ASSOCIATION INTERNATIONALE POUR
L'ETUDE DES ARGILES

COMMISSION VII OF THE INTERNATIONAL SOCIETY OF SOIL SCIENCE

AUSTRALIAN CLAY MINERALS SOCIETY

10TH INTERNATIONAL CLAY CONFERENCE

Adelaide, Australia
18-23 July, 1993

GUIDE BOOK FOR NEW ZEALAND PRE-CONFERENCE FIELD TRIP F.1

Clay Mineralogy of Tephras and Associated Paleosols and Soils, and Hydrothermal Deposits, North Island

D. J. Lowe

Department of Earth Sciences, University of Waikato, Private Bag 3105,
Hamilton, New Zealand

H. J. Percival

Landcare Research New Zealand Ltd, Private Bag 31 902,
Lower Hutt, New Zealand

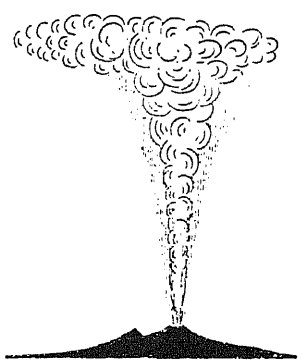

Bibliographic citation:

Lowe, D.J.; Percival, H.J. 1993. Clay mineralogy of tephras and associated paleosols and soils, and hydrothermal deposits, North Island. *Guide Book for New Zealand Pre-Conference Field Trip F.1,* 10th International Clay Conference, Adelaide, Australia. 110pp.

Keywords: clay minerals, allophane, halloysite, ferrihydrite, hydrothermal clays, paleosols, soils, tephra, stratigraphy, New Zealand.

Note: Throughout the text, Ma = millions of years before present, ka = thousands of years before present.

TABLE OF CONTENTS

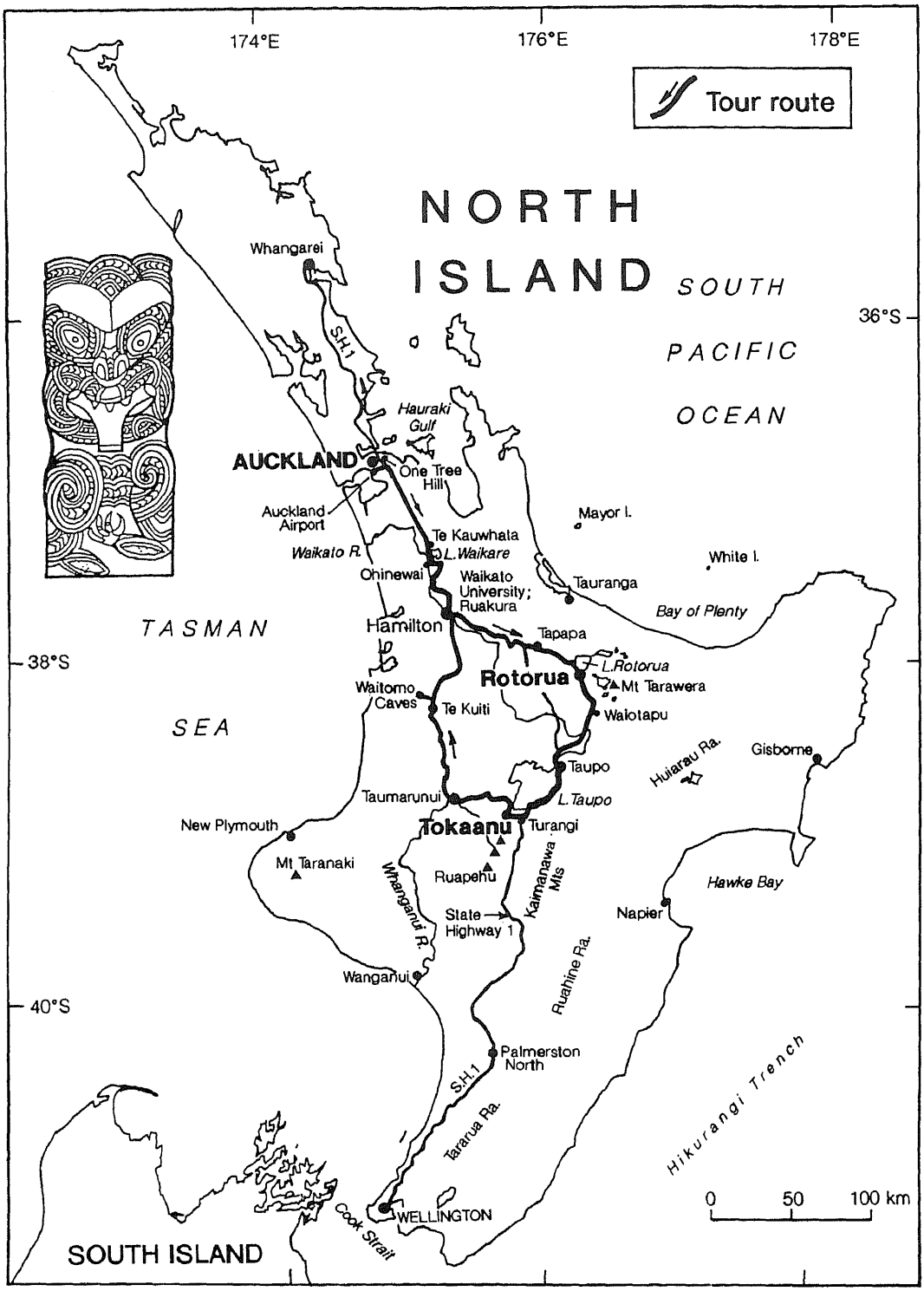

Fig. 0.1 The North Island, New Zealand, and the tour route. Overnight stops are at Auckland, Rotorua, and Tokaanu. The inset depicts a carving of the Waikato tribal area, named after the Waikato River which flows through much of our route. The river was referred to by the Maori people as Waikato-taniwha-rau, meaning 'The flowing river of a hundred water monsters'. The term taniwha was symbolic for a chief, being an expression of admiration. The river is the longest in New Zealand (425 km), rising on the slopes of Mt Ruapehu and ending in the Tasman Sea at Port Waikato.

PREFACE

Welcome to New Zealand or Aotearoa — "Land of the Long White Cloud" — and to the tour. We hope your short stay in New Zealand is both informative and friendly, and to this end we have devised an itinerary comprising a mix of scientific, scenic, and cultural stops. We hope that we have the balance right. Because the tour is being held in mid-winter, we are constrained to some extent by shortish days and the expectation that we will probably have to endure cold and wet conditions for at least part of the tour. Please note that we aim to be on the road at 8.00 or 8.30 am, and to return to our hotel at 5.00 or 5.30 pm each day.

Tour themes and itinerary

The tour centres on the occurrence and genesis of clay minerals, especially allophane, halloysite, and ferrihydrite, associated with both Quaternary rhyolitic airfall tephra (volcanic ash) deposits and volcanogenic alluvium, and on mineralisation and thermal activity in hydrothermal fields. After a brief overview of the basaltic volcanoes of Auckland City, our route essentially traverses the Central Volcanic Region by way of a large loop with overnight stops at Rotorua (2 nights), Tokaanu, and Auckland (Fig. 0.1). We have around five stops planned for each day (including lunch), three of these being scientific stops except on Day 4 when we have only one scientific stop because of the need to travel greater distances.

Our route takes us progressively towards the locus of the most recently active volcanic centres of the Central Volcanic Region, and so the surficial tephra deposits and buried paleosols become successively younger and generally less weathered: tephras at the Mangawara section (Day 1) span c. 1 Ma; at Tapapa (Day 2), c. 140 ka; at Te Ngae (Day 2), c. 20 ka; and at De Bretts, c. 10 ka, and Wairakei, c. 2 ka (Day 3). Interspersed with these tephra-paleosol sections are stops to examine an allophane-halloysite soil drainage (leaching) sequence on volcanogenic alluvium (Day 1), hydrothermal activity and mineral deposits at Whakarewarewa (Day 2) and Waiotapu (Day 3), and pure ferrihydrite seepage deposits in Hamilton (Day 4).

Following introductory and detailed background review material, the tour guide has been arranged on a day-by-day basis and includes an outline of the route and stops, and several pages describing the stratigraphy, mineralogy, chemistry, and pedology of the deposits or features at each of the main stops. We will attempt to point out and describe geological and other features as appropriate during travel periods.

Other activities

Examples of New Zealand's distinctive fauna and flora, including kiwis and tuataras, will be seen at close quarters at Rainbow Springs (Day 2), where we will also enjoy an agricultural farm show. In Rotorua we will partake in a Maori hangi (steam-cooked feast) and concert including traditional dance forms (hakas) and songs (Day 2). In Tokaanu, hot pools will be available to relax in near the slopes of Mt Tongariro (Day 3). At Waitomo, we will visit the Waitomo Cave and in Hamilton spend a short time at the Waikato Museum of Art and History (Day 4). Finally, the tour will conclude with a farewell dinner in Auckland.

Acknowledgements

We thank the following who helped plan, support, or provide data for the tour: C.W. Childs, R.L. Parfitt, W.J. Rijske, T.G. Shepherd, D.N. Eden, P.L. Singleton, B.K.G. Theng, N. Wells, G.G.C. Claridge, M. McLeod, & G.E. Orbell (Landcare Research or DSIR), S.F. Simmons (Auckland University), K.W. Perrott (AgResearch Ruakura), G.J. Churchman, R.W.L. Kimber, & M.J. Wright (CSIRO Soils, S.A.), C.S. Nelson, J.D. Green, R.M. Briggs, P.J.J. Kamp, F. Bailey, & M.R. Green (Waikato University), J.T. McLeod (Environment Waikato), G.A. Spiers (Guelph University), B.E. Green (Asarco Australia), and the various people or organisations who hosted or transported the tour party, or willingly allowed access to private land. M. Lowe is especially thanked for helping collate the guide.

1. INTRODUCTION TO NEW ZEALAND

Geological environment

New Zealand consists of a cluster of islands, the three largest being North, South, and Stewart, in the southwest Pacific Ocean. They have a total land area of about 270 000 km^2 (similar to that of the British Isles or Japan). The islands are the small emergent parts of a much larger submarine continental mass (Fig. 1.1) that was rafted away from Australia and Antarctica by sea-floor spreading in the proto-Tasman Sea between 85 and 60 Ma. Much of this New Zealand subcontinent is a remnant of the former eastern margin of Gondwanaland, the ancient southern supercontinent. The mainland islands form a long, narrow, NE-SW trending archipelago bisected by an active, obliquely converging, boundary between the Australian and Pacific lithospheric plates (Fig. 1.2), which has evolved over the last 25 million years (Kamp 1992). The plate boundary is marked by active seismicity and volcanic arcs, illustrating New Zealand's position as part of the Circum-Pacific Mobile Belt — the so-called "Pacific Ring of Fire". The NE-SW trend of the modern plate boundary cuts across mainly NW-SE oriented structural features inherited from earlier (mid-Cretaceous) rifting events.

In the South Island, continent-continent convergence across the transcurrent Alpine Fault dominates the tectonic scene, with rapid uplift and jagged relief being the result. Rock uplift is most rapid in the central portion of the Southern Alps (about 10 mm/year; Tippett & Kamp in press), and numerous peaks exceed 3000 m in elevation. Fission track dating shows that uplift of the southern end of the Southern Alps began about 8 Ma, and the northern end at 5 Ma (Kamp et al. 1989). Because of such rapid uplift, the late Cretaceous-early Cenozoic cover rocks have been largely removed and therefore the landforms are developed in indurated basement rocks (Fig. 1.3).

In the North Island, in contrast, the ocean-continent convergence has commonly produced marine sedimentary basins and has inverted them, and so generally late Cretaceous-Cenozoic rock sequences, including volcanic ones, are dominant. The uplift of the crust of northern and central North Island originates from high heat flows, but in southeastern North Island it is driven by tectonic thickening. An active volcanic arc of andesite and dacite volcanoes runs from White Island to Mt Ruapehu (Fig. 1.2; Cole 1990). To the northwest of this arc is a backarc region characterised by a much-faulted basin-and-range topography involving basement rocks and basic and rhyolitic volcanism. Large multivent calderas, the sources of voluminous rhyolite lava and of pyroclastic deposits in the form of thick sheets of ignimbrites and widely dispersed airfall tephras, occur immediately behind the active volcanic arc (see section 2 below).

New Zealand's maritime mid-latitude location has made it particularly sensitive to the climatic fluctuations and associated glaciations and sea level changes of the Quaternary Period (Pillans 1992). Glaciations have had their greatest influence in the South Island where the tectonic uplift produced elevated areas for snow accumulation and the relief and structural features necessary for alpine ice caps and major valley glacier systems to develop. Analysis of cores from DSDP Site 594 southeast of New Zealand has shown that the South Island glaciations were in phase with those of the Northern Hemisphere (Nelson et al. 1985a). During the maximum of the last glacial (c. 22-18 ka), an almost continuous glacier complex stretched nearly 700 km along the Southern Alps with snowlines lowered around 800 m below those of the present (Porter 1975). Sea levels were lowered by about 120 m (Pillans et al. 1992). The estimated drop in annual temperature (ignoring regional variations and assuming similar precipitation levels to those of today) is 4.5 to 5.0°C (McGlone 1988). During the periods of glacial advance and retreat, erosion debris of glacial drift, outwash gravels, and loess was deposited in large quantities in inland basins and on both coastlines, with loess deposits especially abundant on the eastern side of the South Island.

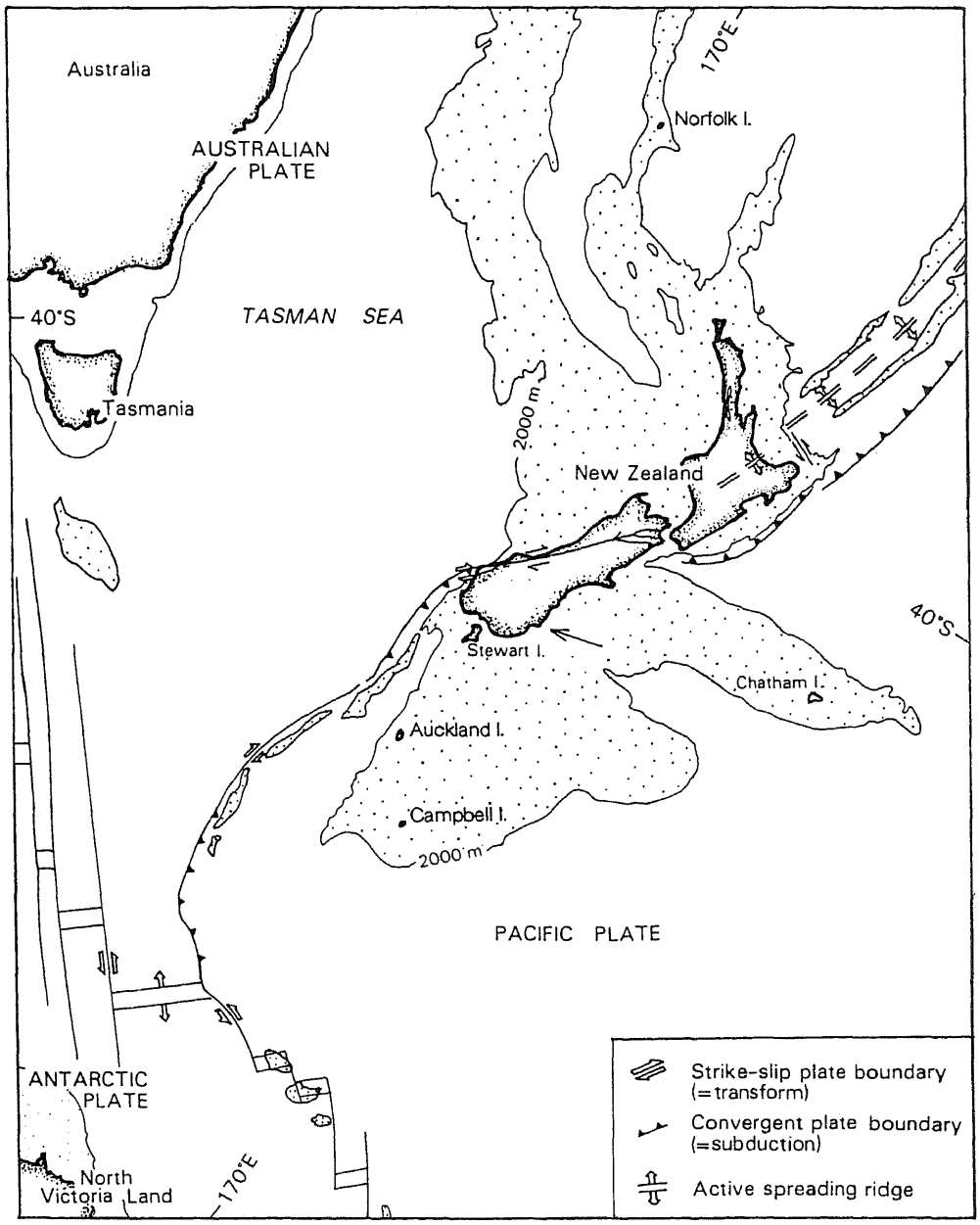

Fig. 1.1 Generalised plate tectonic setting of New Zealand and the southwest Pacific. Sparse stipple represents continental sea floor shallower than 2000 m, and defines the New Zealand subcontinent. The active spreading ridge offshore marks the Havre Trough (after Kamp 1986).

By comparison with the South Island, glaciation in the North Island was minor with cirques and small valley glaciers occurring in the Tararua Range, and a small ice field on the volcanoes in central North Island (Fig. 0.1). Periglacial activity, including severe fluvial and wind erosion at times, occurred in much of the North Island with the notable exception of the Northland peninsula. Loess sheets were deposited in the southern half of the North Island. In parts of central North Island, at elevations >400 m, tephric loess was deposited between airfall tephra units during the colder periods.

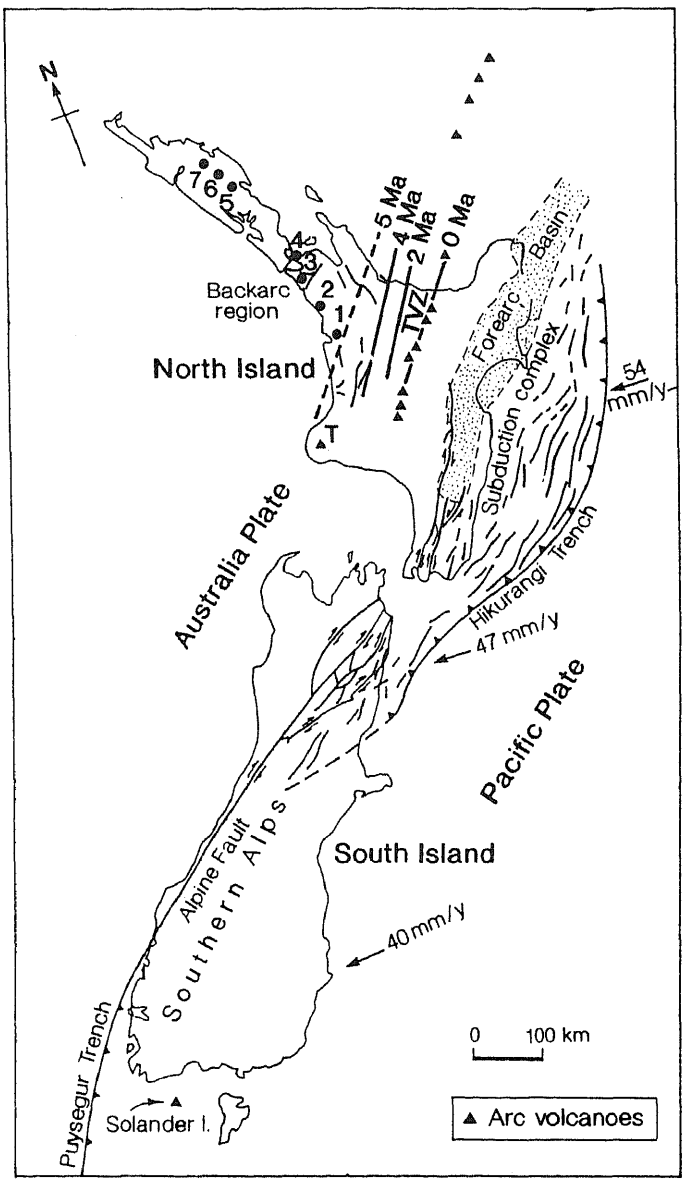

Fig. 1.2 The present tectonic character of the obliquely convergent modern Australia-Pacific plate boundary through New Zealand (after Kamp 1992), and the trenchward migration of the arc volcanoes during the last 5 Ma (after Tatsumi & Tsunakawa 1992). TVZ = Taupo Volcanic Zone. Intraplate basalt volcanic fields are: 1, Alexandra (co-existing intraplate and subduction-related eruptives; Briggs & McDonough 1990); 2, Ngatutura; 3, South Auckland; 4, Auckland; 5, Whangarei; 6, Puhipuhi; 7, Kaikohe-Bay of Islands. T = Mt Taranaki.

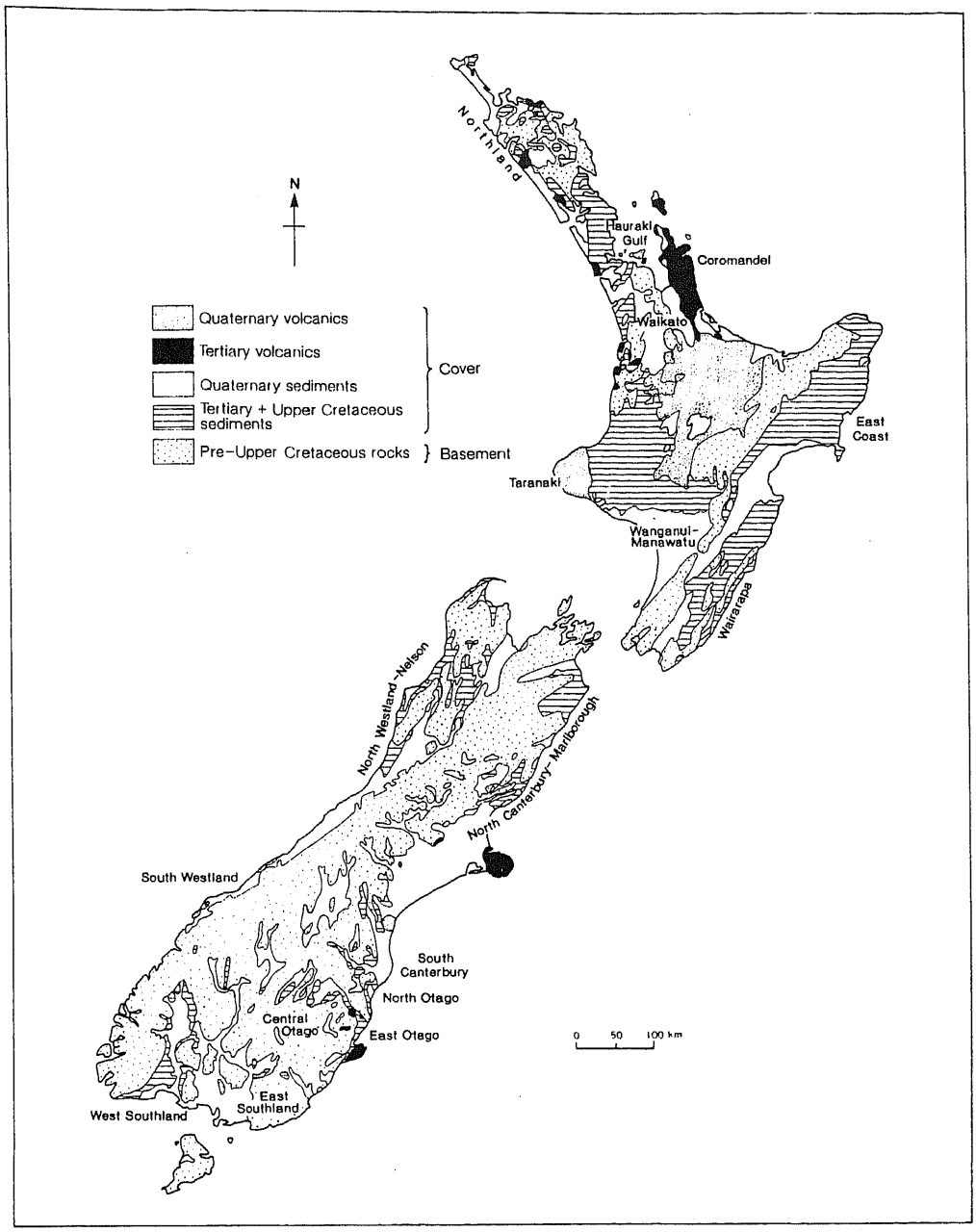

Fig. 1.3 Generalised geological map of New Zealand (from Kamp 1992). Quaternary, 2-0 Ma; Tertiary, 65-2 Ma; Upper Cretaceous, 100-65 Ma; Pre-Upper Cretaceous, pre-100 Ma.

The dominantly hilly and often mountainous nature of much of New Zealand (around 50% is classed as steep, 20% moderately hilly, and 30% rolling or flat), coupled with a generally high rainfall and the widespread occurrence of highly jointed basement rocks and soft sedimentary rocks that are very susceptible to erosion, has produced generally very fast rates of denudation, especially through landsliding, either as deep rock and debris slides or as shallow, regolith slides. Denudation rates may be as high as 5000 m^3/km^2/year in some areas (Crozier et al. 1992). The landsliding is evidently an episodic process controlled chiefly by the frequency of earthquakes and high magnitude climatic events such as rainstorms. In the last millennium human activities, especially deforestation, both by Polynesian and European settlers, have tended to increase rates of erosion.

Thus active tectonism, volcanism, generally abundant rainfall, and high rates of erosion in New Zealand have resulted in a dynamic, sharp textured, and youthful landscape with great landform variety. Almost all of the present landscape has developed within the past two million years, indeed much of it in the second half of the Pleistocene or in the Holocene (Pillans et al. 1992).

Soils

The soil pattern associated with the New Zealand landscape is complex, partly because of the many different kinds of parent materials, and partly because of the varied conditions under which they have been transformed into soils (Soil Bureau Staff 1968; Molloy 1988). All the orders of *Soil Taxonomy* (Soil Survey Staff 1992) are represented in New Zealand, but Mollisols and (especially) Vertisols are very rare (Hewitt 1992).

Northern North Island, which largely escaped the effects of the glacial periods, is warm and humid, and many soils are old, deeply weathered, and clayey, forming mainly Ultisols and some Oxisols (Fig. 1.4). Spodosols, commonly associated with forest species that produce an acid litter (e.g. kauri, rimu), are also represented. Elsewhere in New Zealand the soils are almost all relatively young because of the effects of tectonism, land instability, and the Pleistocene glaciations (especially influential in the South Island). In central and western North Island large areas of soils (and buried paleosols) are developed on the sequences of airfall tephra deposits, forming mainly Udands and Vitrands dominated by short-range order clays. Parts of southern North Island, and eastern South Island, often experience seasonal moisture deficiencies (ustic moisture regimes) and the soils typically are Alfisols or Inceptisols. The very dry inland basins of the South Island (Central Otago) contain Aridisols, whilst in the very high rainfall areas of western South Island, Spodosols, often Aquods, predominate (Fig. 1.4).

Climate

New Zealand lies within the zone of mid-latitude westerly winds extending from 70° to 30°S. These strong, consistent winds are moisture laden after their passage over the surrounding ocean, but moderated in temperature. The main climatic features of the country result from interaction of this air flow with the substantial barrier of the northeast-trending mountain chains (Tomlinson 1975). Because few areas are more than 100 km from the coast, oceanic influence is dominant and the climate is generally moist, windy, and with low annual cloudiness. Most of New Zealand can be classified as warm or cool temperate (McGlone 1988). Annual mean temperatures vary from about 15°C in northern North Island to about 9°C in southern South Island, with summer temperatures relatively cool and winter conditions generally mild. Westerly winds predominate for most of the year although there may be considerable modification by local topography. In many North Island areas, southwesterly flows predominate. In the past year or two, mean monthly temperatures have been about 1°C lower than normal, and winds generally more southerly, because of the influence of the El Nino phenomenon (ocean surface temperature anomalies of the equatorial Pacific) and fine ash fallout from the Pinatubo eruption in the Phillipines in mid-1991.

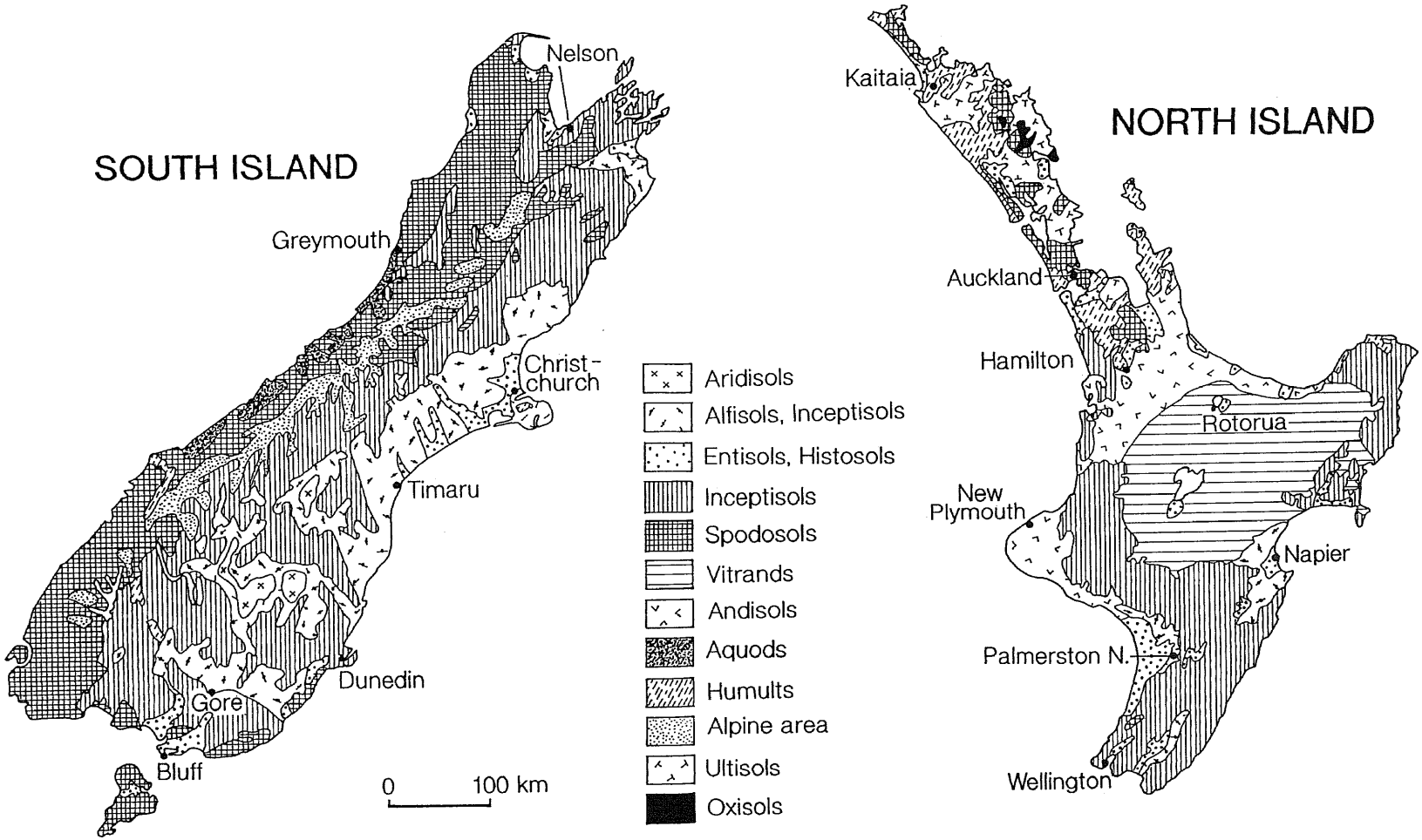

Fig. 1.4 Generalised soil map of New Zealand (after Soil Bureau Staff 1968 and Hewitt 1992).

Rainfall is highly variable and strongly related to the topography, ranging from more than 7000 mm in the central Southern Alps to 350 mm in inland Central Otago east of the main mountain ranges. The average for the whole country is probably >2000 mm but for much it lies between 600 and 1600 mm. Day-to-day weather variation is high and is controlled by a progression of eastward-moving anticyclones and depressions, with associated cold and warm fronts, at approximately 5 to 10 day intervals (Tomlinson 1975). Persistent weather patterns are rare. Sunshine levels are relatively high with much of the country receiving >2000 hours per year.

Flora and fauna

Fossil remains show that New Zealand has long been forested, and recognisable ancestors of some present-day trees such as rimu (*Dacrydium cupressinum*), kahikatea (*Dacrycarpus dacrydioides*), totara (*Podocarpus totara*), matai (*Prumnopitys taxifolia*), miro (*Prumnopitys ferruginea*), and kauri (*Agathis australis*) extend back 250 Ma (Bishop 1992). At that time, New Zealand was part of Gondwanaland. Ancestors of various ancient or 'archaic' animals — the tuatara, native frogs, and giant land snails — lived in New Zealand as far back as 150 Ma. The ancestors of the moas and kiwis, southern beeches (*Nothofagus*), and rewarewa (*Knightia*) were also present when New Zealand first began to separate from Antarctica and Australia c. 85 Ma. When this happened many previously dominant plants and animals became extinct. Dinosaurs and other giant reptiles, many marine invertebrates, and some of the fern-like plants and gymnosperms, were lost as climates changed and new life forms evolved. For the plants and animals left 'aboard' New Zealand when it drifted away from Gondwanaland, the islands became both a paradise and a prison (Bishop 1992). Only a trickle of new plants and animals has subsequently arrived from across the sea. Thus New Zealand's early separation and long isolation have provided opportunities for the evolution of peculiar endemic plants and animals. Since then the country's turbulent geological development, involving tectonism, volcanism, and climate change, has further influenced evolution and extinction in New Zealand (McGlone 1985).

The impact of humans or other exotic invaders (especially mammals) has occurred only very recently, being restricted to the last 1000 years or so. However, the forests have changed significantly in this relatively short time. About 75% of the land was covered in forest in pre-Polynesian times but this was reduced to about 55% by the time European settlement began about 150 years ago. This reduction in forest cover is attributed largely to Polynesian firings (McGlone 1983a). Since European arrival, forest cover has been further reduced to about 25%, with practically all lowland areas being cleared for agriculture. An inevitable result of deforestation on this scale, together with the introduction of carnivorous and herbivorous mammals such as rats, stoats, pigs, deer, and possums, has been the extinction of unique native plants and animals, particulary from the lowland forests, through competition, predation, and disease (Towns & Atkinson 1991). A large proportion of the extinctions can be attributed directly to the loss of habitat or to the reduction of forested areas to patches too small to provide adequate resources for survival of populations. Nearly 25% of all the endangered species of birds listed from around the world are from New Zealand, and over 300 of the flowering plants and ferns (10-15% of the total) are currently at risk (Hackwell 1983). Those offshore islands free of introduced pests have assumed special significance as 'safe havens' to transfer native animals whose existence is threatened elsewhere. Such transference to offshore islands, together with programmes of pest eradication on them, now form the mainstay of New Zealand's threatened species management (Towns & Atkinson 1991; Bishop 1992).

The flora of New Zealand is not rich as the total number of higher plants — slightly more than 2000 — is small compared with other countries of similar size and latitude. However, c. 85% of species and c. 10% of genera are found nowhere else, including one endemic genus of fern and 38 endemic genera of flowering plants. Twenty-four of these 39 endemic genera are represented by a single species (Hackwell 1983). The early naturalist Sir Joseph Banks, visiting New Zealand in 1769 with Captain Cook, remarked that "The entire novelty of what we found recompensed us as natural historians for the want of variety".

About 80% of New Zealand's higher plant genera are found also in Australia, but the most distinctive and widespread Australian genera, *Eucalyptus*, *Acacia*, and *Banksia*, do not occur in New Zealand (McGlone 1988).

New Zealand forests are of two major types, dominated either by (1) conifers (podocarps, 'cedar', kauri) and broadleaf 'hardwood' (e.g. tawa, taraire, rata, kamahi, rewarewa) trees, or (2) by one or more of the four southern beeches. Conifer-broadleaved forests are very diverse, occurring throughout the country under all climates but are best developed on warm, fertile, lowland sites. Beeches tend to occupy sites climatically less favourable for plant growth than those dominated by conifer-broadleaved forests, hence are concentrated in cooler, southern regions, and in uplands rather than lowlands (McGlone 1988). The largest tree, kauri (*Agathis australis*), occurs only in warmer regions north of latitude 38°S; it rarely exceeds heights of more than 30 m but has massive, cylindrical boles normally up to 3 m in diameter but some may be as large as 7 m.

As a whole, New Zealand forests are quite different from those of the Northern Hemisphere and other temperate regions, resembling tropical rain forest in many ways: they are moist, dense, and evergreen with many multi-storied vegetation layers, and both the forest floor and trees are often covered in mosses and ferns, with the trees also carrying vines and other plants on trunks and upper branches. Other characteristics include a dearth of deciduous species or annuals; trees frequently have differing juvenile and adult forms; many shrubs and juvenile trees have divaricating forms with widely-angled branches and a tangled growth habit; flowers are usually inconspicuous and lack bright colours; many plants produce colourful, bird-dispersed, small fleshy fruits; and an unusually high proportion (c. 12%) of native species have male and female flowers on separate plants (Hackwell 1983). Finally, New Zealand forests differ from all others in that they have developed in the absence of herbivorous mammals, and hence they more closely resemble the ancient forests of Gondwanaland than those of any other southern continent. New Zealand also has the world's largest buttercup (*Ranunculus lyallii*), the smallest member of the pine family (*Lepidothamus laxifolius*), the largest tree fern (*Cyathea medullaris*), tree-sized daises (*Olearia, Senecio*), mosses 0.3 m high (*Dawsonia superba*), and numerous cushion plants including the huge 'vegetable sheep' of the South Island mountains (*Haastia, Raoulia*).

Like the flora, the fauna of New Zealand is a curious mixture of 'archaic' animals of Gondwanaland lineage and later arrivals from more recent times, mostly from Australia. Only a few examples are described here. Among the birds, there has been an evolutionary trend towards increasing size, loss of flight, and dark plumage. Kiwis (*Apteryx*), together with the now extinct moas (*Dinornis*), are endemic representativesof the ratites, which also include the emu, cassowary, rhea, and the ostrich. Until recently, both kiwis and moas were thought to have become flightless on Gondwanaland, but new work has suggested that kiwis are of more recent origin than moas, their lineage dating back only 40 million years. If so, how the kiwi's ancestors reached New Zealand, well isolated from Gondwanaland by then, is a puzzle (Bishop 1992). Kiwis, of which four species are known (more probably exist), are unusual amongst living ratites because of their small size and adaptation to life on the forest floor. They are nocturnal and feed on small insects and other invertebrates. Their long beak has nostrils at the tip and cat-like sensory hairs at the base. Moas were herbivores of different sizes, the largest being over 2 m tall and weighing c. 200 kg, and the various species may have browsed in different habitats.

One of New Zealand's rarest flightless birds is the bright green kakapo or New Zealand ground parrot (*Strigops habroptilus*), the world's largest parrot. It has evolved a solitary, nocturnal existence and sometimes climbs trees to get its food. Other flightless herbivorous birds include the rare takahe (*Porphyrio mantelli*), formerly widespread but now restricted to parts of Fiordland, and the weka (*Gallirallus australis*), an opportunist feeding on a variety of animal and vegetable matter (Bishop 1992).

The tuatara (*Sphenodon punctatus*) is the sole remaining species from a family of reptiles (Sphenodontida) with a lineage going back more than 225 million years and little changed from its ancient predecessors. It resembles a lizard and a crest of fexible spines along the back, the shape of the skull and jaw, and the enlarged pineal gland suggestive of a 'third eye' are among its special features.

Another distinctive animal, the 'velvet worm' or peripatus (*Peripatoides novaezelandiae*), occupies what appears to be a half-way position in the evolutionary scale between worms and insects. It has the soft, flexible, unjointed body of a worm yet clawed feet and air-conducting tracheae of an insect (Bishop 1992).

The ancestors of New Zealand's three native frog species (*Leiopelma*) probably date back to Gondwanaland times. They are considered to be the most primitive of all living frogs. They lack vocal sacs hence are non-croaking, have tail-wagging muscles but no tail, and have fish-like vertebrae. Lacking fully webbed feet for swimming, they deposit eggs in moist ground or seepages rather than in water. The young of Hamilton's frog (*L. hamiltoni*) are hatched as virtually tailed froglets which then crawl onto the moist back of the adult male to complete development (Bishop 1992).

Perhaps the most 'deadly' archaic animals of the forest floor are the giant snails (*Powelliphanta*) that grow up to 10 cm in diameter. These members of the ancient Gondwanaland snail family, Rhytididae, are voracious carnivores and hunt earthworms, slugs, and smaller snails which are consumed with the hundreds of tiny dagger-like teeth covering their radula, or tongue (Bishop 1992).

2. CENTRAL NORTH ISLAND VOLCANISM AND PYROCLASTIC DEPOSITS

Late Cenozoic intraplate and subduction-related volcanism

The North Island, located on the leading edge of the Australian plate, is being underthrust by the Pacific plate at the Hikurangi Trench with the subducting slab dipping to the NW at c. 50°. Since about 5 Ma, a series of NE-trending frontal arc volcanoes have migrated c. 100 km southeastwards across the central North Island, probably because of gradual steepening of the subducted slab, to reach the present-day locus of activity in the Taupo Volcanic Zone (TVZ) about 2 Ma (Fig. 1.2; Kamp 1984; Tatsumi & Tsunakawa 1992).

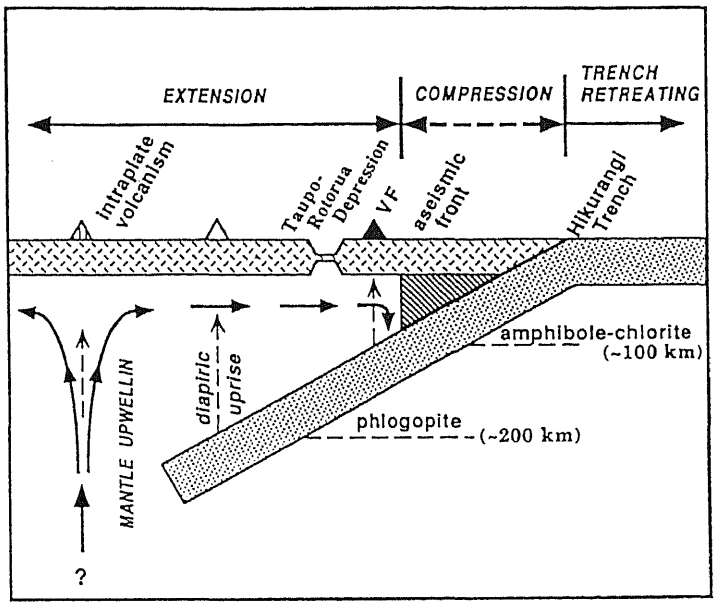

Fig. 2.1 Model for the origin of backarc rifting and pattern of stress in North Island as related to intraplate and subduction-related volcanism (from Tatsumi & Tsunakawa 1992). VF = volcanic front (TVZ); hatching = forearc mantle wedge.

Two types of volcanism resulting from this tectonic setting are manifest in the North Island, as outlined below.

(1) Mainly basaltic, intraplate volcanism in the backarc region. Effectively confined to western and northern North Island in seven volcanic fields (Fig.1.2), this volcanism may be caused by the upwelling of asthenospheric materials from deeper parts of the mantle (Fig. 2.1). There is a progressive younging in age of the fields from the Alexandra Volcanics (2.74-1.60 Ma), to Ngatutura (1.83-1.54 Ma), to South Auckland (1.56-0.51 Ma), and to Auckland (0.14 Ma to 600 years) (Briggs et al. 1989; Kermode 1992). However, the Northland fields (numbered 5-7 in Fig. 1.2) show a wide range of ages from c. 10 Ma to c. 1.2 ka. On our tour we will travel over, or near to, the Auckland, South Auckland, and Alexandra volcanic fields (Fig. 2.2).

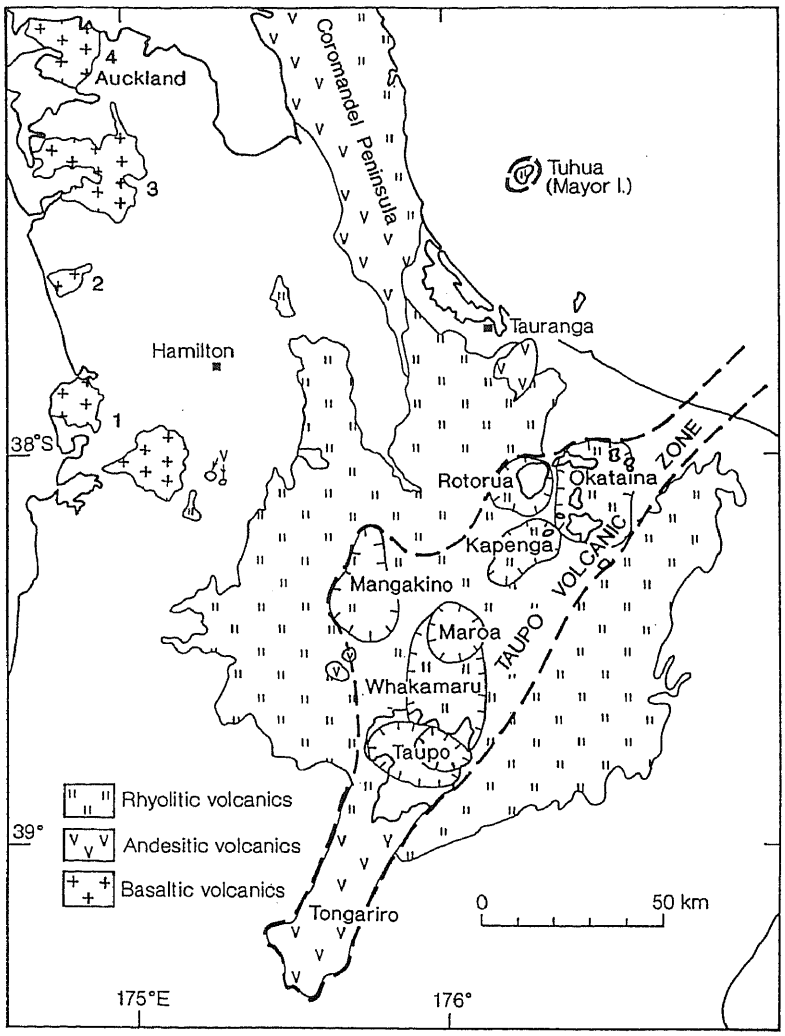

Fig. 2.2 Generalised distribution of basaltic, andesitic, and rhyolitic volcanics (including welded ignimbrites) in central North Island, and the locations of seven multivent calderas and Tongariro Volcanic Centre in the Taupo Volcanic Zone (after Briggs et al. in press). The TVZ forms the eastern part of the geologically and geophysically distinct wedge-shaped Central Volcanic Region. The Tuhua volcano of Mayor Island is a peralkaline caldera complex most recently active in the Holocene (Houghton et al. 1992). The Coromandel Peninsula lies in the Coromandel Volcanic Zone, an area of active volcanism in Miocene-Pleistocene times (Skinner 1986). Intraplate basalt fields (numbered) are as in Fig. 1.2.

(2) Mainly andesitic and rhyolitic, subduction-related volcanism along the frontal arc and in the backarc region (collectively referred to as the Central Volcanic Region). Since c. 2 Ma, this volcanism relates chiefly to activity in the TVZ, a relatively narrow (<≈50 km) volcanotectonic depression comprising a young backarc basin — the Taupo-Rotorua Depression — formed within thin continental crust in an area of active extension (rifting) and very high heat flow (700-800 mW/m^2), and the adjacent frontal arc (Cole 1990; Tatsumi & Tsunakawa 1992). The arc extends about 250 km NE-SW from the active volcanoes of White Island in the Bay of Plenty to those of Tongariro Volcanic Centre south of Lake Taupo (Fig. 2.1) (cf. Wilson 1993). It is primarily andesite-dacite in composition, making up about 3% (volumetrically ≈800 km^3) of the TVZ deposits. Very rare basalts (proportionally <1%; ≈2 km^3) also occur in the region (Gamble et al. 1990). The Taupo-Rotorua Depression in the TVZ is evidently the southern extension of active oceanic back-arc rifting along the Havre Trough offshore (Fig. 1.1; Wright et al. 1990), and is currently widening at the rate of 18 ± 5 mm/yr (Darby & Williams 1991). A possible mechanism for this rifting is the injection of asthenospheric materials into the mantle wedge which, together with the subducted slab, is being pushed trenchwards (Fig. 2.1; Tatsumi & Tsunakawa 1992).

A second (part) subduction-related volcanic chain in the backarc region is that of the mainly basaltic Alexandra Volcanics and the andesitic Taranaki volcanoes (aged c. 1.8 Ma to A.D. 1755) in western North Island. These will not be considered further here but are described in Briggs & McDonough (1990), Neall (1979), and Neall et al. (1986).

Taupo Volcanic Zone and associated pyroclastic deposits

The central part of the TVZ, which is comparable in size and longevity to the Yellowstone volcanic area in the United States (Wilson et al. 1984), has erupted huge quantities (≈10 000 to 16 000 km^3) of rhyolitic lavas and pyroclastic deposits, including both welded and non-welded ignimbrites, of ≈2 km or more thickness (Wilson et al. 1984; Stern 1987). These silicic materials make up c. 97% of the TVZ deposits, and drillholes reveal that they are underlain in places by andesite lavas locally >1 km thick (Browne et al. 1992). The deposits have been erupted mainly from seven multivent centres marked by large calderas (Fig. 2.2), the earliest known eruptives originating from Mangakino caldera at least 1.6 Ma (Pringle et al. 1992; Soengkono et al. 1992). The Taupo volcano is an 'inverse' volcano, so called because it is concave with the flanks sloping gently inwards towards the vent locations (Walker 1984), rather than forming the steep convex cones characteristic of andesite stratovolcanoes (e.g. Mt Taranaki) or rhyolite domes (e.g. Mt Tarawera). This inverted form, also shown by the Rotorua volcano, arises largely because eruptions from rhyolitic volcanoes of this sort are typically so powerful that accumulation of erupted material near the vent is insufficient to counteract subsidence due to caldera collapse because of magma withdrawal and regional tectonic extension, and because later effusion of steep-sided domes is comparatively minor. The Mangakino and Kapenga calderas are probably extinct, Rotorua and Maroa may be feebly active, and Taupo and Okataina are very active, the latest eruptions occurring c. 1850 years ago (Taupo) and in A.D. 1886 (Tarawera), respectively. The Whakamaru caldera is probably extinct but intense faulting in the area may be partly due to resurgence (Wilson et al. 1986).

The known history of eruptions from these calderas is summarised by Wilson et al. (1984, 1986), Wilson (1986, 1993), and Briggs et al. (in press). Such eruptions include one of the largest late Quaternary eruptions known, that of the Whakamaru-group ignimbrites and an associated airfall component, the Rangitawa Tephra, from Whakamaru caldera c. 0.35 Ma, producing >≈1200 km^3 of pyroclastic material (Froggatt et al. 1986; Kohn et al. 1992). Fallout from this eruption very likely reached South America, 10 000 km to the east of New Zealand, and beyond (Froggatt et al. 1986). Another enormous eruption was that of Kawakawa Tephra from Taupo volcano c. 22.6 ka, producing ≈500 km^3 of fall deposits, 300 km^3 of ignimbrite, and 500 km^3 of intra-caldera fill (Wilson 1993).

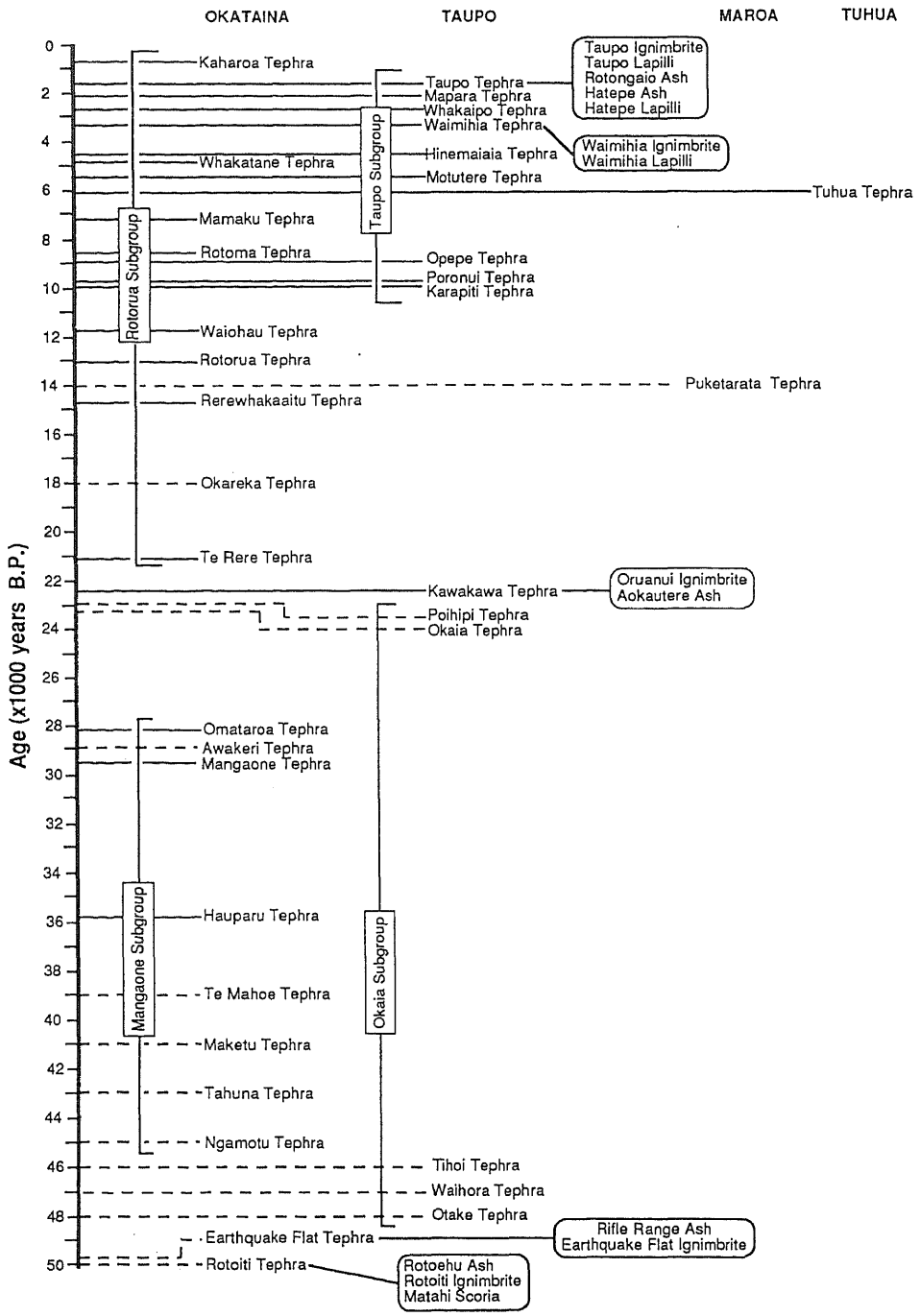

Fig. 2.3 The stratigraphic relationships of named late Quaternary silicic tephras in time and space, showing the interfingering of tephras from four volcanic centres (Fig. 2.2). Solid tie lines to the age scale are based on mean radiocarbon ages; dashed lines indicate that dates are not available, the relative chronology being derived from stratigraphic relations and degree of paleosol development (from Froggatt & Lowe 1990). Two additional tephras (basaltic) were erupted from the Okataina centre: Rotokawau (c. 3.5 ka) and Tarawera (10 June 1886). The age of the oldest formation (Rotoiti) is estimated at c. 50 ka by Froggatt & Lowe (1990) but ages ranging from c. 45 ka to 64 ka have also been proposed (Berryman 1992; Buhay et al. 1992; Wilson et al. 1992). Note: Wilson (1993) has recently revised the stratigraphy of the Taupo subgroup eruptives and now records 28 eruptive events in this period.

Pyroclastic fall deposits associated with the central TVZ caldera eruptions are widespread in the North Island, with some forming important stratigraphic markers extending to the South Island and in deep sea cores both west and east of New Zealand (e.g. Nelson et al. 1985b; Pillans et al. 1992). Apart from a few exceptions, the earliest tephra deposits ('tephra' is a widely-used collective term for all the unconsolidated, primary pyroclastic products of an eruption; Froggatt & Lowe 1990) at distal localities peripheral to TVZ have generally not been well dated. However, recent work using improved fission track dating techniques and the K-Ar and $^{40}Ar/^{39}Ar$ methods, together with paleomagnetism, is making great advances (e.g. Kohn et al. 1992; Pringle et al. 1992; Soengkono et al. 1992; Alloway et al. 1993).

In the Waikato region, there are two groups of old, strongly weathered tephra sequences: the Kauroa Ashes (erupted from c. 2.3 to ?1 Ma; Briggs et al. 1989), and the Hamilton Ashes (erupted from c. 0.35 Ma to 0.1 Ma; Selby & Lowe 1992). Both groups have uncertain sources — the Kauroa beds possibly represent very early eruptions from TVZ (?Mangakino caldera), and the Hamilton beds may relate to the eruptions from the Taupo, Whakamaru, or Maroa centres. Representatives of these deposits will be seen on Day 1 of the tour.

Pyroclastic eruptives from TVZ over the past c. 50 ka are much better documented and their chronology (by radiocarbon dating) and distribution are generally well established (Froggatt & Lowe 1990; Lowe 1990; Wilson 1993). In this time there have been around 50 pyroclastic eruptions from the Taupo and Okataina calderas alone, a mean rate of one every ≈1000 years (Fig. 2.3). Many eruptions produced volumes of deposits >>1 km^3 (in comparison, the 1980 eruption of Mt St Helens in USA produced about 1 km^3 of pyroclastic material). The three largest, volumetrically, were the Rotoiti (240 km^3), Kawakawa (800 km^3), and Taupo (90 km^3) eruptive episodes, with the total volume of rhyolitic material erupted from TVZ in the past c. 50 ka conservatively estimated at ≈800 km^3 of airfall tephra, 540 km^3 of ignimbrite, and 550 km^3 of extrusive lava, together equivalent to more than 700 km^3 of magma (Froggatt & Lowe 1990; Wilson 1993). A number of these Okataina and Taupo-derived tephra deposits will be seen during Days 2 and 3 of the tour.

Numerous andesitic tephras have been erupted from the Tongariro Volcanic Centre in late Quaternary times but these generally have a limited distribution (e.g. Topping 1973; Cole et al. 1986; Lowe 1988; Donoghue et al. 1991).

3. OCCURRENCE OF CLAYS IN TEPHRAS AND ASSOCIATED SOILS AND PALEOSOLS IN CENTRAL AND NORTHERN NORTH ISLAND

Studies in New Zealand on tephra-derived clay minerals, especially allophane, have been facilitated in three main ways (Parfitt 1990a). (1) Tephra parent materials have been erupted from relatively few volcanic centres of rhyolitic, andesitic, and basaltic composition, and the distribution of many tephra layers can be readily traced across the landscape, as noted above (e.g. Lowe 1990). At many sites, therefore, the tephra stratigraphy is well documented and thus the time since deposition, and primary composition, are known (e.g. Lowe 1986, 1988). (2) Most of New Zealand was under native forest before Polynesian and European settlement in only the last ≈1000 and 150 years, respectively (section 1 above), and so many soils have generally been little modified apart from recent conversion to pasture. (3) The climate is moist and temperate with rainfall usually exceeding evapotranspiration for most of the year in central and northern North Island areas (i.e. it has an udic moisture regime), conditions that favour the formation of allophane in particular (Parfitt & Kimble 1989).

With increasing age the amount of clay-sized (<2 μm) material in tephra deposits generally increases as glassy and other components are weathered and transformed to clay minerals. In central North Island, tephras less than c. 3 ka generally have <5% clay; tephras c. 3 to 10 ka contain ≈5-10% clay, whereas those c. 10 to 50 ka contain ≈15-30% clay; tephras older than c. 50 ka have >70% clay (Table 3.1). The amount of clay formed in these deposits thus broadly correlates with tephra age. This general relationship applies only where the tephras are weathering under similar conditions, however, as the rates of clay formation differ according to environment and composition. Environmental parameters such as frequency and depth of burial, climate, vegetation, and degree of leaching may influence the proportion of clay-sized material in a tephra deposit, and, together with its primary composition, determine the types of clay minerals within the clay fraction (Lowe & Nelson 1983; Lowe 1986).

Table 3.1 Relationship between tephra age and clay content of some rhyolitic tephras from New Zealand[a]

Tephra	Age (ka)[b]	Clay % (< 2 μm)[c]	No. of samples
Kaharoa	0.70	6	2
Taupo	1.85	5	8
Mapara	2.16	5	1
Whakaipo	2.69	5	1
Waimihia	3.28	5	2
Whakatane	4.83	7	6
Mamaku	7.25	8	9
Rotoma	8.53	6	2
Waiohau	11.85	16	5
Rotorua	13.08	10	2
Rerewhakaaitu	14.70	9	8
Okareka & Te Rere	18 - 21	15	7
Kawakawa	22.59	18	11
Mangaone subgroup	≈28 - 45	16	10
Rotoehu	≈50	25	9
Hamilton group	≈100 - 350	71	31
Kauroa group	≈1? - 2.3 Ma	85	43

a Mainly after Lowe (1986) plus data from Shepherd (1984) and Green (1987). Some tephras may contain small proportions of admixed andesitic material.
b After Briggs et al. (1989), Froggatt & Lowe (1990), and Selby & Lowe (1992).
c Mean of n analyses including paleosols (usually buried Bw or Bt horizons).

The clay fractions of tephras consist mainly of authigenic clay minerals along with smaller amounts of residual or accessory minerals. The outstanding feature of almost all tephra-derived clay fractions is the occurrence of short-range order (SRO) clay minerals in addition to well-ordered or crystalline species, with a key characteristic being 'active' Al (and often Fe) in various mineralogical forms. SRO minerals can also occur in non-tephric materials (e.g. soils derived from basalt lavas) and in non-volcanic (usually quartzo-feldspathic) materials chiefly through strong leaching or podzolisation (e.g. Young et al. 1980; Farmer 1982; Childs et al. 1983; Parfitt & Webb 1984; Parfitt & Saigusa 1985; Hewitt 1992).

Types of clay components

The most abundant secondary minerals occurring in the clay fraction of tephras and associated soils and paleosols in North Island are allophane and halloysite. Imogolite and ferrihydrite are also common but are found usually in only small amounts except in special circumstances. Gibbsite, goethite, and hematite may also occur in some tephra deposits, whilst subordinate amounts of secondary silica polymorphs (mainly opaline or amorphous silica), humus complexes, vermiculite and other 2:1 minerals, interstratified or mixed-layer minerals, and kaolinite have additionally been reported. Residual minerals including quartz, feldspar, cristobalite, tridymite, glass, and (rarely) diatoms may occur in tephra clay fractions but in varying amounts. Some notes on these minerals and their formation, particularly allophane, are summarised below. More detailed information is summarised in Lowe & Nelson (1983), Lowe (1986), Parfitt (1986), Parfitt & Childs (1988), Parfitt & Kimble (1989), Parfitt (1990a), and Childs (1992). Overseas data are summarised in, for example, Wada (1985, 1987, 1989), Dixon & Weed (1989), Mizota & van Reeuwijk (1989), and Huang (1991).

Allophane

Allophane is the name given to a group of aluminosilicate clays characterised by SRO and containing silica, alumina, and water in chemical combination (Parfitt 1990a). This definition excludes imogolite because this mineral, comprising bundles of fine tubes (see below), has long-range order in one dimension. Volcanic glass is also excluded because it has no order. There are three main types of allophane found in New Zealand, the first two predominantly in soils: (1) an Al-rich allophane (Al:Si molar ratio ≈2.0 or more), often referred to as 'imogolite-like allophane'; (2) a Si-rich allophane (Al:Si ≈1.0), perhaps best referred to as 'halloysite-like allophane'; and (3) stream deposit allophane (Al:Si ratios 0.9-1.8), also known as 'hydrous feldspathoid allophane'. Their properties are listed in Table 3.2.

Table 3.2 Types of allophane found in New Zealand (from Parfitt 1990a)

Measurement	Al-rich (soil)	Si-rich (soil)	Stream deposit
Al:Si ratio	2–4	~1	0·9–1·8
Infrared bands (cm^{-1})	975, 690, 570, 500, 428, 348	1020, 680, 580 450	1020, 880, 670, 610, 450
^{29}Si n.m.r. Possible structure	−78 ppm orthosilicate	−90, (−78) ppm polymerized silicate (orthosilicate)	−86 ppm layer silicate
^{27}Al n.m.r.	5 ppm Al^{VI}	5, 60 ppm Al^{VI}, Al^{IV}	3, 51 ppm Al^{VI}, Al^{IV}
Names proposed	Proto-imogolite allophane,[A] Imogolite-like allophane[B]	Pumice allophane[A] (Defect kaolin,[C] Halloysite-like allophane[C])	Hydrous feldspathoid allophane[A]

[A] Farmer *et al.* (1979).
[B] Parfitt and Wilson (1985).
[C] Yoshinaga (1986).

Al-rich allophanes (Al:Si ≈2.0) are composed of discrete, spherically shaped particles, usually clumped together into aggregates as shown by high resolution electron microscopy. The diameter of an individual spherule is about 4 to 5.5 nm and its wall appears to be ≈0.7-1.0 nm thick. Infrared spectroscopy and other studies indicate that Al-rich allophane comprises fragments having the imogolite atomic structure over a short range, the fragments linking to give a porous, hollow spherule, each containing about 8-10 micropores (broken bond defects) (Fig. 3.1). The defects in the structure presumably arise where the proto-imogolite fragments combine, making edge to edge contact, as they form spherules (Parfitt 1990a). The defect sites may account for the variable charge characteristics of allophane (Theng et al. 1982). Water molecules occupy the interior of the spherules and are also adsorbed onto the outer AlOH surface. The units are curved with a gibbsite-like octahedral sheet on the outer surface with hydroxyls at the surface (Fig. 3.1). The inner surface consists of O_3SiOH tetrahedra with the oxygens replacing the inner hydroxyls of the octahedral layer (Parfitt 1990a). Specific surface area measurements range from about 400 to 900 m^2/g (Childs & Parfitt 1987). Al-rich allophane, initially characterised as such in Taranaki soils (Russell et al. 1981), is the dominant form of allophane in New Zealand.

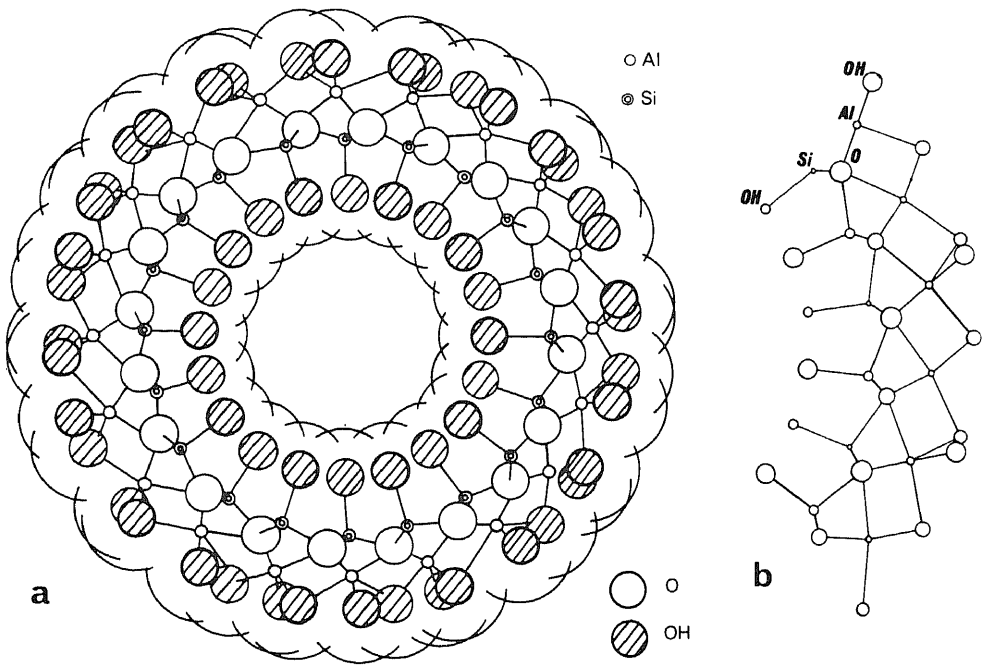

Fig. 3.1 (a) Cross section of an imogolite tube viewed down the tube axis. The outside diameter is 2.14 nm, the inside diameter 0.64 nm. The external surface of the tube comprises a gibbsite-like Al octahedral structure but the internal surface has exposed Si-OH groups (SiO_3OH) with the Si in isolated tetrahedral sites (after Parfitt 1980). (b) Curling of the gibbsite hydroxide sheet sheet by contraction of one surface to accomodate the SiO_3OH tetrahedra (after Wada 1989).

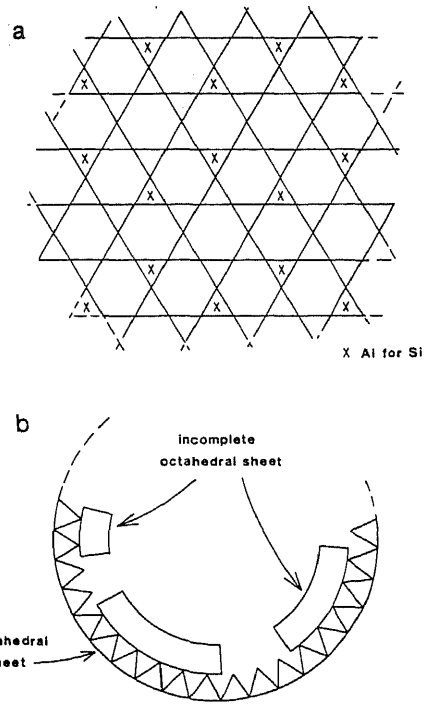

Fig. 3.2 Diagrammatic representation of a structural model of Silica Springs allophane. (a) Possible 1:3 Al-for-Si substitution in tetrahedral sheet. (b) Fragment of curved 1:1 aluminosilicate with incomplete octahedral sheet (from Childs et al. 1990).

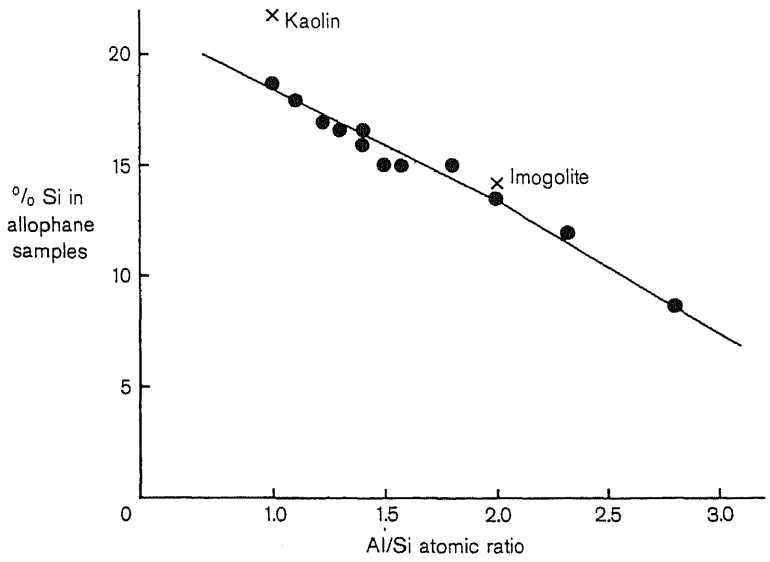

Fig. 3.3 Si content of allophanes of various Al/Si atomic ratio (from Parfitt & Wilson 1985).

Si-rich allophanes (Al:Si ≈1.0) have different infrared spectra from those of Al-rich allophanes (the Si-O stretching band occurs at a higher frequency — 1020 cm^{-1} — and the 348 cm^{-1} band is much weaker), indicating that some of the silicate is polymerized (Parfitt 1990a). NMR spectra also show the presence of polymerized silica, together with orthosilicate. The Al appears to be present in mainly octahedral sites, with some in tetrahedral sites. As with Al-rich allophanes, this Al-octahedral layer provides the structural framework for Si-rich allophanes and is linked to silicate polymers (Parfitt 1990a). Soil allophanes with Al:Si ratios between 1 and 2 have infrared spectra showing the presence of proto-imogolite (2:1) together with the polymerized silicate (1:1) structure. Such allophanes have been interpreted as mixtures of Al-rich and Si-rich allophanes, either as mixed allophane particles or as mixtures of structures within the particles, or both (Parfitt 1990a).

Stream deposit allophanes have Al:Si ratios in the range 0.9 to 1.8 and their structure differs from those of soil allophanes. The so-called Silica Springs allophane, found in the stream bed below the vents of Silica Springs on Mt Ruapehu, is the major New Zealand example of this type of allophane. Childs et al. (1990) suggested that a Silica Springs allophane primary particle consists of a tetrahedral sheet, with a curvature corresponding to a diameter of about 2-3 nm, and containing one Al for every three Si (Fig. 3.2). Excess Al is bound octahedrally (probably on the inside of the curved surfaces) to the apical O of the tetrahedra, and to OH and H_2O groups. In some cases the curvature may lead to the formation of more or less complete hollow spherules, usually manifest as globular aggregates. Thus, Childs et al. (1990) suggested that in Silica Springs allophane, the Si(Al) tetrahedral sheet forms the framework. This structure contrasts to the proposals outlined above for Al- and Si-rich allophanes in which the Al octahedral sheet forms the framework. Silica Springs allophane does not precipitate until the pH of the stream reaches 5.9, and this indicates the initial presence of tetrahedrally coordinated Al species (Al^{iv}), especially $Al(OH)4^-$, in solution (Childs et al. 1990).

The distinctive and very reactive properties of allophane are controlled by the structure, shape and small size of the allophane particle, the high surface area, and the chemical groups present at the surface, -O, -OH, and -OH_2 groups. The pH dependent charge, interaction with organic matter, phosphate and sulfate adsorption, and physical properties associated with allophane, are summarised by Parfitt (1990a). Further information, especially on the properties of Andisols, is reviewed in Theng (1980), Allbrook (1983), Neall (1984), Wada (1985), Mizota & van Reeuwijk (1989), Parfitt & Clayden (1991), and Soil Survey Staff (1992).

In the field, allophane deposits may be identified by the characteristic greasy feel, and by various chemical tests such as NaF (Fieldes & Perrott 1966) or toluidine blue (Wada & Kakuto 1985). The fluoride test is not entirely specific for allophane because fluoride may also react with Al-humus complexes (and $CaCO_3$). Synthetic allophanes, which are free of iron, have a whitish colour but natural soil allophanes are usually associated with ferrihydrite or goethite, or both, and are probably coloured by these iron oxides (Parfitt 1986). The Silica Springs allophane has a very low Fe content and so the material is a creamy-white colour. In the laboratory, infrared spectroscopy may be used for allophane identification under certain conditions (Parfitt 1990a), but the main method is by dissolution in acid oxalate reagent (Parfitt & Wilson 1985; Parfitt & Childs 1988; Mizota & van Reeuwijk 1989). Imogolite also dissolves in acid oxalate, but this is usually a minor constituent in New Zealand soils. The values of silicon (Si*o*) and aluminium (Al*o*) extracted by acid oxalate are used together with the value of aluminium extracted from Al-humus complexes by pyrophosphate (Al*p*) (Parfitt & Wilson 1985; Fig. 3.3). The Al:Si atomic ratio of the allophane is calculated from (Al*o*-Al*p*)/Si*o*, and the amount of allophane in the sample is estimated by multiplying Si*o* by an appropriate factor (Table 3.3). Quantities ranging from 0.5% to 60% allophane have been measured using this method (e.g. Childs & Parfitt 1987; Parfitt 1990a). The Al:Si ratio of allophanes in New Zealand soils ranges from 0.4 to 4.0 (Fig. 3.4a), the median being 1.9, very close to the value for imogolite-like allophane which is used as a reference point in the series (Parfitt & Kimble 1989). Kodama & Ross (1991) have recently reported that alkaline Tiron dissolution treatment is as effective as acid oxalate in the dissolution of allophane, imogolite, and poorly crystalline Fe oxides.

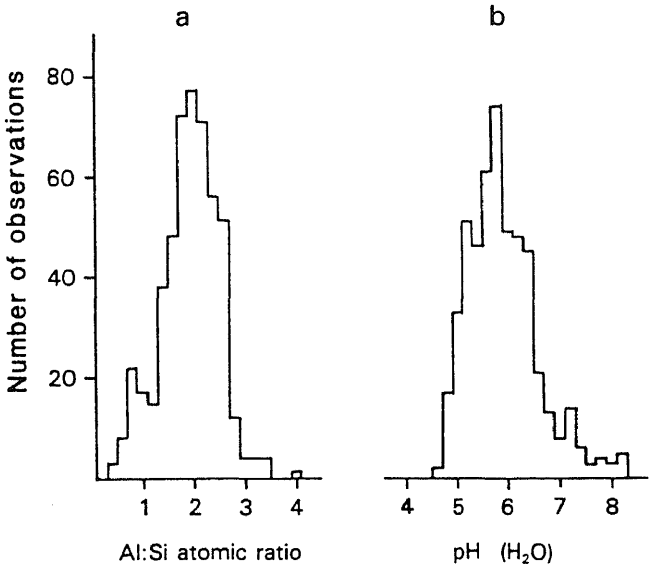

Fig. 3.4 Histograms of (a) allophanic Al/Si atomic ratios, and (b) pH(H_2O) of allophanic horizons, in <2 mm material in New Zealand soils (512 samples; from Parfitt & Kimble 1989). The samples with Al/Si values <1.0 are from glass-bearing alluvial soils weathering in an ustic moisture regime; samples with Al/Si ratios >3.0 are from non-volcanic soils that have been podzolized (both groups contain only ≈2% allophane). Most samples occur in soils with an udic moisture regime and a mean annual rainfall between 800—2500 mm; samples with pH >7.4 occur in soils in an ustic moisture regime and the allophane is usually the Si-rich type.

Table 3.3 Al:Si atomic ratios of allophane and the Si$_o$ multiplying factor to use to estimate allophane (from Parfitt 1990a)

Al:Si	Factor	Al:Si	Factor
1.0	5	2.5	10
1.5	6	3.0	12
2.0	7	3.5	16

Allophane formation and weathering in tephras and associated soils in New Zealand were comprehensively reviewed by Lowe (1986), who stated that the type of clay and rate of formation are controlled chiefly by macro- and micro-environmental factors together with the mineralogical and physicochemical composition of the parent deposits (e.g. andesitic versus rhyolitic tephra), and that the effect of time is subordinate to these factors. In essence, the important environmental factors are the activity of silicic acid in the soil solution, the availability of Al species, and the opportunity for co-precipitation. These are controlled by the leaching regime, the organic cycle, and pH (Birrell et al. 1977; Parfitt et al. 1983, 1984; Shoji & Fujiwara 1984; Parfitt 1990b; Farmer et al. 1991). In turn, these factors are influenced by climate (especially rainfall), drainage, vegetation, tephra thickness, depth of burial, and the frequency of additions of fresh tephra (Fig. 3.5).

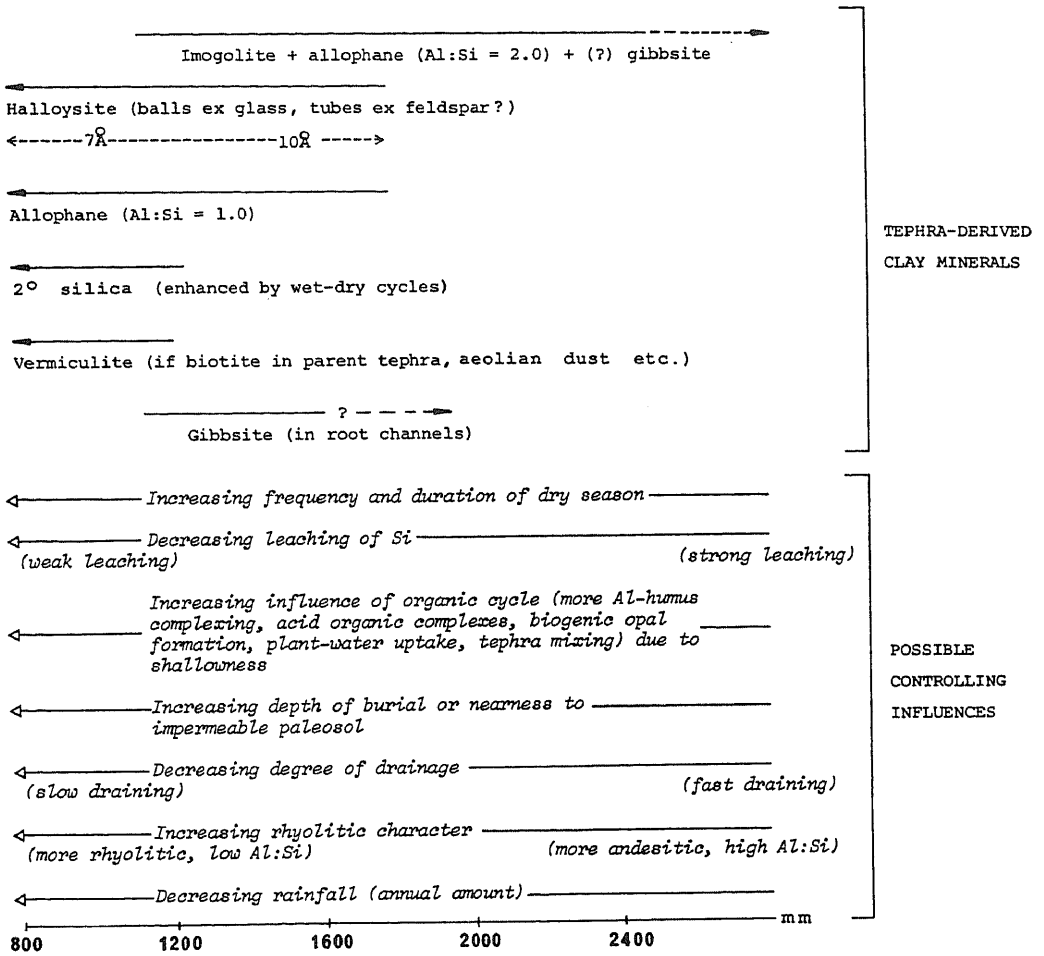

Fig. 3.5 Weathering sequence for tephras in the Waikato region, New Zealand, showing clay mineral formation and persistence with respect to various environmental controls other than tephra age. The clay minerals increase in amount (in direction of solid arrows) as a function of the environmental influences (open arrows). Part of the diagram is based on Parfitt et al. (1983) (after Lowe 1986).

Allophane (chiefly Al:Si ≈2) can persist in tephra beds for hundreds of thousands of years under favourable conditions (e.g. Kirkman 1980a; Stevens & Vucetich 1985; Lowe 1986) and is therefore a mineral relatively stable (metastable) or easily formed in soils (Parfitt 1990a). Imogolite is also relatively stable, and stability diagrams (Fig. 3.6) show that it is more stable than halloysite over a wide range of silica activity (Percival 1985). Halloysite is more stable than imogolite only at high silica activity, both minerals being less stable than kaolinite, however. The stability line for Al-rich allophane (Al:Si ≈2) is parallel to that of imogolite, and is probably in a similar position, i.e. its stability is similar. There is some evidence that this allophane might be more stable than imogolite (Farmer et al. 1991a).

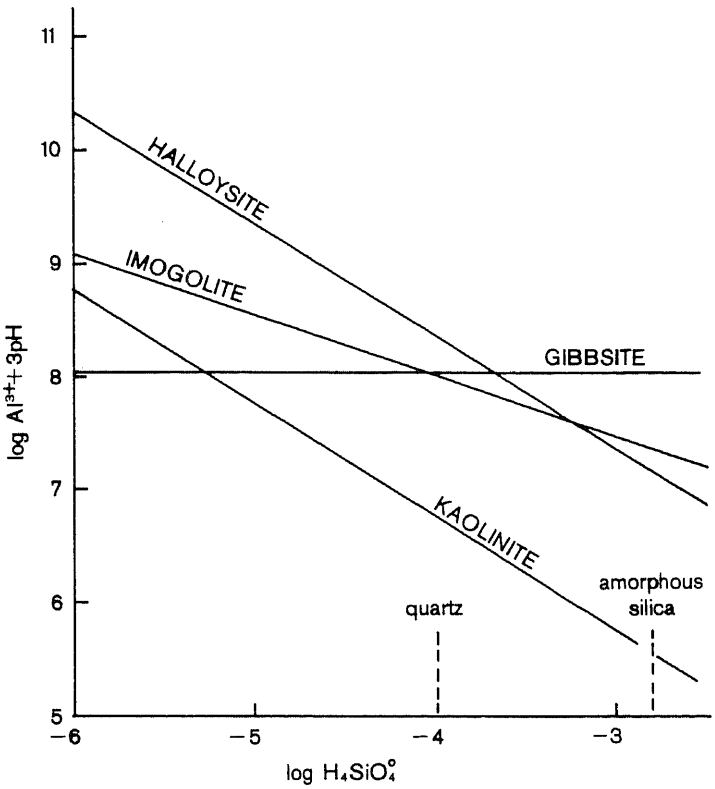

Fig. 3.6 Stability of kaolinite, halloysite, and imogolite compared with that of gibbsite (from Percival 1985).

In general, allophane forms from the weathering of glass in tephra at pH(H_2O) values between 5 and 7, a pH of at least 4.8 being required for allophane to precipitate (Fig. 3.4b). Parfitt & Kimble (1989) demonstrated that the Al-rich allophanes, which predominate in New Zealand tephras and soils, tend to form in acid, well drained soils where the Si in soil solution is likely to be low (about 1 to 3 g/m^3), and that the Si-rich allophanes, and halloysite, tend to form in environments where Si in soil solution is likely to be high (about 6 to 20 g/m^3). The importance of silica activity in governing the formation of allophane or halloysite, as predicted in earlier studies by Parfitt et al. (1983, 1984) and Lowe (1986), was confirmed by Singleton et al. (1989). They showed from study of a soil drainage sequence (see Stop 5, Day 1) that halloysite forms, directly from glass, in preference to allophane when Si in soil solutions exceeds 10 g/m^3, whereas allophane forms where Si is less than this. A previous idea, that allophane weathers to halloysite with time because it often occurs in older tephras (e.g. Kirkman 1975), has been largely replaced by the models of silica activity (Lowe 1986; Parfitt 1990a). Moreover, for imogolite-like allophane to alter to halloysite would require rearrangement of atomic structures (the allophane needs to turn 'inside out') and this can only take place by dissolution and reprecipitation (Parfitt 1990a). Kirkman & McHardy (1980) and Lowe (1986) demonstrated that higher silica activity is more likely in rhyolitic than in andesitic tephras, the latter being inherently less siliceous (e.g. andesitic glass SiO_2:Al_2O_3 ≈3.8, rhyolitic ≈6.4; Lowe 1986).

From a study of the kinetics of clay formation in relatively weakly weathered tephra-derived paleosols, Hodder et al. (1990) suggested that allophane formation occurs in a two-stage process: an initial hydration of volcanic glass via a parabolic rate law, followed by a first-order (linear) reaction to produce the clay minerals. Indirect confirmation of this model comes from the activation energies calculated from the rate constants, suggesting that the process of formation of Al-rich allophane (or imogolite) is diffusion controlled — i.e. the rate of reaction is proportional to the rate at which the reactants can arrive and depart — whereas the rate of formation of Si-rich allophane is controlled by the chemical processes at the site of reaction.

Because Si in soil solution is controlled by variables such as drainage, rainfall, and tephra composition, tephra sequences and paleosols may contain varying proportions of allophane and halloysite (as will be seen at some stops on Days 1 and 2 of the tour). Attempts have been made to relate such stratigraphic variations in mineralogy to the influence of past environments, especially paleoclimate, so that allophane-rich beds are considered to have weathered under warm, moderate to high rainfall conditions (hence promoting strong Si leaching) during interglacials whereas halloysite-rich beds weathered under cold, low rainfall conditions (hence promoting weak Si leaching) during glacials (Birrell & Pullar 1973; Birrell et al. 1977; Parfitt et al. 1983; Stevens & Vucetich 1985; Green 1987). This concept is supported by Alloway et al. (1992a) who recently demonstrated that glacial-interglacial climatic change had influenced the weathering characteristics and mineralogy of Andisols in Taranaki (using changes in Al/Si ratios and variations in 15-bar water retention as a measure of drying history). However, the weathering model in Fig. 3.5 emphasises that many site-specific environmental conditions and compositional factors, rather than just rainfall for example, may control the concentration of Si in solution and its distribution through the profile, and provide circumstances for either its loss, its precipitation, or its co-precipitation with available Al. Because these many possible controlling influences have operated both in the past and the present, then studies relating tephra clay mineralogy to paleoenvironment must be interpreted cautiously (Lowe 1986).

Imogolite

Imogolite is a hydrous aluminosilicate that was first described in a Japanese soil known as 'imogo', derived from glassy tephra. It appears in electron microscopy as smooth and curved threads several micrometres long and arranged into bundles ≈10 to 30 nm across (Wada 1989). The threads comprise fine tubular units with inner and outer diameters of about 1.0 and 2.0 nm, respectively (Fig. 3.1), and an external surface area of about 1450 m^2/g (Theng et al. 1982). Cradwick et al. (1972) described the tubular units as paracrystalline because the atomic

arrangement in its tube unit is regular despite some randomness involved in the arrangement of tube units to form the thread. The tubes comprise a single octahedral (gibbsite-like) sheet in which the OH groups on one side lose protons and bond to Si atoms, forming an inner surface of O_3SiOH groups (Schulze 1989). Because Si-O bonds are shorter than Al-O bonds, the unit is forced to contract to form a cylinder with a circumference of 10 to 12 modified gibbsite unit cells (Fig. 3.1; Parfitt 1980). As described previously, the structure of Al-rich allophane (Al/Si ≈2.0) is related to that of imogolite, hence it was originally named 'proto-imogolite' or 'imogolite-like allophane' (Table 3.2).

Imogolite, with an ideal composition of $SiO_2.Al_2O_3.2.5H_2O(+)$, is commonly found in association with allophane and has similar chemical properties (Wada 1989). It may be formed from volcanic glass or pumice either by precipitation (neoformation) from weathering solutions low in silica activity, presumably by a diffusion-controlled process (Hodder et al. 1990), or by transforming from allophane through desilication (Wada 1989). It is more stable than halloysite over a wide range of silica activities (Fig. 3.6); halloysite could in principle dissolve to precipitate imogolite under intense leaching conditions (Percival 1985). Imogolite, as with allophane, also occurs in non-volcanic materials through strong leaching or podzolization (e.g. Childs et al. 1983).

Together with allophane, imogolite can be estimated by the acid oxalate dissolution method described previously, but electron microscopy is usually necessary to positively identify the characteristic imogolite threads. Infrared spectroscopy is also used. Imogolite is usually present in many New Zealand tephra-derived soils, but in small amounts (e.g.Yoshinaga et al. 1973; Kirkman 1975, 1976a; Parfitt et al. 1982; Lowe & Nelson 1983; Childs & Parfitt 1987).

Allophane-like constituents

These are defined as SRO aluminosilicates distinguishable from allophane according to their dissolution by citrate-dithionite and 20 g L^{-1} Na_2CO_3 solution (Wada 1989). However, their existence is controversial. Parfitt et al. (1980) suggested that they may represent the Fe- or Al-rich part of the allophane wall or other defects, rather than a separate structure, and Wada (1980, 1989) suggested they are possibly polymeric hydroxy-aluminosilicate cations or partly dissolved allophane. They have not been reported in New Zealand tephras except by Mizota (1982) who concluded that 'allophane-like constituents' and 'hydrous alumina', but not allophane, were present in a basaltic tephra-derived soil in Northland. Parfitt & Childs (1983), however, suggested that Mizota's 'allophane-like constituents' could be explained as partially dissolved proto-imogolite allophane together with ferrihydrite and hematite.

Ferrihydrite

Ferrihydrite was recognised as a mineral by the International Mineralogical Association in 1975 and is a hydrous iron oxide of short-range order. Because of its SRO, it gives broad XRD peaks — usually up to five or six in natural ferrihydrite, which may be considered (relatively) 'well ordered', down to those which show only two peaks and which may be called 'two-line ferrihydrite' or 'protoferrihydrite' (Childs 1992a). Previously, terms such as 'amorphous ferric hydroxide' and 'iron oxide gel' have been used for ferrihydrite. Natural ferrihydrites commonly contain up to ≈9% Si (typically ≈5%) and the role and location of silicate is still a subject of debate and research (Childs 1992a; Parfitt et al. in press).

Various formulae for ferrihydrite have been proposed, including $5Fe_2O_3.9H_2O$, $Fe_5O_8.4H_2O$, and $Fe_2O_3.2FeOOH$ (Parfitt et al. in press). Its structure is not as well understood as those of other iron oxide minerals but most evidence indicates hexagonal-close-packed layers of O^{2-}, OH^-, and H_2O with Fe(III) occupying octahedral positions and giving a trigonal unit cell, with a = 0.508 nm and c = 0.94 nm (Schwertmann & Taylor 1989; Childs 1992a). Eggleton & Fitzpatrick (1988) proposed a different structural model incorporating ≈35% of total Fe in tetrahedral positions.

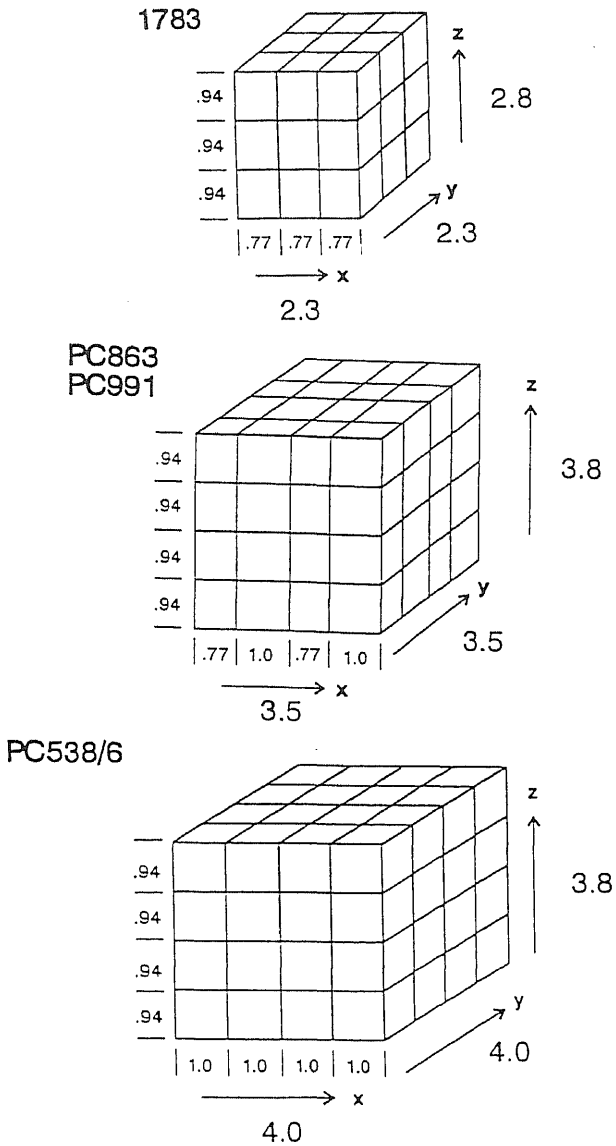

Fig. 3.7 Proposed models of (siliceous) ferrihydrite particles showing crystalline domains. The diagrams illustrate domain and particle sizes (in nm) consistent with low-angle XRD and infrared data for ferrihydrite. The omission of corner domains would produce a primary particle tending towards a spherical shape (from Parfitt et al. in press). Samples: 1783 from paddy race, Aso-Dani in Mt Aso caldera, Japan; PC538/6 & PC863 from streambed on Mt Egmont; PC991 from streambed on Mt Ruapehu.

More recently, Parfitt et al. (in press) have developed a new model using low angle XRD of four naturally-occurring ferrihydrite samples. They determined that the mean diameter of primary particles decreases from 4.1 nm to 2.5 nm as the domain size in the xy-plane decreases from 1.0 nm to 0.77 nm (Fig. 3.7). The Si_o content increases from 4.1% to 6.1% as both domain and particle sizes decrease, but other factors (e.g. pH, speciation, and rate of precipitation) are likely to be important in influencing particle size (Parfitt et al. in press). It is suggested that most silicate bonds to, and bridges, the surfaces of the domains (i.e. mainly within the interior of the particles). The relatively few silicate anions exposed on the particle exterior would be readily accessible for exchange (e.g. with phosphate), but exchange with those in the interior would be restricted. Although Si is evidently not an essential structural component, its presence seems to favour the formation of ferrihydrite instead of more crystalline iron oxides, and, in some cases, the formation of poorly-ordered ferrihydrite at the expense of relatively well-ordered forms (Childs 1992a). The simple Parfitt et al. (in press) model helps explain the apparent stability that silicate confers on ferrihydrite.

Primary ferrihydrite particles are very small and have a high specific surface area (between 200 and 500 m^2/g) and adsorptive capacity, and a variable charge surface (Childs 1985, 1987a, 1992a). Electron microscopy shows that the primary particles are spheroidal with diameters ranging from ≈2 to 7 nm. This combination of reactive surface groups and high specific surface area makes ferrihydrite an important soil component analogous to allophane. Ferrihydrite influences colour (it is a strong pigmenting agent, usually 5YR-7.5YR), anion adsorption, aggregation, and other properties. Even at concentrations of only 1-2%, ferrihydrite can represent most of a soil's specific surface area (Childs 1992a).

Ferrihydrite in soils is difficult to identify and quantify using conventional mineralogical techniques because of the relatively weak and nondescript signals it gives unless it is present in realtively high concentrations (>5-10%). Other techniques, notably differential XRD, Mossbauer spectroscopy, and dissolution chemistry have proved more successful. Acid-oxalate extractable iron (Fe_o), with a multiplier of 1.7, is currently the best available indicator of the presence and quantity of ferrihydrite in a soil, though it cannot be regarded as a means of positive identification alone (Parfitt & Childs 1988; Childs 1992a).

Ferrihydrite is a common component of tephra-derived soils and spodosols, of soils undergoing rapid early weathering, of soils containing soluble silicate or organic materials that inhibit the formation of more crystalline iron oxides (i.e. stabilise ferrihydrite), of iron pans or placic horizons, and of soils subject to periodic reduction and oxidation (Childs 1992a). Because it is thermodynamically unstable in relation to hematite and goethite, ferrihydrite is likely to be replaced by these crystalline oxides over long periods of weathering. In New Zealand, ferrihydrite occurs in a wide range of soils in small amounts, including various tephra-derived soils, ranging from 0.5% to 8.0% (weighted) (e.g. Childs 1987a; Green 1987). However, it also occurs in drainage ditches and seepages, with the best deposits occurring in streams on the slopes of the andesitic stratovolcanoes of Mts Ruapehu (Childs et al. 1982) and Taranaki (Egmont) (Childs et al. 1986, 1990). We will see a good examples of ferrihydrite in seepage and stream deposits by the Waikato River in Hamilton City at Stop 4, Day 4.

Halloysite

Halloysite is a kaolin subgroup 1:1 layer-structured aluminosilicate minerals of the same ideal composition as kaolinite (Dixon 1989). It occurs mainly as spherical, roughly concentrically-banded particles, or as tubes, scrolls, or curled flakes (Churchman & Carr 1975). Kirkman (1981a) described these morphologies in New Zealand tephras as squat and elongate ellipsoids. Platy, tabular, and disk-shaped halloysite has also been reported (Kirkman 1977).

Halloysite can occur in two phases, one with two interlayer water molecules per formula unit (hydrated or 1.0 nm halloysite) and the other without (dehydrated or 0.7 nm halloysite) (Churchman & Carr 1975). These phases represent end members of a continuous series of hydration states in which average interlayer water contents encompassing all values between 0

and 2 molecules per unit cell are possible (Churchman et al. 1972). Dehydration, accompanied by shrinkage, occurs through an interstratification in which there is partial segregation of the two basic layer types (Churchman et al. 1972; Lowe & Nelson 1983). The layer of water lessens the interlayer restraining force between adjacent layers in halloysite so that they typically curl along the *b* axis (Churchman 1986). Halloysite can be distinguished from kaolinite based on the relative abilities of these minerals to intercalate polar organic compounds such as formamide — the prior intercalation of halloysite with a water monolayer ensures easier intercalation than in kaolinite (Churchman & Theng 1984; Churchman et al. 1984; Theng et al. 1984). The existence of so-called 'embryonic halloysites' with poorly ordered characteristics (Wada et al. 1987) is disputed (Parfitt & Churchman 1988).

Halloysites have much larger unit particles than allophane (≈300—600 nm cf. 4 nm) and their properties and reactivities relate to this particle size as well as morphology, a relatively high degree of crystallinity, and a Si-O-Si outer surface in contrast with the Al-OH-Al surface of Al-rich allophanes (Theng et al. 1982). They are usually identified quantitatively by XRD (typically in conjunction with the formamide test) and DTA methods, aided by electron microscopy and occasionally infrared spectroscopy (e.g. Lowe & Nelson 1983; Parfitt & Wilson 1985; Churchman 1986; Dixon 1989). The degree of crystallinity of halloysite may be gauged partly from the sharpness of the 0.7 and 1.0 nm peaks, but broad peaks, indicative of relatively poor crystallinity, may also reflect the effect of partial dehydration (interstratification) of the halloysite (Lowe & Nelson 1983).

The different morphological forms of some halloysite may relate directly to primary mineralogy, spherical halloysite possibly originating from glass, tubular halloysite from feldspar, and by various possible mechanisms (Kirkman 1981b; Lowe 1986; Nagasawa & Noro 1987). More recent work by Soma et al. (1992) indicates that particle morphology is apparently influenced by structural Fe content. The long tubular halloysite has very little structural Fe, and its concentration tends to increase with the proportion of non-tubular particles in the samples. The spherical halloysite has the most structural Fe which, however, does not appear to influence particle shape directly. X-ray photoelectron spectroscopy indicates that Fe substitutes for Al in octahedral positions in approximately 1:2 proportion. Halloysite layers within a crystal are generally inhomogenous in composition. Individual halloysite crystals are probably built up like 'onion skins' in that surface layers would be enriched or depleted in Fe depending on the chemical environment in which crystal growth occurs (Soma et al. 1992).

In central North Island, halloysite is often the dominant clay mineral constituent in deeply buried paleosols on strongly weathered Pleistocene tephras, such as the Hamilton Ash, Kauroa Ash, and New Plymouth ash beds (e.g. Hogg 1974; Salter 1979; Kirkman & Pullar 1978; Kirkman 1980a, 1980b, 1981a; Stevens & Vucetich 1985). It rarely occurs in significant amounts in tephra horizons at or near the land surface. Where it does, the soils are either poorly drained (i.e. have a 'stagnant' moisture regime) or are typically strongly weathered and possibly exhumed with relict halloysite derived either from formation at depth due to a burial (or age) effect, or from changes in surface weathering conditions (Lowe 1986). It typically occurs in varying amounts in tephras and associated paleosols older than about 10 to 15 ka and usually at depths of a metre or more below the modern land surface (e.g. Birrell & Pullar 1973; Kirkman 1975, 1976a; Parfitt et al. 1983; Lowe 1986; Green 1987). McIntosh (1979, 1980), however, showed that authigenic halloysite (both spheroidal and tubular) can form by modern processes in siliceous tephra deposits aged as young as 1850 years buried at a depth of ≈2 m. He demonstrated that the halloysite formation at this depth was due to resilication from a silica-rich solution — lysimeter leachate SiO_2:Al_2O_3 mole ratios were ≤≈1.0 in surface horizons but ≈2.0 at depth. This work agrees with observations elsewhere that halloysite can form rapidly and directly from glass (e.g. Dixon & McKee 1974), is thermodynamically more stable than imogolite when Si in soil solution is high (Fig. 3.6), and supports the Si activity (and drainage) models of Parfitt et al. (1983, 1984), Lowe (1986), and Singleton et al. (1989) described earlier. It also emphasises the effect of tephra overburden in determining the availability of silica in solution (e.g. Wada 1989) and the tendency of halloysite XRD peaks to become sharper and better defined with increasing depth (Kirkman 1975, 1980a; Lowe & Nelson 1983). Wada (1980) suggested that because the greatest amounts of allophane and imogolite seem to coexist

with the smallest particles of halloysite, then the halloysite may be a recrystallisation product of resilication of (dissolved) allophane and imogolite.

Churchman & Gilkes (1989) and Churchman (1990) presented evidence suggesting that halloysites appear to transform to *kaolinites* with increasing weathering, and that kaolinite occurs in upper horizons of several tephra-derived soils in New Zealand. Similar occurrences, generally small in quantity, are reported by Parfitt et al. (1981) and Mizota (1982), but are rare in comparison with halloysite. The occurrence of b-axis disordered kaolinite 'books' and micaceous kaolinite in some of the strongly-weathered Kauroa and Hamilton Ash beds, respectively, is reported by Salter (1979) and Shepherd (1984) (see Stop 3, Day 1). Kaolinite is also associated with hydrothermal alteration in active or recently active thermal areas of TVZ (e.g. Wells et al. 1985; Simmons et al. 1992; see Stop 1, Day 3).

Silica polymorphs

Clay fractions in New Zealand tephras and associated soils often contain silica in various forms including quartz, cristobalite, tridymite, volcanic glass, (biogenic) opaline silica, amorphous silica, silica 'flakes', and diatoms (e.g. Kirkman 1975, 1976a, 1981b; Henmi & Parfitt 1980; Parfitt et al. 1983; Shepherd 1984; Stewart et al. 1984, 1986; Stevens & Vucetich 1985; Weatherhead 1988; Hosono et al. 1991), sometimes in significant amounts. (Feldspar, a tectosilicate, is also reported as a minor residual constituent.) It is likely that most of these components originated from the parent materials i.e. they are essentially residual 'primary' minerals. Studies, including oxygen isotope analysis, of quartz in soils derived from basaltic and andesitic tephras have demonstrated that most of it is aeolian in origin (e.g. Stewart et al. 1984, 1986; Alloway et al. 1992b). Similarly, oxygen isotope analysis of well-ordered cristobalite indicates that it is likely to be of primary (high temperature) origin (e.g. Mizota et al. 1987), in contrast to a secondary origin as suggested by Lowe (1986). Nevertheless, Drees et al. (1989) indicate that silica minerals (e.g. amorphous silica) may synthesise in soil environments through neoformation from soluble silica or from in situ dissolution-reprecipitation transformation reactions.

Opaline silica (or plant phytolith) formation through uptake of Si in solution by living plant cells is favoured in near-surface tephras by the supersaturation of silica by evaporation and plant evapotranspiration, an abundant supply of silica, wet-dry cycles, and the suppression of Al activity by humus accumulation (Henmi & Parfitt 1980; Parfitt et al. 1983; Lowe 1986; Wada 1989; Huang 1991). Identification of different types of phytoliths is being used to infer paleovegetation (e.g. Hoson et al. 1991; Childs 1992b). Although probably resistant, the biogenic silica may be redissolved and either leached or precipitated with available Al to form Si-rich allophane, halloysite, or amorphous silica or silica 'flakes' or 'plates'. For example, Kirkman (1981b) reported the presence of such flakes associated with halloysite in rhyolitic tephras and suggested that they precipitated as excess Si from solution during dry periods. In contrast to oxalate extraction, Tiron dissolution treatment (Kodama & Ross 1991) removes opaline silica, and so the difference between silica extracted by oxalate and Tiron could be used as a measure of opaline silica quantity.

Humus and humus complexes

Extraction and infrared spectroscopy analysis indicate that humus evolves from forms with a very low complexing ability for Al and Fe to forms that complex Al and Fe in the humified organic-bearing (A) horizons of soils, both surficial and buried (Wada 1980). The organic matter is probably adsorbed onto allophane surfaces by ligand exchange (Parfitt 1990a; Huang 1991). Such Al- and Al/Fe-humus complexes are very stable and are an important feature of Andisols (e.g. Churchman & Tate 1987; Parfitt & Clayden 1991). That hydroxy Al-humus complexes occur in some tephra-derived soils in which allophane and imogolite are largely absent suggests that its formation inhibits the formation of allophane and imogolite through

competition with orthosilicic acid for the coordination sites of Al released by weathering (Wada 1989). The Si/Al ratio of the precipitates decreases with increasing organic C% (Huang 1991).

The Al-humus complexes are typically identified by selective chemical dissolution and difference infrared spectroscopy or DTA. Al in humus complexes is estimated by pyrophosphate extraction (Al*p*) but pyrophosphate-extractable Fe should not be used to estimate Fe in humus complexes (Parfitt & Childs 1988).

The strikingly dark, deep A horizons characteristic of andic soils in Japan ('Kurobokudo'), thought to have developed under the influence of grasses, especially *Miscanthus sinesis* (Otowa 1986), are not generally evident in New Zealand. Yamamoto et al. (1989) found that Japanese andic soils contained much higher total organic and humic acid C contents than in New Zealand, and that humic acids extracted from the Japanese soils were blacker and apparently more humified; humic acids from the New Zealand soils were mostly of the B or P type, those from Japanese soils mostly of the A type. The reasons for these differences are likely to relate to differences in vegetation, parent materials, and climatic factors (Yamamoto et al. 1989; Hosono et al. 1991). For example, warm, wet summers and cool, dry winters are typical in Japan, whereas in New Zealand summers are generally warm but dry, winters cool and wet. Birrell et al. (1971) and Birrell & Pullar (1973) attributed the chemical properties of the organic matter in buried black horizons on three New Zealand tephras to decomposition of bracken fern rhizomes (*Pteridium aquilinum*).

Humus composition in buried tephra-derived soils undergoes some changes with age (Tsutsuki & Kuwatsuka 1989). Goh (1972) found that amino acids occur in buried paleosols in New Zealand tephras. Limmer & Wilson (1980) showed that such mineral bound amino acids were relict and proposed a dating method based on amino acid analysis. Kimber et al. (in press) successfully applied amino acid racemization to a tephra-loess-paleosol section at Tapapa — which will be examined at Stop 1, Day 2.

Gibbsite and crystalline iron oxides

Gibbsite [$Al(OH)_3$] is the most common Al hydroxide mineral in soils. It can form rapidly, coexisting with allophane and imogolite in young deposits, but is generally associated with older and strongly weathered deposits (Lowe 1986; Schulze 1989). In New Zealand tephras, both rhyolitic and andesitic, and young and old, it almost always occurs in only small or trace amounts, sometimes as root pseudomorphs (e.g. Hogg 1974; Salter 1979; Russell et al. 1981; Kirkman 1975, 1980a, 1980b; Parfitt et al. 1981, 1983; Lowe 1986). Two exceptions include 17% of the clay fraction of one andesitic bed in a strongly-weathered tephra sequence near Te Kuiti (Stevens & Vucetich 1985), and up to 22% of the clay fraction of a soil derived from Hamilton Ash near Pukekohe (Parfitt et al. 1981). More is usually found in weathered basalt-derived soils in Auckland and Northland where it may form nodules (e.g. Orbell et al. 1981; Mizota 1982). Such generally low concentrations of gibbsite in tephras have been explained either by unfavourable site conditions that minimise desilication (e.g. Kirkman 1980b) or by the presence of 'iron oxide gel' inhibitors (Kirkman & McHardy 1980). Hogg (1974) and Parfitt et al. (1983) suggested that Si removal by plants may account for the occurrence of some gibbsite in root channels (Fig. 3.5).

Crystalline iron oxides (i.e. excluding ferrihydrite which has SRO) in New Zealand soils usually include hematite, goethite, lepicrocite, maghemite, and magnetite, the last two being end members of a series (Childs 1987b). They are typically present as very fine particles evenly dispersed, or concentrated in discrete horizons or nodules. Even at low concentrations, iron oxides have a high pigmenting power and determine the colour of many soils (Schwertmann & Taylor 1989). They can usually be identified by conventional methods such as XRD but dissolution methods are widely used for quantitative work (Parfitt & Childs 1988). Dithionite extraction (Fe*d*) removes all iron oxide minerals from a sample except for coarse (sand-sized) grains which are likely to be primary in origin. As noted earlier, ferrihydrite is best estimated by oxalate extraction and so (Fe*d*-Fe*o*) is used to estimate the iron present in pedogenic, crystalline

iron oxide minerals, and is commonly reported in terms of Fe_2O_3 i.e. 1.43 x Fe value (Childs 1987b).

Concentrations, expressed as Fe_2O_3, in clays derived from tephra-derived soils in New Zealand range from 0.6% to 9.3%, the greatest amounts occurring in basaltic soils (10-18% occurs in soils developed on weathered basalt lava) (Childs 1987b). In some cases the iron oxides are identified as hematite and goethite, usually in small quantities (e.g. Kirkman 1975; Parfitt et al. 1981; Mizota 1982; Parfitt & Childs 1988). Lepidicrocite is rare (McQueen 1975; Kirkman 1980a).

2:1 and interstratified minerals

2:1 minerals include micas (including illite), vermiculite, smectites, and chlorites (Schulze 1989). They often occur as interstratified, or mixed-layer, minerals. Their origin in tephras has been controversial. Some Japanese studies suggested that they formed pedogenically from 'amorphous' minerals including K-enriched volcanic glass, but other explanations are more widely accepted now. The most favoured is the transformation of mafic minerals either from the primary tephra or from postdepositional contamination by aeolian accessions as loess or dust (Russell et al. 1981; Stewart et al. 1984, 1986; Lowe 1986). Other sources of 2:1 type clays include 'exotic' layered silicates incorporated into the tephra during eruption, or detrital 2:1 clays mixed into tephra deposits from underlying materials. Smectites may form from plagioclase under conditions of restrictive drainage (Lowe 1986).

In New Zealand, 2:1 and interstratified minerals are uncommon in tephras except in special circumstances. Vermiculite has been reported in a number of tephra-derived soils of both rhyolitic and basaltic composition — the occurrence is attributed to either aeolian accessions (basaltic soils) or to weathering of primary biotite (rhyolitic soils) (McIntosh 1979; Parfitt et al. 1981; Orbell et al. 1981; Mizota 1982; Lowe 1986). Mica and smectite (and a zeolite, mordenite) is reported in the hydrothermally-altered Rotomahana Mud (erupted during the 1886 Tarawera eruption) (Birrell & Pullar 1973; Kirkman 1976b; Vucetich & Wells 1978; Parfitt et al. 1981). Smectite, montmorillonite-vermiculite, and a K-depleted micaceous kaolinite intergrade are identified in several beds and paleosols of the Hamilton and Kauroa ash sequences (Hogg 1974; Salter 1979; Parfitt et al. 1981; Lowe & Nelson 1983; Shepherd 1984), and vermiculite-chlorite and kaolinite-montmorillonite interstratified minerals occur in small amounts in a Northland basaltic soil (Mizota 1982).

4. DAY 1: AUCKLAND—HAMILTON—ROTORUA

Outline of Day 1 (Tuesday 13 July)

8.00 - 8.30 am	Depart Travellers' International Hotel and travel to One Tree Hill, Auckland (15 km)
8.30 - 9.15 am	STOP 1 — View of basaltic volcanoes of Auckland
9.15 - 10.30 am	Travel to Te Kauwhata area (75 km)
10.30 - 11.00 am	STOP 2 — Morning tea near Te Kauwhata
11.00 - 11.30 am	Travel to Welch Road (Mangawara) via Ohinewai (27 km)
11.30 -12.30 pm	STOP 3 — 1 Ma sequence of tephra beds and paleosols (Mangawara)
12.30 - 1.00 pm	Travel to University of Waikato, Hamilton (40 km)
1.00 - 2.00 pm	STOP 4 — Lunch and group photograph at University of Waikato
2.00 - 2.15 pm	Travel to Ruakura Research Centre, Hamilton (2 km)
2.15 - 3.45 pm	STOP 5 — Allophane-halloysite volcanogenic soil drainage sequence, Ruakura, and afternoon tea
3.45 - 5.30 pm	Travel to Lake Plaza Hotel, Rotorua (110 km). Overnight stop.
	Dinner
	Evening free

The tour route (Fig. 4.1) takes us initially to One Tree Hill for a view of the multiple basaltic cones and explosion craters of Auckland, New Zealand's largest city (population ≈0.95 million). We then head south through South Auckland urban sprawl until climbing over rolling land and the Bombay Hills marking the South Auckland basalts (aged c. 0.5 to 1.5 Ma). The basalts are rarely soil forming, most being mantled with a series of distal tephra beds including Hamilton Ash from which commonly Humults are formed. These are used primarily for intensive horticultural production.

South of the Bombays we enter the Waikato region, a range-and-basin province with a patchy mantle of distal tephras. Occasionally following the Waikato River, we eventually arrive in Hamilton in the Hamilton Basin, marked by gently rolling, tephra-covered hills and alluvial plains and bogs. Here, and in other parts of the Waikato lowlands, the dominant land use is agriculture, particularly dairying, and horticulture. As we drive southeastwards towards Rotorua, the terrain beyond Cambridge tends to steepen in response to increased thickening of the underlying welded ignimbrite sheets. This landscape, except for eroded steeplands, is still mainly smooth and softened, being entirely draped in tephra deposits that generally increase in thickness and become successively younger and less weathered towards the Taupo Volcanic Zone (TVZ). The main soils are classed as Andisols. The final part of our route climbs over eroded ignimbrite sheets forming the Mamaku Plateau, and we then descend into the Rotorua Caldera to Rotorua.

STOP 1 — Basaltic volcanoes of Auckland, One Tree Hill

Auckland Volcanic Field

Auckland City, straddling a narrow isthmus separating the Manukau and Waitemata Harbours, is known both as the City of Sails and City of Volcanoes. A total of 48 eruptive centres have been identified in the Auckland Volcanic Field, all lying within a 360 km^2 area centred on One Tree Hill (Fig. 4.2; Kermode 1992). Most of the erupted material has a typical intraplate basalt chemistry (e.g. Table 4.1) and consists chiefly of alkali basalts and basanites derived from the mantle at depths of 75—125 km (Searle 1981; Heming & Barnet 1986; Kermode 1992). The dominant minerals are olivine, clinopyroxene (mainly titanaugite), plagioclase, and Fe-Ti oxides.

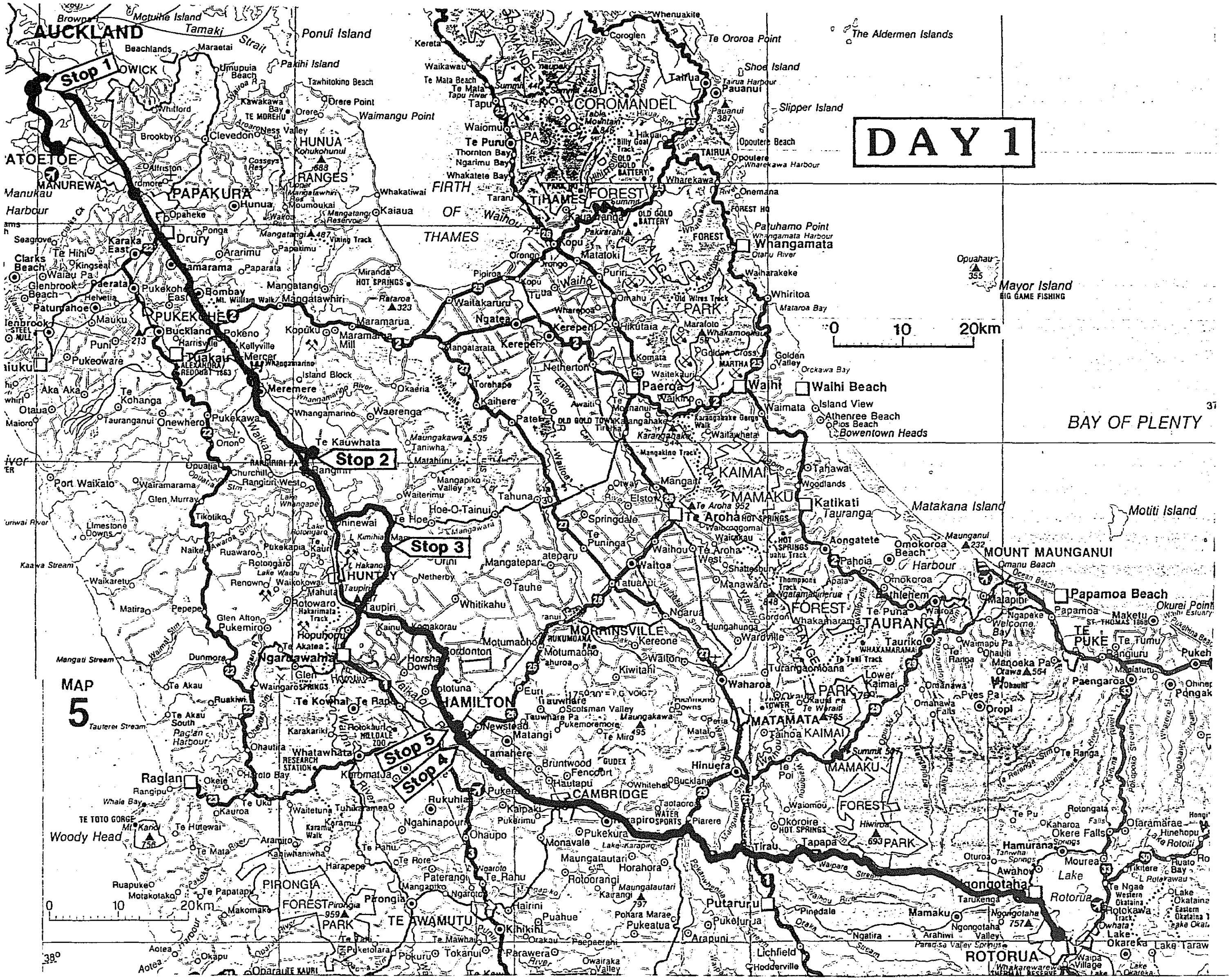

Fig. 4.1 Tour route and stops, Day 1.

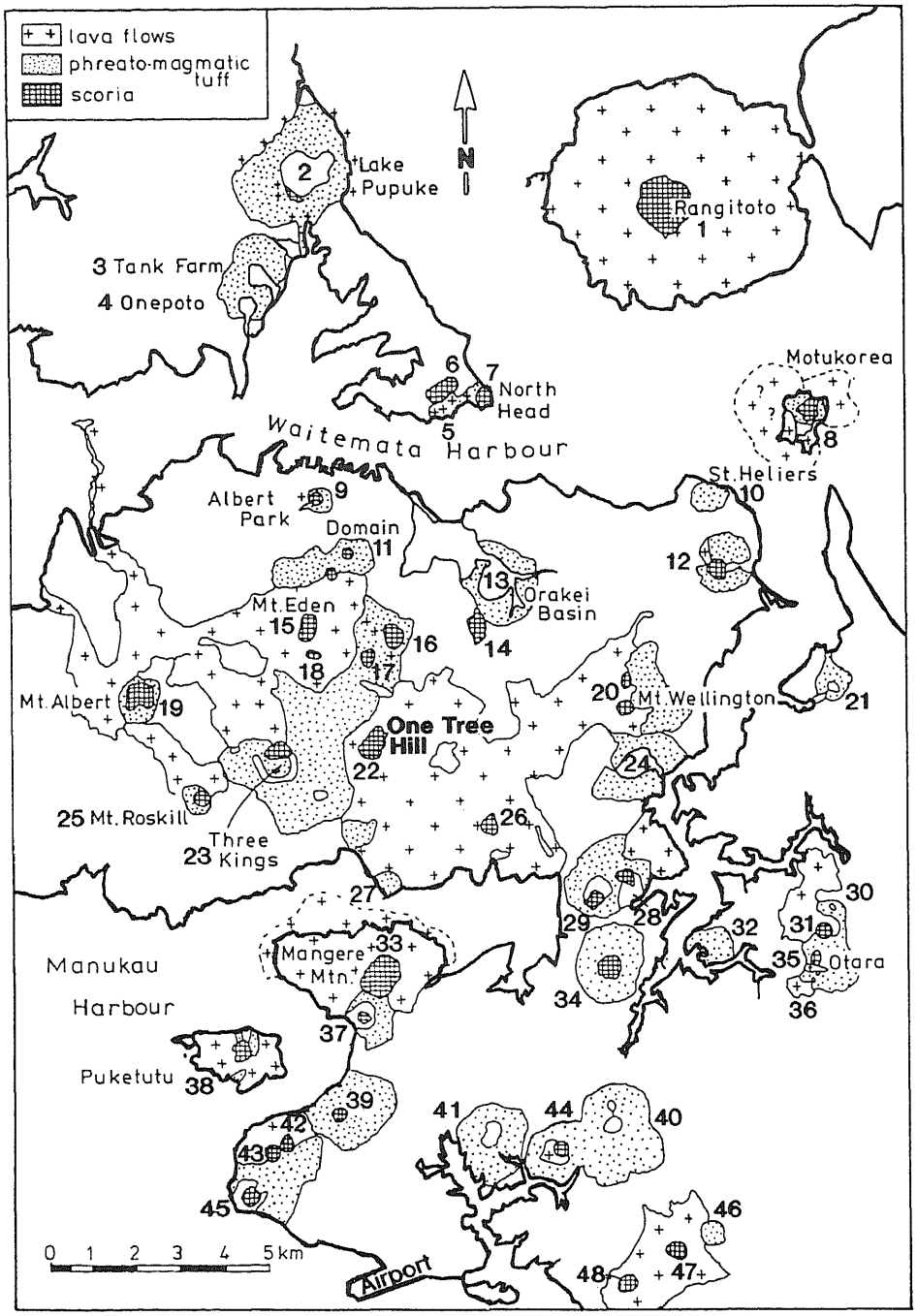

Fig. 4.2 The Auckland Volcanic Field and distribution of main rock types. Volcanoes not named on the map are: 5, Mt Victoria; 6, Mt Cambria; 12, Taylor Hill; 14, Little Rangitoto; 16, Mt Hobson; 17, Mt St John; 18, Te Pouhawaiki; 21, Pigeon Mtn; 24, Panmure Basin; 26, Mt Smart; 27, Hopua; 28, McLennan Hills; 29, Mt Richmond; 30, Styaks Swamp; 31, Green Hill; 32, Pukekiwiriki; 34, Robertson Hill; 36, Hampton Park; 37, Mangere Lagoon; 39, Waitomokaia; 40, Kohuora; 41, Pukaki; 42, Pukeiti; 43, Otuataua; 44, Crater Hill; 45, Maungataketake; 46, Ash Hill; 47, Manurewa; 48, Matakarua (after Heming & Barnet 1986 and Kermode 1992).

Eruptive activity of the Auckland volcanoes comprises either strongly explosive or quietly effusive to mildly explosive eruptions. The explosive eruptions produced craters (34 in total), some now inundated by the sea (e.g. Orakei Basin), and scoria cones (23 in total), whereas the effusive activity generated lava fields (15 in total) (Fig. 4.2; Kermode 1992). The largest volcano by far is the youngest, Rangitoto Island, which has produced about half of the field's total volume of erupted material.

Each of the eruptive centres of Auckland has apparently resulted from a single eruption, or short sequence of eruptions, that probably lasted no longer than about 10 years (Kermode 1992), although Newnham & Lowe (1991) showed that eruptions from Mt Wellington may have been several hundred years apart. The ages of activity, based mainly on radiocarbon and thermoluminescence [TL] dating, range from c. 140 ka (Lake Pupuke) to around 600 years (c. 1400 A.D.) for Rangitoto (Wood 1991; Kermode 1992; Nichol 1992), and the field is considered active. In fact, Wood (1991) suggests that an increased frequency and greater volume of eruptive material evident for the past 22 ka may mean that the Auckland field is finally 'getting into full swing'. Compositionally, Rangitoto eruptives mark a subtle but fundamental change in the field — the magma source was shallower and more melting occurred than in previous eruptions — and it is predicted that future eruptions may therefore be bigger and more frequent (I.E.M. Smith in Jamieson 1992). Studies of xenoliths included within the erupted material of Auckland volcanoes indicate an ascent time for magma of the order of hours to days, providing minimal warning time for the next event. Three seismograph stations, spaced about 40 km apart around Auckland, are used to monitor movement of magma (Kermode 1992).

One Tree Hill (Maungakiekie)

One Tree Hill is (volumetrically) the second largest volcano in the Auckland field and, at 183 m altitude, is a dominant topographic feature on the Auckland Isthmus. It is made up of a complex scoria cone (now 73 m high) produced by fire fountaining, and overlies extensive lava flows 60-80 m thick that cover an area of at least 11 km^2 (Kermode 1983, 1992). Analyses of these lavas are given in Table 4.1. The summit atops an elongated rim of the main oval-shaped crater which is 180 m across and 50 m deep; two breached horseshoe-shaped craters lie on the southwestern and southeastern sides of the cone (flanking the access road). The age of the volcano is estimated by TL dating at 16.5 ± 1.4 ka (Wood 1991).

Apart from those shallower than 35 cm, the soils on One Tree Hill (Papakauri hill soils) are probably Hapludands. Mean annual rainfall is 1270 mm; mean annual temperature is 14.5°C. Native vegetation was mixed broadleaved forest with podocarps and some kauri (Newnham & Lowe 1991). A brief description (from Cox 1973) from a site (R11/693765*) 15 m below the summit is as follows:

0-8 cm A	Dusky red fine sandy loam; friable; strongly developed medium and fine granular structure crushing to crumbs; many small basalt scoria fragments,
8-23 cm Bw	reddish brown stony sandy loam; friable; strongly developed medium nutty [subangular blocky] structure; many basalt scoria fragments,
23-46 cm BC	as above grading into weathering basalt scoria.

No analyses have been done at this site but a sample from the Bw horizon of a soil at nearby Mt Albert (Fig. 4.2), analysed using acid oxalate extraction, contains the following (%): Al*o*, 6.85; Si*o*, 3.43; Fe*o*, 5.11 (G.A. Spiers pers. comm. 1993). Assuming Al*p* is negligible, the Al/Si ratio is 2.0 and hence the allophane content (whole soil basis) is ≈24%.

---

* Grid reference based on the national 1000 m grid of the 1:50 000 topographical map series NZMS260.

Ferrihydrite content is very high at ≈8.7%. Other clay minerals likely to be present include hematite, vermiculite, gibbsite, and kaolinite, all of which are found in Papakauri soils in Northland (Orbell et al. 1981; Parfitt & Childs 1983; Childs 1987a,b).

One Tree Hill is the most extensively terraced of all Auckland's volcanoes — the crater walls as well as the outer slopes of the cone have been modified — and was the largest of the prehistoric Maori settlements. The earthworks provided housing sites and fortifications. From its summit, most features of the two harbours and the Hauraki Gulf (beyond Rangitoto) may be seen, as well as other distinctive cones including Rangitoto (260 m), North Head (66 m), Mt Eden (196 m) and The Domain to the north, Mt Wellington (135 m) to the east, Mt Albert (134 m) to the west, and Mt Mangere (104 m) to the south (Fig. 4.2).

The One Tree Hill area was gifted to the people of Auckland by Sir John Logan Campbell, whose tomb is at the summit between the obelisk, built in 1940 to commemorate the Maori race, and the pine tree (replacing, in c. 1880, the original totara which gave the hill its European name) (Clark 1989). On Sir John's tomb is engraved the Latin phrase 'Si monumentum requiris circumspice', which freely translates to 'If you seek a monument, look about you.' (This same phrase commemorates Christopher Wren in St Paul's Cathedral in London.) The phrase is also appropriate for the Maori initiative and industry which produced the terracing of the Auckland volcanic cones, as well as the still-existing forces responsible for their eruptions.

Table 4.1 Major and trace element analyses of One Tree Hill basalts (from Heming & Barnet 1986)

No.*	1	2	3	4
Wt%				
SiO_2	44.22	46.81	47.40	48.03
TiO_2	2.55	2.33	2.84	2.14
Al_2O_3	12.94	13.28	13.70	12.08
Fe_2O_3	7.84	5.87	2.57	2.95
FeO	4.60	7.00	9.10	9.00
MnO	0.19	0.18	10.11	10.92
MgO	11.71	9.52	9.40	9.59
CaO	10.19	9.27	3.04	3.10
Na_2O	3.20	2.95	0.59	0.63
K_2O	1.09	0.62	0.43	0.38
P_2O_5	0.53	0.48	0.18	0.16
H_2O-	0.00	0.00	0.22	0.46
LOI	0.42	1.38	0.00	0.00
Total	99.48	99.69	99.58	99.44
ppm				
Ba	357	298	218	211
Rb	19	8	10	11
Sr	503	385	416	423
Zr	197	171	159	167
V	279	215	186	209
Cr	373	301	351	331
Ni	251	218	243	215
Cu	84	79	79	73
Zn	92	109	91	96

*Samples: 1, 30665; 2, 30696; 3, 30672; 4, 30698

STOP 3 — 1 Ma sequence of Kauroa and Hamilton Ash beds and paleosols, Mangawara

Kauroa and Hamilton Ash beds

The Kauroa Ash Formation comprises a sequence of extremely weathered, clay-rich, rhyolitic tephra deposits recognised largely in the Waikato region (Ward 1967; Pain 1975; Salter 1979; Kirkman 1980a). The beds are quite variable in character, ranging from friable to extremely firm in consistence, and with many colours and structures. Much of the sequence has been removed by erosion — in the Hamilton Basin it is seldom thicker than 1-2 m, but in western Waikato it may be up to 9 m thick — and outcrops are sparse (Selby & Lowe 1992). At the type section near Raglan on the west coast, Salter (1979) identified 15 units, labelled K1 to K15 from bottom to top, respectively, and 10 associated paleosols. Stratigraphic interfingering of the Kauroa beds with K-Ar dated basalts of the Alexandra Volcanics enabled K1 to be dated at 2.3 Ma (Briggs et al. 1989). Unit K12 is tentatively correlated with Ongatiti Ignimbrite, which has an age of c. 1.2 Ma (Pringle et al. 1992). The youngest bed, K15, also known as Waiterimu Ash (Ward 1967), has not yet been dated directly but stratigraphic work in progress indicates that it may have been deposited around c. 0.95 Ma. Where preserved, K15 forms an extremely prominent paleosol, dark reddish brown in colour with usually a strongly developed blocky or prismatic structure. It represents the tiny remnants of an old land surface that apparently persisted for perhaps half a million years or so (Selby & Lowe 1992).

The Kauroa Ash beds probably represent distal airfall tephra and ignimbrite deposits from early TVZ eruptions, some probably deriving from Mangakino volcano (Fig. 2.2).

The Hamilton Ash Formation, separated from the underlying Kauroa beds by a well defined erosional unconformity, is a sequence of strongly weathered, clay-textured tephra beds and paleosols well represented in the Waikato-South Auckland regions (Ward 1967; Pain 1975). Usually between 3 and 5 m thick, the beds are sometimes thin and patchy, presumably because of erosion (Selby & Lowe 1992). The sequence has been divided into eight units numbered H1 to H8 from bottom to top, respectively. The oldest bed (H1) is typically a pale yellowish brown colour with a sharp lower boundary marked by a coarse yellow, quartz-rich sandy layer forming a prominent marker bed. Based on correlations with other tephra deposits in central and southern North Island, and in deep sea cores, H1 has been identified as the Rangitawa Tephra, which has an age (based on fission track analysis of zircons) of 0.35 ± 0.04 Ma (Nelson 1988; Kohn et al. 1992). The overlying beds (H2 to H8), all clayey in texture, range from friable to firm in consistence with reddish-yellow to strong brown colours. Their ages are currently unknown. The presence of paleosols in the sequence suggests that there were considerable periods without eruptions. The youngest bed (H8) is estimated to be aged ≈100 ka (Selby & Lowe 1992). Where the Hamilton Ash materials are exposed at or near the surface, well-developed and strongly structured soils occur, usually Humults or Udults

The Hamilton Ash beds are evidently rhyolitic in origin (based on trace element analysis of titanomagnetites; Shepherd 1984). The Rangitawa Tephra (H1) is probably a distal correlative of the biotite and quartz-bearing Whakamaru-group ignimbrites erupted from Whakamaru or Taupo volcanoes (Kohn et al. 1992), and the remaining beds may well have originated from these sources too (Fig. 2.2) .

Stratigraphy and composition of Welch's Road section

The section, ≈6.2 m high, is located near the end of Welch's Road at S13/097053 at 40 m elevation in the northern Waikato Basin. Mean annual rainfall is 1250 mm and mean annual temperature is 14°C. Native vegetation since c. 14 ka has been mixed broadleaf-podocarp forest (Newnham et al. 1989). The Hamilton Ash beds at this section have been studied by Shepherd (1984), and his findings form the basis of most of the following notes. Nicholson (1986) also

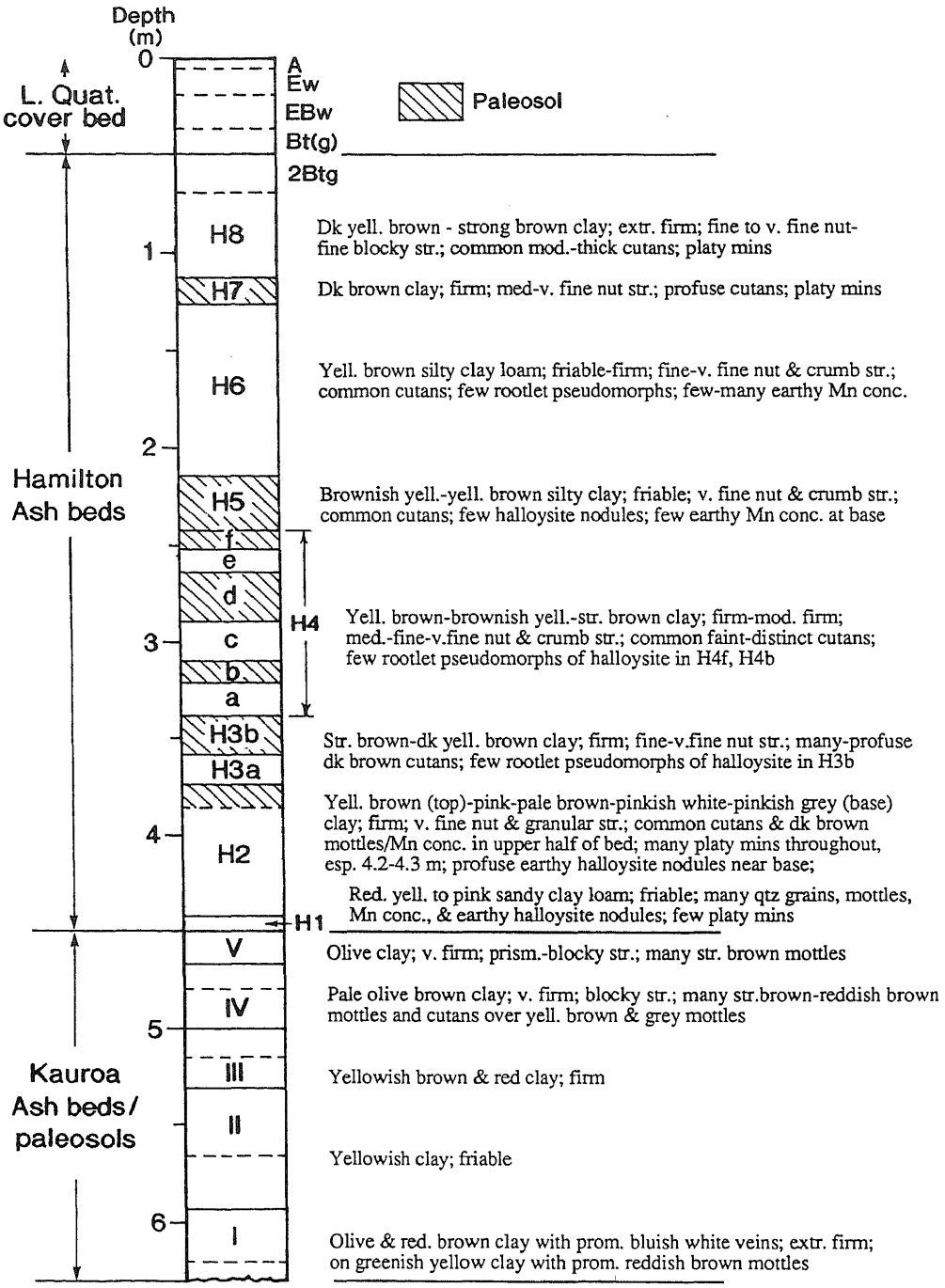

Fig. 4.3 Generalised stratigraphy and description of the Welch Rd section, Mangawara (after Shepherd 1984).

examined the Hamilton beds here, concentrating on their physical and mechanical properties. However, the Kauroa Ash beds have not been analysed at this site. The stratigraphy and main characteristics of the section are outlined in Fig. 4.3.

The *Kauroa beds* (base of section to 4.5 m) comprise five informal units, I-V (Fig. 4.3). These have been tentatively correlated with similar beds at Waikato University in Hamilton by Davoren (1976). They seem to represent the upper part of the group as the top bed is probably K15, but the relationship of the remaining beds to the type sequence near Raglan is uncertain. Analyses by Davoren (1976) at the University site showed that beds I-V contain 85 to 95% clay-sized material. The sparse sand fractions are made up of quartz, cristobalite, plagioclase, Fe-Ti oxides, and zircon. Clay minerals, identified using XRD, DTA, and TEM, are predominantly halloysite with subordinate allophane: beds I, III, IV, and V contain ≈70% halloysite (both 0.7 and 1.0 nm) in the form of short, stubby irregular tubes and rods, and minor allophane; bed II contains ≈40% halloysite, dominantly as long tubes and rods, and perhaps ≈40% allophane. This predominantly halloysite-allophane dual composition agrees in general with analyses on Kauroa Ash beds near Raglan (Salter 1979; Kirkman 1980a). However, a sample from bed II analysed using acid oxalate extraction contains the following (%): Al$_o$, 0.25; Si$_o$, 0.07; Fe$_o$, 0.13 (G.A. Spiers pers. comm. 1993). Assuming Al$_p$ is zero, the Al/Si ratio is ≈3.5 and hence the allophane content (whole soil basis) is apparently only ≈1%. Ferrihydrite content is very low (≈0.2%).

The *Hamilton beds* (from 4.5 m to 0.5 m) comprise eight main units, H1-H8, some divided into subunits and 7 paleosols (Fig. 4.3). The paleosols, some only weakly expressed, are distinguished typically by darker colours, the frequent presence of root traces, rootlet pseudomorphs or rhizomorphs, and slightly more strongly developed sub-angular blocky structures. Clay skins (cutans) occur commonly throughout the sequence; manganese concretions and halloysite nodules also occur; and a distinctive sand-sized golden platy mineral (a micacaeous kaolinite intergrade - see below) is found in beds H1, H2 (especially), H7, and H8. Evidence elsewhere suggests that there is an unconformity between H4 and H5. H5 stands out because of its distinctly yellowish colour and friable consistence. The dark brown topmost bed of the sequence, H8, is overlain by an erosional unconformity and a 0.5 m-thick composite cover bed of weathered ≈50 ka Rotoehu Ash and intermixed younger deposits (derived mainly from TVZ). The modern soil (Kainui silt loam) is developed in both the younger tephra cover bed and the upper Hamilton beds, and is halloysitic with no allophane. It is classified as an Aquic Hapludult.

Laboratory analyses of the Hamilton beds show they are dominated by clay (≈60-85%) with almost no sand except in the lowest two beds (Table 4.2). Aggregates of halloysite clay were found to make up ≈50-99% of the silt- and sand-sized fractions in most beds. The aggregates were broken up by CO_2 charged water to calculate the grain size percentages.

Sand fractions typically comprise quartz, cristobalite, feldspar, Fe-Ti oxides, zircon, and traces of glass and ferromagnesian minerals. The sand-sized golden platy mineral, especially abundant in bed H2, was examined by optical microscope, SEM, XRD, and XRF. Under SEM, it has morphological characteristics similar to those of vermiculite and is made up of ≈9 primary (each 6-8 μm thick), 4 secondary (1-1.5 μm), and 5-7 tertiary (0.7 μm) lamellae units. Both the secondary and tertiary lamellae show some buckling along basal planes. XRD traces of the mineral are shown in Fig. 4.4, which contains both dioctahedral and trioctahedral layer silicates with 060 reflections at 0.149 nm and 0.154 nm, respectively. Shepherd (1984) determined the mineral's unit cell parameters (Table 4.3) and suggested that it is a 2:1:1 partially random interstratified micaceous kaolinite intergrade, with a tendency to segregation, and containing >50% partially disordered dioctahedral kaolinite and <50% of 1 M trioctahedral mica. XRF analysis (Table 4.4) indicates that the mica component is K-depleted. Shepherd (1984) proposed that the platy mineral is authigenic, initially crystallising out of solution as a kaolinite-mica intergrade in approximately equal amounts, followed by the hydrolysis of the mica component to form micaceous kaolinite. However, more recent studies in the literature (e.g. Fanning et al. 1989) indicate that it may alternatively be the result of kaolinization of biotite (biotite is characteristic of unweathered Rangitawa Tephra, the parent ash for the H1 and

possibly H2 beds) via a number of possible mechanisms including dissolution of biotite and recrystallisation of kaolinite at linear boundaries (Ahn & Peacor 1987).

Table 4.2 Grain size analyses and <1 μm clay mineralogy (approx.) of Hamilton Ash beds at Welch's Road (after Shepherd 1984)

Bed[a]	Sand% >63 μm	Silt% 2-63 μm	Clay% <2 μm	Halloysite%	Allophane%
H8	1	21	78	75	22
H7	4	20	76	65	30
H6	1	21	78	48	47
H5[b]	1	37	62	60	35
H4f	1	21	78	80	15
H4e	1	22	77	80	15
H4d	1	22	77	80	15
H4c	1	22	77	90	10
H4b	1	18	81	75	20
H4a	1	19	80	85	10
H3b	1	18	81	70	25
H3a	1	15	84	80	15
H2-upper	3	17	80	85	12
H2-lower	18	18	64	93	3
H1	17	24	59	85	10

a Corrected for aggregated clay; mean values of two or more analyses per bed. b Also contains ≈6% gibbsite.

Clay fractions were analysed by XRD, DTA, and TEM. Beds H1, H2, H3, H4, H7, and H8 are dominated by halloysite with only small amounts of allophane, while H5 and H6 contain perhaps 45-50% allophane as well as halloysite (Table 4.2). (Because allophane estimates are not based on acid oxalate dissolution analysis, then they must be considered as approximate.) Where proportions of allophane apparently increase, the crystallinity of halloysite decreases. An XRD pattern typical of all samples is shown in Fig. 4.5. The halloysite occurs in three common morphologies: large and small spheroids, long tubes, and short and medium sized laths and tubes. Most beds, except H4c and H8, comprise mainly medium size laths and tubes with lesser amounts of small spheroids. H4c is dominated by small spheroids and H8 by short laths and tubes. All beds also contain traces of 'silica plates' (≈0.2-0.6 μm) in the clay fractions (Shepherd 1984).

Table 4.3 Unit cell parameters of platy mineral in Hamilton Ash (from Shepherd 1984)

Lattice parameters	Dioctahedral	Trioctahedral
a-dimension	0.516 nm	0.533 nm
b-dimension	0.894 nm	0.924 nm
c-dimension	0.722 nm	1.010 nm
ß	10.38 nm	10.01 nm

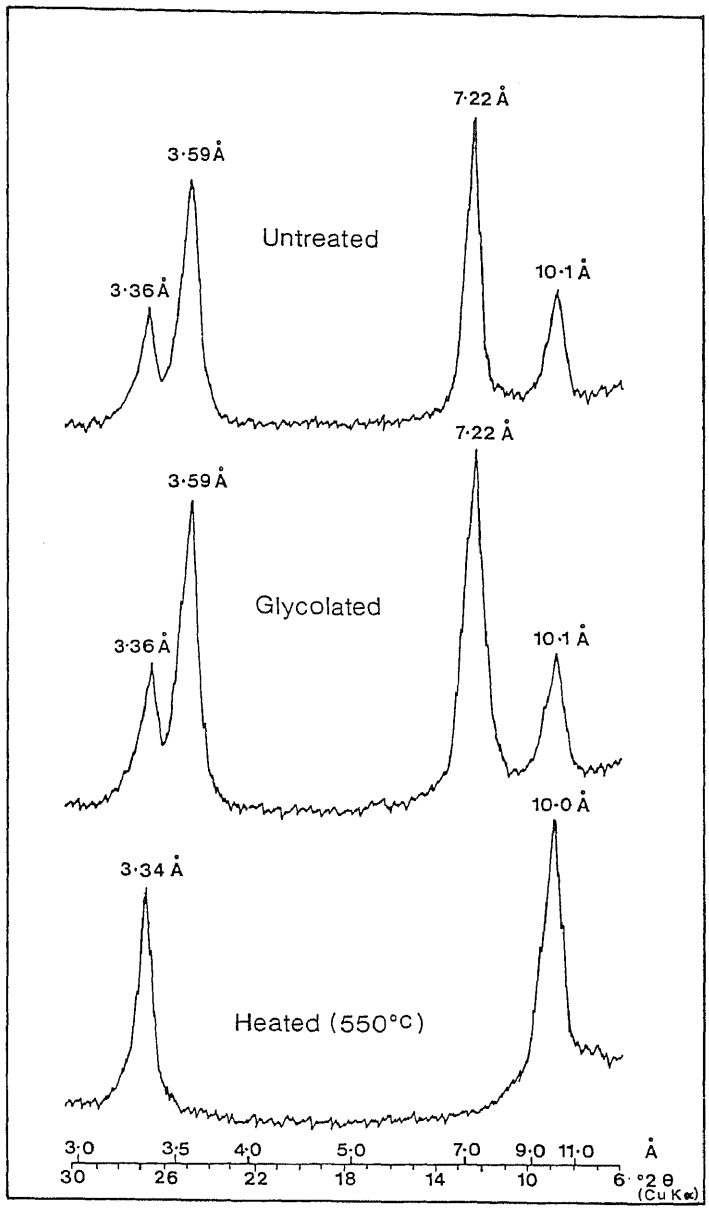

Fig. 4.4 XRD patterns of Hamilton Ash platy mineral using different treatments (from Shepherd 1984).

Table 4.4 Composition of platy mineral in Hamilton Ash (from Shepherd 1984)

SiO_2	Al_2O_3	Fe_2O_3*	MgO	CaO	K_2O	H_2O+	SiO_2/Al_2O_3
42.8	31.9	6.9	1.7	tr	1.2	14.7	1.3

* Total Fe

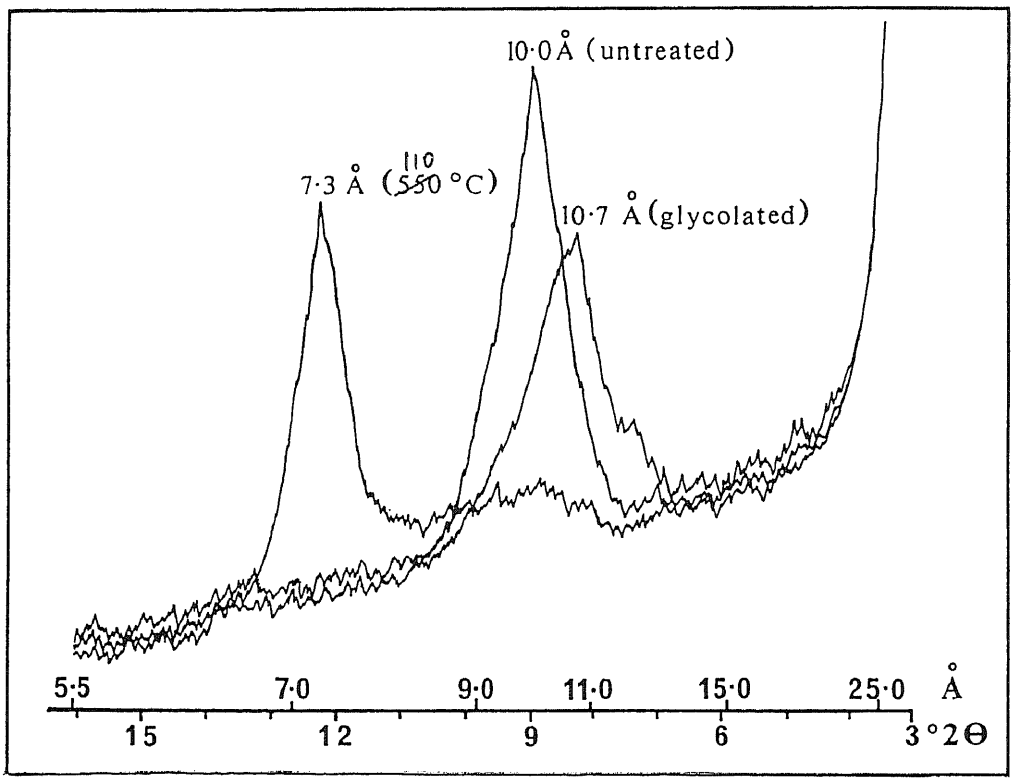

Fig. 4.5 XRD patterns for untreated and treated <1 μm clay minerals in sample H4c (from Shepherd 1984).

Table 4.5 Chemical analyses of Hamilton Ash beds (whole samples) by XRF (after Shepherd 1984)

	H8	H7	H6	H5	H4	H3	H2	H1	Rhyolite†
SiO_2	41.2	44.0	40.7	41.8	42.5	43.1	45.8	45.6	74.2
Al_2O_3	40.1	37.4	40.8	39.4	42.4	40.8	40.7	32.4	13.3
TiO_2	1.1	1.3	1.3	1.1	1.0	1.1	0.8	1.0	0.3
Fe_2O_3*	9.9	11.3	11.2	9.7	8.2	8.5	5.3	9.3	1.8
MnO	tr	tr	tr	tr	tr	tr	tr	0.1	0.05
MgO	3.7	3.2	4.3	3.3	3.3	3.8	4.3	5.4	0.3
CaO	3.0	3.0	3.0	3.0	3.0	3.0	3.0	3.1	1.6
K_2O	0.2	0.3	0.2	0.2	0.2	0.2	0.5	0.3	3.2
P_2O_5	0.1	0.1	0.1	0.1	0.1	0.1	0.1	0.1	0.05
Total	99.3	100.6	101.6	98.6	100.7	100.6	100.5	97.3	94.8
n	2	1	2	2	6	2	5	1	25

* Total Fe † Mean of 25 analyses of (unweathered) rhyolites from TVZ (Ewart 1966)

Analysis of the Hamilton beds using XRF (Table 4.5) showed little variation throughout the sequence, although H1 and H2 were slighly lower in alumina and higher in silica, respectively. Comparison of the analyses with those of unweathered rhyolites show that Al_2O_3 and TiO_2 content is 3-4 times greater, and SiO_2 content ≈40% lower, in the Hamilton beds. This indicates respective accumulation and loss of these components (Shepherd 1984).

It is interesting to speculate, based on the Si leaching leaching models, that the allophane-rich beds of H5 and H6 may have weathered under warm, moderate to high rainfall conditions during interglacials whereas the remaining halloysite-rich beds weathered under cold, low rainfall conditions during glacials (cf. Stevens & Vucetich 1985). The Waikato lowlands have experienced significant fluctuations in climate and vegetation since 18 ka (Newnham et al. 1989) — mean temperature at 18 ka was ≈4°C below that of the present, and the region was largely unforested between 18 and 14 ka — and so it is likely that environmental changes of similar magnitude occurred during the past 350 ka. Kohn et al. (1992) demonstrated that the Rangitawa Tephra (bed H1) was erupted near the end of oxygen isotope stage 10 (a glacial period), and the very high halloysite content in H1 and H2 accords with this. New analyses and age determinations are required, however, before any firm relationships between clay mineralogy and paleoevironments can be made at this site.

STOP 5 — Allophane-halloysite soil drainage sequence (Horotiu-Bruntwood-Te Kowhai soils), Ruakura

Hamilton Basin alluvial plains

The Hamilton Basin has been partly infilled by thick deposits of mainly rhyolitic volcanogenic alluvium known as the Hinuera Formation (Kear & Schofield 1978). Carried by a high energy, ancestral Waikato River system, the Hinuera Formation was deposited as a large low angle fan chiefly between c. 19 and 17 ka, during the coldest part of the last glaciation when the region was essentially unforested (Hume et al. 1975; Green & Lowe 1985; Newnham et al. 1989; Selby & Lowe 1992). Sedimentation more or less finished by c. 15 ka, coinciding with regional reafforestation and climatic amelioration. The sediments are dominated by quartz, feldspar, rounded rhyolitic rock fragments, pumice, and heavy minerals (Hume et al. 1975). The surface of the plains is flat to gently undulating, and is marked by a complex pattern of ridges and swales of generally coarse and fine materials, respectively, which reflect the original pattern of alluvial deposition by the braided Waikato River system. Since deposition ceased 15 ka, the Hinuera surface has been mantled by successive increments of distal tephras, derived from various sources (mainly rhyolitic), which add up to ≈0.4 m in total thickness (Lowe 1986, 1988) (based on cores from lakes and bogs overlying the Hinuera Formation). The modern soils are therefore derived from vitric alluvial and airfall deposits and form a pattern of well drained to poorly drained soils relating to the ridge and swale microtopography (McCraw 1967; Singleton 1991).

Ruakura soil drainage sequence: Horotiu-Bruntwood-Te Kowhai soils

The sequence of three soils occurs on the campus of AgriResearch Ltd., Ruakura, Hamilton (at approximate grid reference S14/134777). The soils are spaced over a distance of ≈100 m and have similar ages and vitric parent materials. Mean annual rainfall at Ruakura is 1200 mm, mean annual temperature is 13.3°C, and rainfall exceeds evaporation for seven months of the year (winter surplus 426 mm, summer deficit 223 mm). Native vegetation since ≈14 ka has been mixed broadleaf-podocarp forest (Newnham et al. 1989). The improved ryegrass-clover pasture at Ruakura is generally used for the grazing of dairy cattle and sheep (and for deer and goat farming on the Horotiu soils). Maize and swedes are grown on the Horotiu and Bruntwood soils, which are also used for the disposal of dairy shed effluent (Singleton 1991). The soils range from the well drained Horotiu silt loam (a Vitric or Typic Hapludand), the moderately drained Bruntwood silt loam (Aquic Hapludand), and the poorly drained Te Kowhai silt loam (Typic Humaquept).

Horotiu soils occur on the ridges or levees on the Hinuera surface (Fig. 4.6). Profiles are commonly silty over sandy or gravelly material and characterised by a dark brown silt loam topsoil over a yellowish brown, moderately weak, non-sticky silt loam subsoil that becomes sandier with depth. Sand or gravel can occur below 60 cm. A brief (generalised) profile description is (after Singelton 1991, 1992):

0-20 cm Ap	Dark brown silt loam; moderately weak soil strength; non-sticky; moderately developed medium nut structure breaking to strongly developed fine crumb; sharp boundary,
20-60 cm Bw	yellowish brown silt loam; moderately weak soil strength; moderately developed medium nut structures breaking to strongly developed fine crumb; diffuse boundary,
60-80 cm BC	yellowish brown to brownish yellow sandy loam; v. weak soil strength; weakly developed fine nut structure breaking to fine crumb; diffuse boundary,
80-100 cm 2Cu	yellowish brown sand or gravelly sand; loose; massive (single grained).

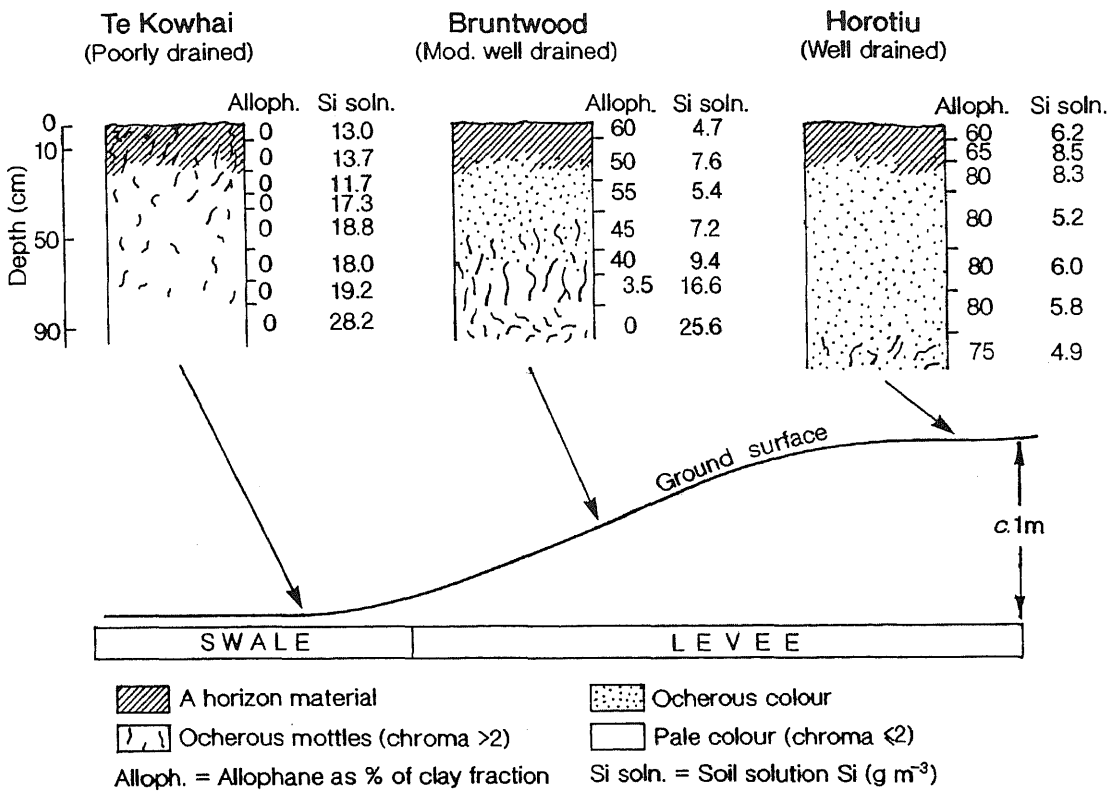

Fig. 4.6 Horotiu-Bruntwood-Te Kowhai soil drainage sequence at Ruakura (after Singleton et al.1989).

Bruntwood soils occur on the sides of the levees in an intermediate position between Horotiu and Te Kowhai soils (Fig. 4.6). Profiles are commonly silt loams over sand (or silty clay loams), and characterised by a very dark greyish brown silt loam topsoil on a yellowish brown silt loam upper subsoil to at least 60 cm, which has yellowish brown mottles. This overlies a pale, poorly drained grey sand (or sometimes silty clay loam) with brownish yellow mottles. A brief profile description (after Singleton 1991, 1992) is:

0-20 cm Ap	Very dark greyish brown silt loam; moderately weak soil strength; non-sticky; moderately developed fine nut structure breaking to strongly developed fine crumb; sharp boundary,
20-60 cm Bw	yellowish brown silt loam; moderately weak soil strength; moderately developed medium nut structure breaking to fine nut; diffuse boundary,
60-80 Bg	pale yellowish brown silt loam with yellowish brown mottles; moderately developed medium and fine nut structure; diffuse boundary,
80-100 cm 2Cg	pale grey loose sand with brownish yellow mottles; massive (single grained).

Te Kowhai soils occur in the depressions or swales (Fig. 4.6). Profiles are commonly layered and are mainly silty over sandy material. They are characterised by a dark greyish brown silt loam topsoil on a pale grey silt loam upper subsoil which has many brownish yellow mottles and is moderately weak and slightly sticky. The lower subsoil is pale grey and commonly a sandy loam. Layers of different soil textures are common. A brief profile description (after Singleton 1991, 1992) is:

0-20 cm Ap	Dark greyish or very dark greyish brown silt loam (may be humic or peaty); moderately weak soil strength in place; slightly sticky; moderately developed fine nut structure breaking to very fine nut; distinct boundary,
20-50 cm Bg	pale grey silt loam or silty clay loam with many medium yellowish brown mottles; moderately weak to moderately firm soil strength in place; moderately developed medium prismatic and block strucure; diffuse boundary,
50-80 cm BCg	pale grey silt or silty clay loam with many fine brownish yellowish mottles; weakly developed coarse nut structure,
80-100 cm 2Cg	pale grey medium sandy loam with many medium yellowish brown mottles; massive (single grained).

Mineralogically, sand fractions of all three soils are dominated by very abundant glass and very common plagioclase. Quartz and cristobalite are also common in the Te Kowhai soils.

The clay fractions differ significantly in composition, however, with regard to the dominant clay minerals allophane and halloysite (Parfitt et al. 1981; Singleton et al. 1989). The Horotiu soil is dominated by allophane (Al/Si ≈2:1) (probably including traces of imogolite) with subordinate halloysite followed by kaolinite and minor cristobalite, glass, and gibbsite; the allophane increases with depth whilst halloysite decreases (Table 4.6). In contrast, the Te Kowhai soil is dominated by halloysite with subordinate amounts of glass followed by minor kaolinite and cristobalite. The Bruntwood soil fits in between these: allophane (Al/Si ≈2:1) predominates in the upper horizons but decreases with depth as halloysite increases in the lower horizons (Table 4.6). Other minerals in the Bruntwood clay fractions include small amounts of cristobalite, glass, and kaolinite.

These marked differences in allophane and halloysite are attributed to the amount of Si in soil solution, which is controlled by leaching and influenced by soil drainage (Singleton et al. 1989). This is illustrated in Fig. 4.6 and Table 4.6. In well drained soils, such as Horotiu, Si in solution is leached from the profile. This maintains low Si concentrations ($\leq$ 10 g m^{-3}) in soil solution, favouring allophane (Al/Si = 2:1) formation. In poorer drained soils, such as Te Kowhai, Si in solution is not readily leached from the profile, high Si levels ($\geq$10 g m^{-3}) are maintained in soil solution, and halloysite forms in preference to allophane (Fig. 4.6). The Bruntwood soil has low levels of Si in solution in the well leached upper profile, which is thus allophanic, but high levels in the poorly drained lower profile, which is thus halloysitic.

Well drained horizons have ochreous colours and contain allophane and halloysite. Poorly drained horizons have dominant pale colours (chroma $\leq$2) due to gleying and contain halloysite and no allophane (Fig. 4.6). Where soil drainage and rainfall appear to be the same, a slight decrease in profile permeability can be sufficient to cause a decrease in allophane and a change from allophane to halloysite dominance.

Table 4.6 Values for pyrophosphate and acid oxalate extractable Fe, Al and Si, soil solution Si, allophane and halloysite content, Ruakura site (from Singleton et al. 1989)

A, allophane; H, halloysite

Depth (cm)	Horizon	Fe_{py} (%)	Al_{py} (%)	Fe_{ox} (%)	Al_{ox} (%)	Si_{ox} (%)	Soil soln Si ($g\ m^{-3}$)	Atomic ratio[A]	A (% of clay)	H (% of clay)
				Horotiu silt loam, well drained (Sample No. SB 9944)						
0–6	Aw1	0·20	0·56	0·80	3·1	1·1	6·2	2·4	60	35
6–17	Aw2	0·18	0·53	0·79	3·3	1·3	8·5	2·2	65	30
17–31	B/A	0·08	0·34	0·83	3·7	1·6	8·3	2·2	80	15
31–55	Bw1	0·02	0·19	0·79	3·3	1·6	5·2	2·0	80	15
55–73	Bw2	0·02	0·18	0·76	3·7	1·9	6·0	1·9	80	15
73–91	Bw3	0·01	0·12	0·77	3·4	1·6	5·8	2·1	80	15
91–107	2C	0·01	0·12	0·46	2·3	0·97	4·9	2·3	75	20
				Bruntwood silt loam, moderately well drained (SB 9952)						
0–7	Aw1	0·24	0·69	1·1	4·0	1·7	4·7	2·0	60	25
7–24	Aw2	0·25	0·76	1·1	4·2	1·6	7·6	2·2	50	25
24–38	Bw	0·02	0·27	1·0	4·5	2·5	5·4	1·6	55	20
38–57	Bg1	0·01	0·16	0·67	3·9	1·6	7·2	2·4	45	25
57–67	Bg2	0·01	0·10	0·66	1·6	0·98	9·4	1·6	40	35
67–79	Bg3	0·02	0·03	0·24	0·23	0·09	16·6	2·3	3·5	60
79–105	2Cr	0·01	0·02	0·10	0·10	0·02	25·6	—[B]	0	75
				Te Kowhai silt loam, poorly drained (SB 9945)						
0–9	Aw	0·20	0·06	0·33	0·33	0·05	13·0	—	0	35
9–22	A/B	0·11	0·06	0·34	0·35	0·05	13·7	—	0	35
22–32	B/A	0·09	0·04	0·44	0·44	0·06	11·7	—	0	40
32–39	Br1	0·08	0·02	0·28	0·28	0·05	17·3	—	0	40
39–57	Br2	0·08	0·02	0·32	0·11	0·06	18·8	—	0	40
57–70	2Br1	0·09	0·04	0·30	0·13	0·06	18·0	—	0	45
70–80	2Br2	0·06	0·07	0·11	0·19	0·07	19·2	—	0	40
80–93	3Cr	0·01	0·05	0·03	0·11	0·04	28·2	—	0	55

[A] $(Al_{ox}–Al_{py})/Si_{ox}$

[B] Insufficient allophane present.

5. DAY 2: ROTORUA—ROTORUA

Outline of Day 2 (Wednesday 14 July)

8.30-9.15 am	Depart Lake Plaza Hotel, Rotorua, and travel to Tapapa (43 km)
9.15-10.15 am	STOP 1 — 140 ka sequence of tephra, tephric loess, and paleosols (Tapapa)
10.15-11.00 am	Travel to Rainbow Springs, Rotorua (37 km)
11.00-2.00 pm	STOP 2 — Rainbow Springs: Morning tea (11.00 am) Farm show (11.45 am) View trout, native trees, kiwis, tuatara Lunch (1.00 pm)
2.00-2.30 pm	Travel to Te Ngae (19 km)
2.30-3.15 pm	STOP 3 — 20 ka sequence of tephra beds and paleosols (Te Ngae)
3.15-3.30 pm	Travel to Whakarerewrewa Thermal Area (13 km)
3.30-5.15 pm	STOP 4 — Afternoon tea and tour of thermal area and village
5.15-5.30 pm	Travel to Lake Plaza Hotel (3 km). Second night Rotorua. Evening: Hangi feast and Maori Concert, Lake Plaza Hotel (7.00-9.30 pm)

We will not be travelling too far today (Fig. 5.1). We leave the Hotel on the shores of Lake Rotorua, a lake formed c. 140 ka following the eruption of the Mamaku Ignimbrite and associated caldera collapse (see Fig. 5.5 below). The lake has an area of 80 km^2 and a maximum depth of 45 m (Lowe & Green 1992). The highest level, about 90 m above present lake level (280 m), occurred when deposits of the Rotoiti Tephra, erupted from the Okataina volcano c. 50-60 ka, blocked the northward drainage from the lake. This level is marked by extensive terraces around the lake on which part of Rotorua City (population ≈60 000) is built. Tephrochonological studies show that the lake remained high until drastically lowered to near its present level c. 22 ka when the Rotoiti deposits were breached (Kennedy et al. 1978). The lake dropped to below its present level between c. 19 and 9 ka, creating further small terraces in the process. Subsequent changes in depth, including a rise of about +10 m at c. 7 ka after the Mamaku eruption, were caused mainly by growth of the volcanic pile in the adjacent Okataina Volcanic Centre (Nairn 1989). Since then lake levels have steadily dropped, probably because of downcutting at the Ohau outlet. The higher lake levels between c. 7 and 4 ka may have partly resulted from higher rainfall than at present (McGlone 1983b). Mokoia Island in Lake Rotorua is a rhyolite dome.

As we skirt the southwestern margins of the lake we pass the rhyolite domes of Mt Ngongotaha (757 m), around the base of which are remnants of the +90 m lake level terraces and associated diatomite, and climb the margins of the caldera onto the Mamaku Plateau (Fig. 5.2). The Plateau surface, ≈1250 km^2 in area, lies between 150 and 650 m elevation, but much is at ≈500 m; it slopes mainly from east to west. It is composed largely of welded and partly welded greyish to pinkish Mamaku Ignimbrite (dated by fission track at 0.14 ± 0.08 Ma; Murphy & Seward 1981), covering an area of >3000 km^2 and with a volume >300 km^3 (Wilson et al. 1984). The ignimbrite is up to 180 m thick near the highest part of the Plateau (Kennedy 1988). The topography is generally flat to rolling with some deeply dissected valleys and gullies, particulary to the west. The main soils are Andic Haplohumods (Mamaku series) under rainfalls of >≈2000 mm per annum (Rijske 1979; Parfitt et al. 1981). Noteable conical hillocks or tor-like features (probably strictly inselbergs: erosion remnants of interfluvial ridges) occur on the central parts of the Plateau above ≈450 m elevation. They represent scattered remnants of jointed ignimbrite, possibly hardened (silicified) in zones by degassing during cooling, which stand on a more welded unit resistant to erosion (Healy 1992).

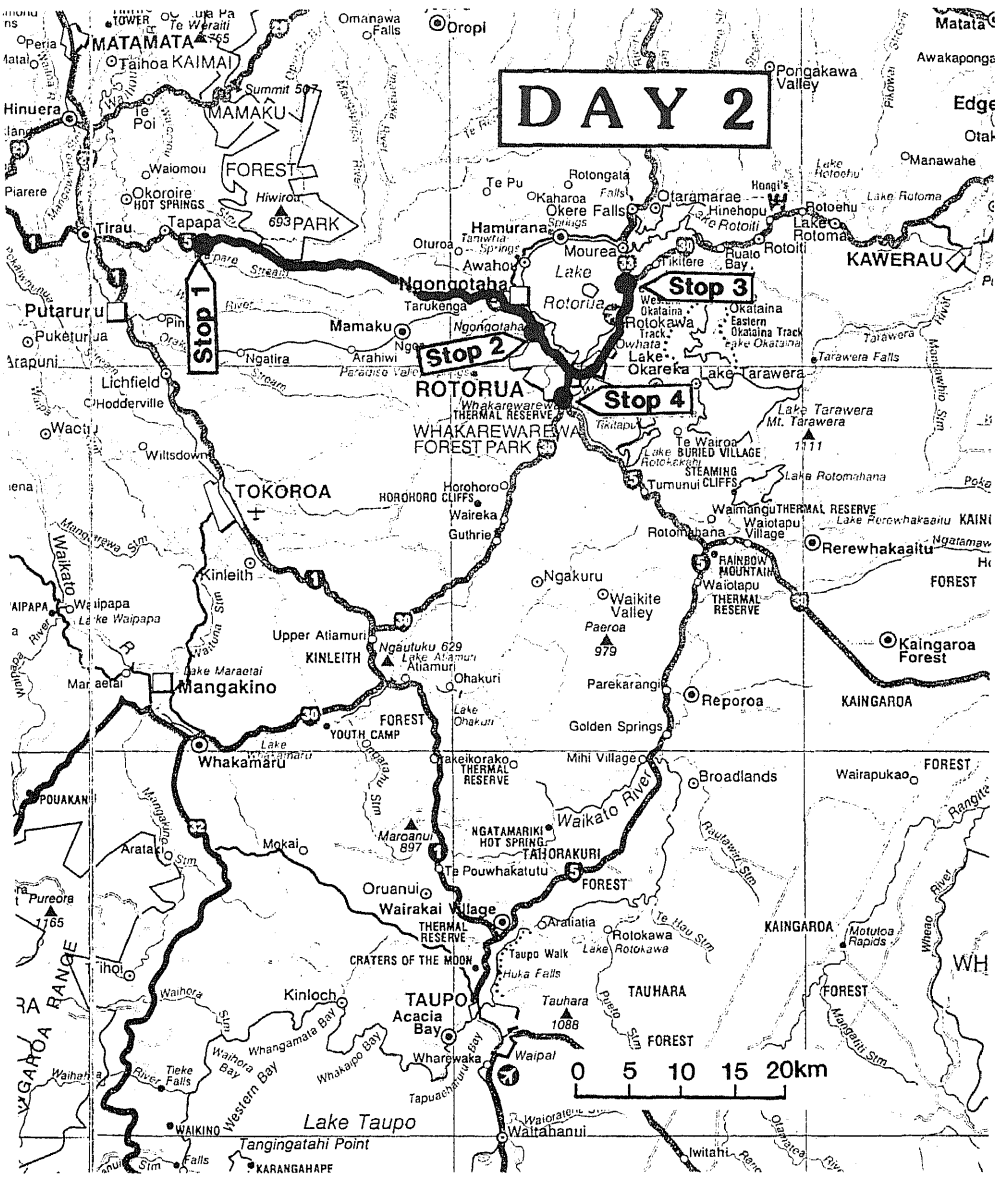

Fig. 5.1 Tour route and stops, Day 2.

The Mamaku Ignimbrite is overlain by a distinctive yellowish-orange lapilli — the Rotorua Tepha — and younger tephras. The Rororua Tephra was erupted c. 13 ka and so there is a major erosional unconformity between it and the Mamaku Ignimbrite, the surface of which is practically unweathered (in places the upper 15 cm is laminated as if shattered by frost, and a thin layer of sand commonly occurs at the interface). Analyses of basal Rotorua Tephra, which is characterised by marked seepage at the interface with Mamaku Ignimbrite, show a predominance of Al-rich allophane and significant iron oxide minerals including ferrihydrite and probably lepidicrocite (Green 1987). Catastrophic fluvial and wind erosion occurred soon after the emplacement of the Mamaku Ignimbrite with huge quantities of material being eventually deposited in the Waikato lowlands (Fig.5.2; Kennedy 1988). Periglacial activity was possibly another process involved in stripping the pre-Rotorua tephras from the Plateau, chiefly prior to deposition of the Rotoehu Ash c. 50-60 ka and between c. 25-15 ka during glacial periods, but there is little evidence of solifluction. At lower elevations, especially on the western margins of the Plateau, the deeply dissected ignimbrite is mantled by a sequence of tephric loess and tephra cover beds up to 7 m thick, and these will be seen at Stop 1. We then retrace our route to Rotorua and travel to the eastern margins of Lake Rotorua (Stop 3), and finish the day at Whakarewarewa thermal area (Stop 4).

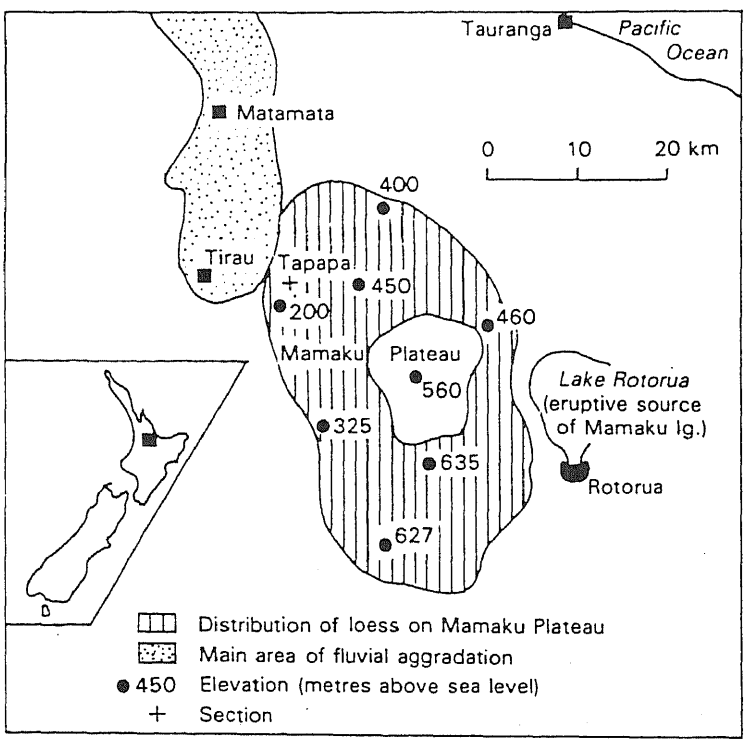

Fig. 5.2 Distribution of tephric loess on the Mamaku Plateau (from Kennedy 1988).

STOP 1 — 140 ka sequence of tephras, tephric loess, and paleosols, Tapapa

The Tapapa section, on privately owned land at T15/635524, lies at an elevation of 260 m, has an annual rainfall of 1600 mm, and a mean annual temperature of ≈13°C. Native vegetation since c. 15 ka was almost certainly mixed broadleaf-podocarp forest (Newnham et al. 1989). The modern soils (Waiohotu series) are Typic Hapludands (McLeod 1992).

Stratigraphy and chronology

The 7 m section exposed here contains a comprehensive stratigraphic record of tephra deposits, tephric loess, and buried paleosols representing alternating periods of deposition and soil formation over the past 140 ka (Kennedy 1982, 1988). The section is described in Table 5.1 and the stratigraphy summarised in Fig. 5.3.

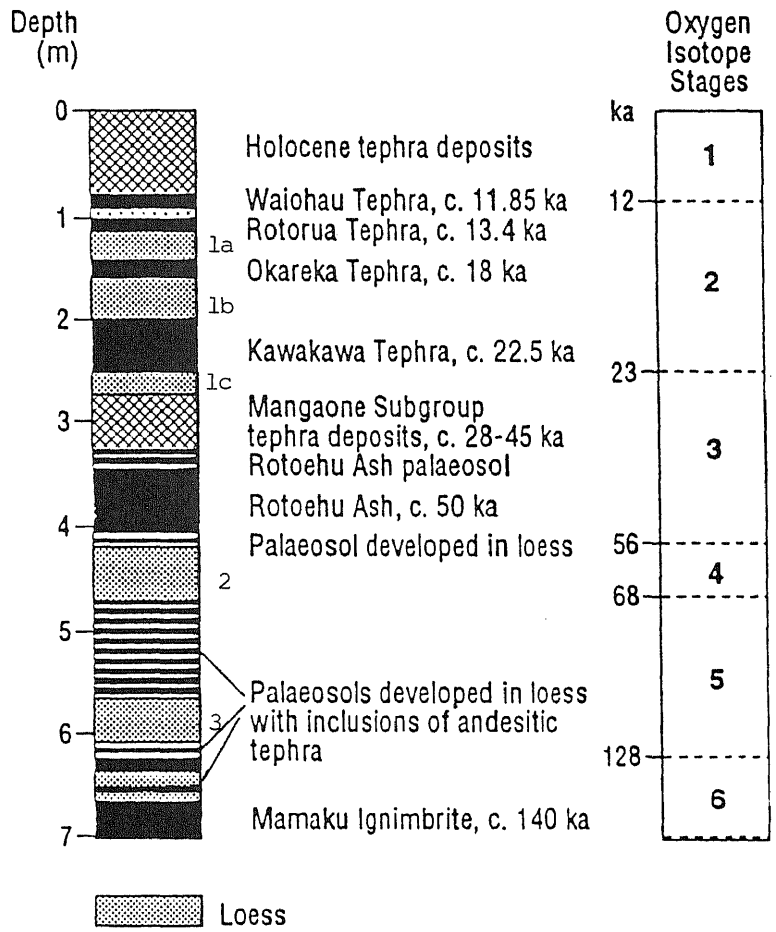

Fig. 5.3 Stratigraphy and chronology of the Tapapa core/section and comparison with oxygen isotope stages (from Kimber et al. in press based on Kennedy 1988).

Table 5.1 Description of Tapapa section (from Kimber et al. in press)

Depth (m)	Description	
0.00 - 1.00	Multiple Holocene tephra deposits (not differentiated): dark yellowish brown (10YR 5/6) to yellowish brown silt loam; moderately weak; weakly developed nut and block structure; indistinct boundary,	Waiohotu gritty silt loam
1.00 - 1.15	Rotorua Tephra (c.13.4 ka): brownish yellow (10YR 6/6) coarse sand; moderately weak; massive breaking to single grain structure; indistinct boundary,	Rr
1.15 - 1.45	Loess: yellowish brown (10YR 5/4) silt loam; moderately firm; weakly developed coarse blocky structure; distinct boundary,	Loess 1a*
1.45 - 1.60	Okareka Tephra (c.18 ka): yellowish brown (10YR 5/6) sandy loam; moderately firm; massive structure; distinct boundary,	Ok
1.60 - 2.00	Loess: yellowish brown (10YR 5/4) silt loam; moderately firm; massive structure; distinct boundary,	Loess 1b
2.00 - 2.45	Kawakawa Tephra (c. 22.5 ka): very pale brown (10YR 7/3) and pink banded silt loam, and sandy loam; moderately firm; massive structure; sharp boundary,	Kk
2.45 - 2.65	Loess: light yellowish brown (10YR 6/6) silt loam; moderately firm; massive structure; few Fe/Mn concretions; indistinct boundary,	Loess 1c
2.65 - 3.35	Palaeosol (in tephra): yellowish brown (10YR 5/6) gritty silt loam; moderately firm; weakly developed coarse blocky structure; horizon includes some Mangaone Subgroup tephras (c. 28-45 ka); indistinct boundary,	Pal 2a
3.50 - 3.95	Rotoehu Ash (c. 50 ka): light grey, yellow and very pale brown layered loamy sand to silt loam; moderately firm to very firm; massive structure; indistinct boundary,	Re
3.95 - 4.20	Weak palaeosol (in loess): brown (10YR 5/3) silty clay loam; moderately firm; massive structure; indistinct boundary,	Pal 2b
4.20 - 4.73	Loess: yellowish brown (10YR 5/4) silty clay loam; moderately firm; massive structure; indistinct boundary,	Loess 2
4.73 - 5.63	Strong palaeosol (in loess but includes some andesitic tephra deposits): dark yellowish brown (10YR 4/4) to yellowish brown (10YR 5/6) silty clay loam; very firm; massive breaking to moderately developed coarse blocky structure; indistinct boundary,	Pal 3
5.63 - 5.98	Loess: yellowish brown (10YR 5/4) silty clay loam; moderately firm; massive structure; few small soft black Fe/Mn concretions; indistinct boundary,	Loess 3
5.98 - 6.33	Palaeosol (in loess but includes some andesitic tephra deposits): yellowish brown (10YR 4/4) silty clay loam; moderately firm; massive structure breaking to moderately developed medium nutty structure; few small black Fe/Mn concretions; indistinct boundary,	Pal 4
6.33 - 6.63	Pal.(?): yellowish brown (10YR 5/4) silty clay loam; moderately firm; massive breaking to weakly developed blocky structure; few weakly weathered ignimbrite fragments; indistinct boundary,	Pal 4
6.63+ *on*	Pale grey (10YR 7/2) soft Mamaku Ignimbrite (c. 140 ka).	

* Loess and paleosol units from Eden et al. (in prep)

The macroscopic rhyolitic tephra layers, derived from mainly the Okataina and also the Taupo volcanic centres and dated by the radiocarbon method, and the Mamaku Ignimbrite at the base, provide the main chronology for the section via tephrochronology (Froggatt & Lowe 1990). They range from c. 140 ka to 1.85 ka in age. Intermixed tephras in addition to those shown in Fig. 5.3, including small additions from andesitic sources, have been recorded in the upper part of the sequence (post-Rotoehu Ash) at an adjacent site (Lowe 1986). The age of the Rotoehu Ash is estimated at c. 50 ka by Froggatt & Lowe (1990) while others have suggested ages ranging from c. 45 ka to 64 ka (Berryman 1992; Buhay et al. 1992; Wilson et al. 1992; Kimber et al. in press).

The loess layers, dominantly yellowish brown (10YR 5/4-5/6), contrast with the interbedded tephras and paleosols and are evidently derived largely from aeolian reworked rhyolitic tephra materials. Such deposits are widespread on the Mamaku Plateau, having been first recognised by Vucetich & Pullar (1969). The loess is dominated by subangular volcanic glass but may also contain charcoal and freshwater diatoms, consistent with accumulation during devegetated, drier and windier periods (Barratt 1988; Kennedy 1988). An exception is the oldest loess-like layer (6.3-6.6 m; Table 5.1), which appears to have formed partly from weathering of the underlying ignimbrite (hence is referred to as a paleosol by Eden et al. in prep and in Table 5.1). Textures range from clay in the oldest loesses (pre-140 ka) to clay loams in the younger loesses (c. 140-50 ka, units 2-3) to silt loams and fine sandy loams in the youngest loess (c. 25-15 ka, units 1a-1c). The loess layers have been matched with cold climate intervals in the marine $\partial^{18}O$ record and correlated with quartzo-feldspathic loess sequences in southern North Island (Fig. 5.3; Kennedy 1988). The paleomagnetic properties of the loess were examined by Froggatt (1988), who found peaks in magnetic susceptibility corresponding to paleosols (at $\partial^{18}O$ stages 3, 5a, and 5e). Lower values related to periods of loess deposition, but Froggatt (1988) suggested that some loess (e.g. Loess 3) evidently accumulated during $\partial^{18}O$ stage 5 (the Last Interglacial).

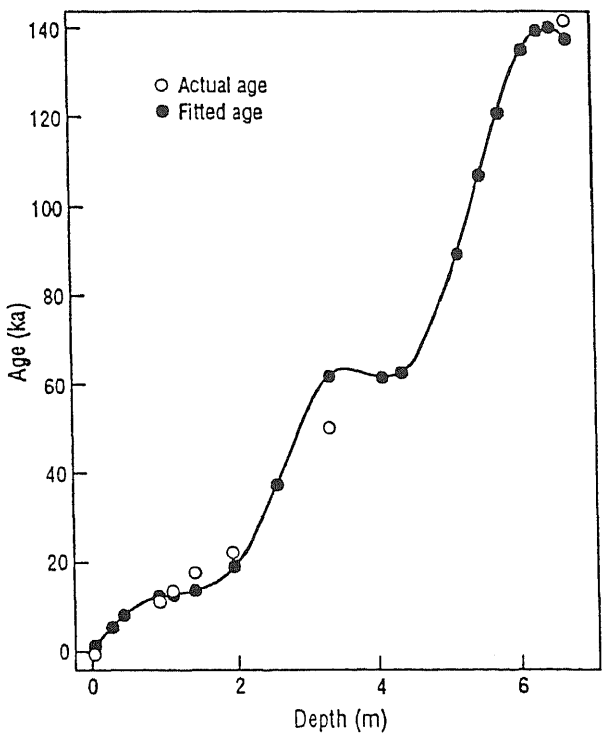

Fig. 5.4 A smoothed spline describing the 'best curve' relationship between depth and age based on calibration age and corresponding D/L values at Tapapa (from Kimber et al. in press).

Table 5.2 Analysis of racemization data and comparison of age estimates with those from previous work (after Kimber et al. in press)

Sample No.	Deposit/palaeosol	Depth (cm)	I		Age (ka)		Previous age (ka) estimates
			Observed	Smoothed	Observed	Fitted	
0		0	0.1	0.16		1	0
2	Holocene tephra	15 – 31	0.25	0.23		5	
3	Holocene tephra	31 – 58	0.35	0.28		8	
5	Waiohau Tephra	87 – 99	0.35	0.35	11.85	12	11.85
6	Rotorua Tephra	100 – 115	0.36	0.36	13.4	13	13.4
7	Loess 1a	127 – 137	0.41	0.38		14	
9	Okareka Ash	159 – 162	–	–	18		18
12	Loess 1b	185 – 203	0.34	0.46		19	19 – 20
14	Kawakwa Tephra	203 – 248	–	–	22.5		22.5
16	Loess 1c	248 – 261	0.73	0.77		37	22.5 – 24
21	Rotoehu Ash palaeosol 2a	328 – 342	1.42	1.19		61	28 – 45
23	Rotoehu Ash	342 – 397	–	–	50		50
26	Weak Palaeosol 2b	397 – 422	1.15	1.19		61	55 – 60
27	Loess 2	422 – 450	1.07	1.2		62	65 – 75
31	Strong Palaeosol 3	508 – 536	1.59	1.65		88	80 – 110
33	Strong Palaeosol 3	542 – 567	2.07	1.95		105	80 – 110
34	Loess 3	567 – 687	1.99	2.16		117	110
37	Palaeosol 4	610 – 628	2.59	2.43		133	120 – 130
39	Loess	632 – 649	2.34	2.5		137	130 – 137
40	Loess/Pal	649 – 662	3.06	2.52		138	–
41	Ignimbrite	662 – 699	2.09	2.47	140	136	140

The paleosols are distinguished mainly by their darker colour and greater degree of weathering with more clay. They also show microstructural evidence for greater soil biotic activity under vegetation (Barratt 1988). Organic and weathering processes appear to have reached a maximum in the paleosol (Paleosol 3) corresponding to late $\partial^{18}O$ stage 5 (c. 80-100 ka), where iron-rich pseudomorphs of plant fragments and abundant fine excrements suggest a forest vegetation. This phase was followed by clay mobilisation and redeposition, possibly when conditions became cooler and at least seasonally drier (Barratt 1988). Weathering and organic activity appear to have been minimal in the loess layer corresponding to the coldest part of $\partial^{18}O$ stage 2 (c. 18-22 ka), with silty concentrations indicating mainly mechanical segregation and turbulence, and some associated gleying, indicating temporary water saturation, both possibly caused by seasonal freezing and thawing. Translocated clay derived from weathered minerals also suggests seasonal wetting and drying (Barratt 1988).

A core taken adjacent to the section has recently been analysed by Kimber et al. (in press) for amino acid racemisation age determinations. D/L values (the ratio of D-amino acids to L-amino acids) for aspartic acid extracted from organic matter (by HCl and by HF on HCl residues) increased rapidly with depth and age. The HF-treated D/L values probably provide the best means of estimating the mean residence time of organic matter, and calibration against the tephrochronological ages provided a numerical age framework (Fig. 5.4; Kimber et al. in press). The ages determined largely agree with the previous estimates (Table 5.2), and provisionally fill the gaps between the Rotoehu Ash and the basal Mamaku Ignimbrite.

Physical, mineralogical, and chemical properties

The full Tapapa sequence has been analysed (from the core) by Eden et al. (in prep); Lowe (1986) additionally worked on the post-Rotoehu Ash materials. Eden et al. (in prep) assayed water content, bulk density, particle size distribution, C content, sand, silt, and clay mineralogy, and major and trace elements of whole samples.

In summary, the tephra layers are distinguished from one another by stratigraphic position, sand mineralogy, and major and trace element chemistry patterns. The sand mineral assemblages are dominated by glass with lesser amounts of plagioclase and cristobalite, tridymite, quartz, and kaolin subgroup aggregated clays in the felsic fractions (>91% of sand fraction); amphiboles (both calcic hornblende and cummingtonite, the latter characterising the Rotoehu Ash), clinopyroxenes, orthopyroxenes, biotite, and Fe-Ti oxides occur in varying proportions in the mafic fractions (<9% of sand fraction). Paleosols are distinguished from loess layers in being finer textured and having the lowest bulk densities, highest water contents, and highest C contents; major and trace element compositions also differ (Eden et al. in prep.).

The <2 μm clay fractions, analysed using a combination of XRD, DTA, and acid oxalate extraction (Whitton & Churchman 1987), are dominated by kaolin subgroup minerals, likely to be mostly halloysite, and allophane (Table 5.3). In the modern soil profile, allophane ± imogolite predominate (35-63%) with kaolin minerals (2-40%) and vermiculite (10-15%, presumably derived from biotite in the parent tephras; Lowe 1986), also being common. Feldspar, cristobalite, and rare quartz are also present in trace amounts. Below ≈1 m depth, kaolins increase to ≥70% and predominate throughout the rest of the section, peaking in the Kawakawa and Rotoehu tephra layers (≥95%). Allophane concomitantly diminishes to only a few percent below ≈1 m depth, increasing to around 10% in Paleosol 3, Loess 3, and Paleosol 4 units between ≈4.7 m and 6.5 m (Table 5.3). Small amounts of gibbsite (≤5%) occur in beds below the Rotoehu Ash but attain about 10% (average) in Mamaku Ignimbrite at the base of the section.

The predominance of allophane in the modern soil, formed chiefly in tephra materials deposited since climatic amelioration about 14 ka, supports the notion of leaching of Si in soil solution from the upper horizons during warm, wet interglacial periods (i.e. $\partial^{18}O$ stage 1). The increase of kaolins with increase in depth suggests an increase of Si from leaching of the overlying beds. The high ratio of rhyolitic to andesitic materials at this site may have enhanced this effect (Lowe 1986). The predominance of kaolins in the section, especially during the known cold and drier periods around the time of deposition of the Kawakawa Tephra (i.e. $\partial^{18}O$ stage 2) and Loess 2 ($\partial^{18}O$ stage 4), supports the model of weak leaching of Si during glacials or stadial periods. In contrast, the increase in allophane in Paleosol 3, Loess 3, and Paleosol 4, corresponds to warmer, wetter conditions (hence promoting Si leaching) associated with the Last Interglacial between c. 90-130 ka ($\partial^{18}O$ stage 5), and matches the micromorphological evidence of Barratt (1988) described above. Similarly, gibbsite quantities, although always small, are greatest in units of this same period (Paleosol 3, Loess 3).

Table 5.3 Mineralogy (%) of clay fractions (<2 μm) of Tapapa materials (after Eden et al. in prep)

Depth (m)	Unit*	Vermic.	Kaolin s'group†	Allophane ± imog.	Feldspar (plag.)	Cristob.	Gibbsite
0-0.15	Ap	15	25	46	7	3	
0.15-0.31	AB	15	15	47	7	3	
0.31-0.55	Bw1	15	2	63	5	2	
0.55-0.80	Bw2	15	12	51	3	1	
0.80-0.84	BC	10	40	35	3	1	
0.95-1.27	Loess 1a		80	7	3	2	<1
1.27-1.59	Rr		70-90	4-5	3	3	<1
1.59-2.03	Loess 1b		85-90	4-5	0-3	1-3	0-<1
2.03-2.48	Kk		94-97	1	0-2	2-3	
2.48-2.61	Loess 1c		90	1	2	4	
2.61-3.42	Pal 2a		85-90	5	0-2	1-4	
3.42-3.97	Re		95	1-3	0-3	0-1	
3.97-4.22	Pal 2b		90	3	3	4	<1
4.22-4.75	Loess 2		85	3-8	2-3	4-5	1-3
4.75-5.67	Pal 3		55-85	6-10	0-2	2	<1-4
5.67-6.10	Loess 3		50-70	8-10	0-2	2-3	1-5
6.10-6.49	Pal 4		55-60	10-12		4	<1-1
6.49-7.05	Mam. Ig		35-50	1-5	6-12	2-4	3-15

* Units and nos. of samples analysed: Loess 1a, 1; Rr, Rotorua Tephra, 2; Loess 1b, 4; Kk, Kawakawa Tephra, 3; Loess 1c, 1; Pal 2a, 5; Re, Rotoehu Ash, 4; Pal 2b, 1; Loess 2, 3; Pal 3, 4; Loess 3, 3; Pal 4, 3 (loess-like); Mam. Ig, Mamaku Ignimbrite, 3.
† Halloysite ± kaolinite

STOP 3 — 20 ka sequence of tephras and paleosols, Te Ngae

Late Quaternary tephras from Okataina volcano

The Okataina volcano is the most recently active of the TVZ rhyolitic centres and, with Taupo volcano, one of the two most productive rhyolite volcanoes known (Nairn 1989; Wilson 1993). Lying to the east of Rotorua Caldera, it has been active from c. 380 ka, but since the eruption of the Rotoiti Tephra c. 50 ka, the Haroharo and Tarawera volcanic complexes have grown on the caldera floor to largely fill the structure (Fig. 5.5). A clear age distinction exists between the exposed eruptives within the caldera, all <22 ka, and the rocks forming the caldera margins, all >140 ka (Nairn 1989).

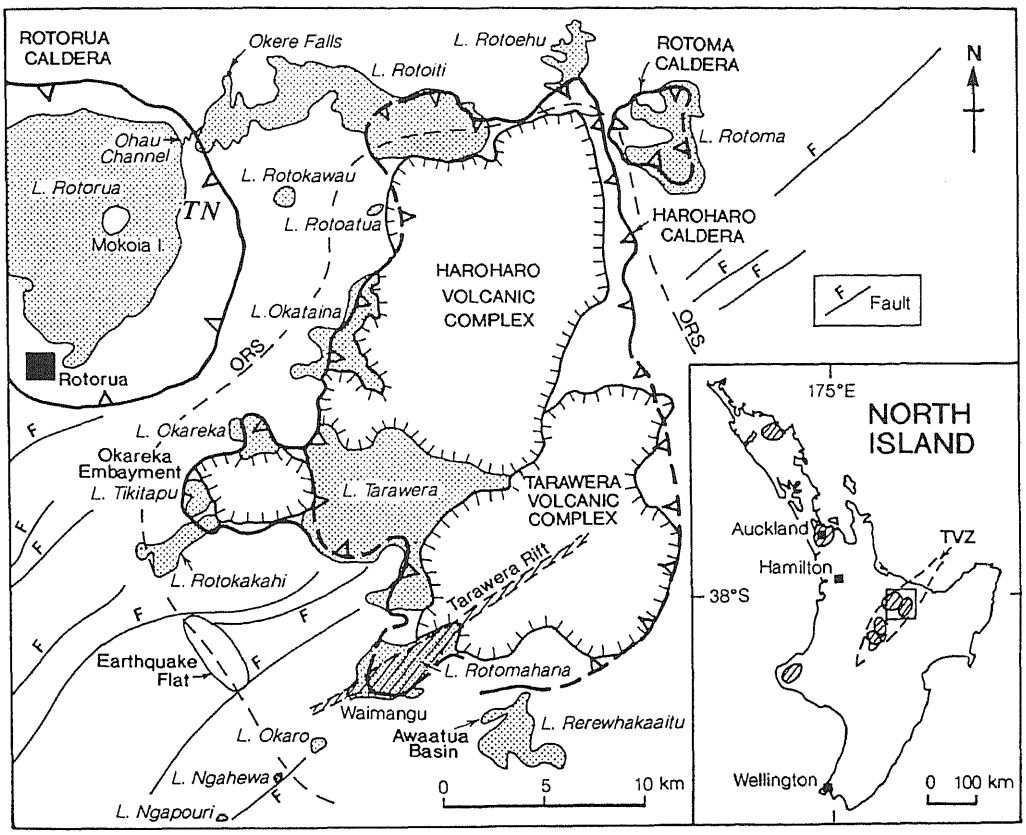

Fig. 5.5 Structural and volcanic features of the Rotorua area associated with the Rotorua and Haroharo calderas. The latter lies within the Okataina Volcanic Centre (marked by ORS, the Okataina Ring Structure). (After Lowe & Green 1992, based on Nairn 1989.) *TN*, Te Ngae site.

There have been 11 eruptive episodes during the past c. 22 ka from vents in the Haroharo and Tarawera complexes, separated by quiescent periods lasting up to a few thousand years (Fig. 2.3, 5.6). All were rhyolitic except for several basaltic events, including the most recent (and one of the smallest), the Tarawera-Rotomahana-Waimangu eruption on 10 June 1886 (Nairn 1979; Walker et al. 1984). The erupted volumes of pyroclastic material are relatively uniform, varying from ≈1 to 15 km^3 (Nairn 1989).

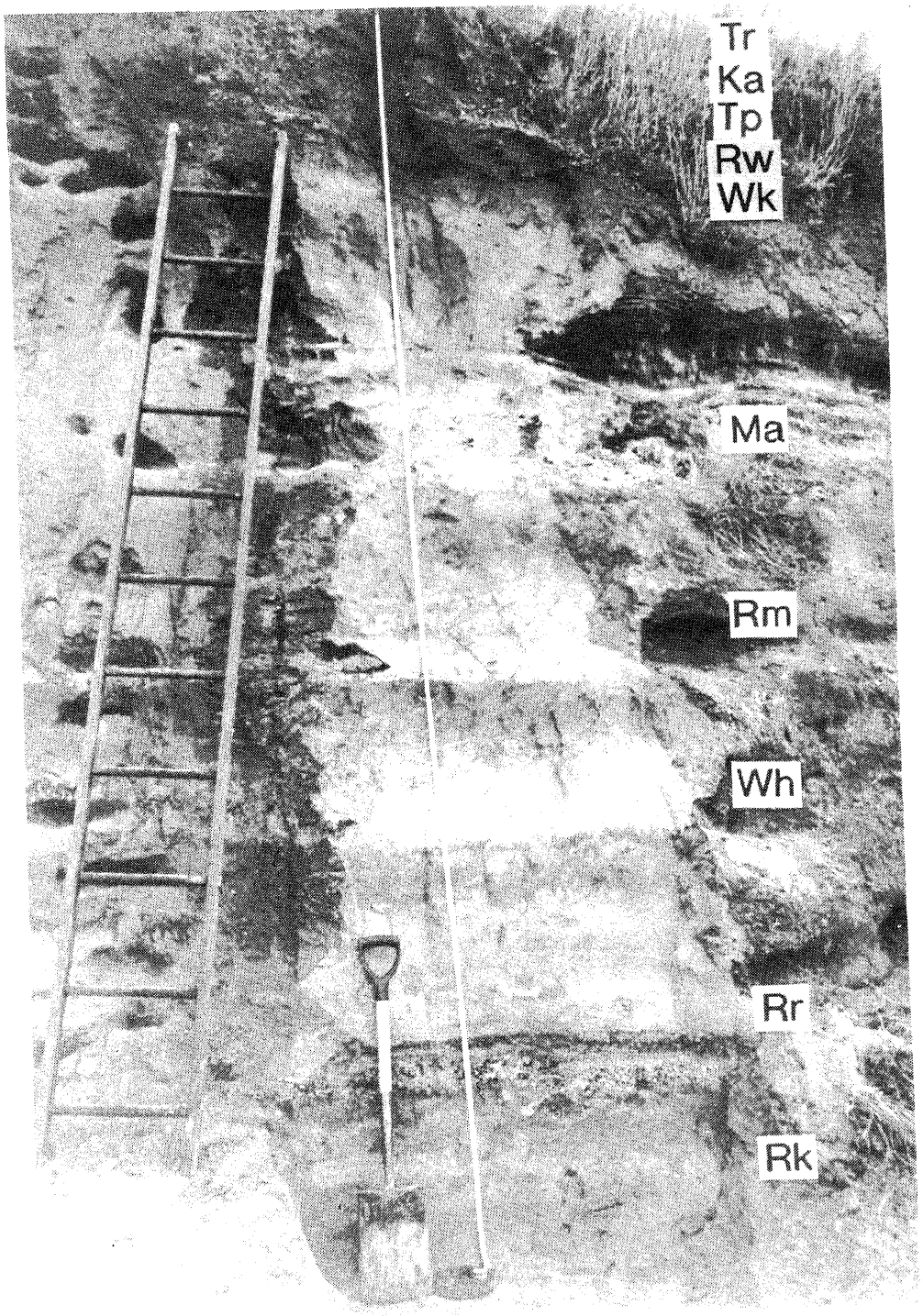

Fig. 5.6 Sequence of late Quaternary tephra deposits and paleosols at Te Ngae Road section. Tephra formations and ages (from Froggatt & Lowe 1990) are: Rk, Rerewhakaaitu, 14.7 ka; Rr, Rotorua, 13.1 ka; Wh, Waiohau, 11.9 ka; Rm, Rotoma, 8.5 ka; Ma, Mamaku, 7.3 ka; Wk, Whakatane, 4.8 ka; Rw, Rotokawau, 3.5 ka (basaltic), Tp, Taupo. 1.85 ka; Ka, Kaharoa, 700 yr ago; Tr, Tarawera (Rotomahana Mud), 1886 A.D. Okareka Tephra (c. 18 ka) also occurs in the section in tephric loess below Rk. All the tephras except Tp (from Taupo volcano) are derived from Okataina volcano. Photo: B.E. Green.

Te Ngae section

The Te Ngae section occurs alongside Highway 33 at Te Ngae (U15/018418) on a sub-vertical terrace cliff face a few hundred metres east of Lake Rotorua. The 6-m high exposure lies at 290 m altitude, and the site has a mean annual rainfall of 1490 mm with a mean annual temperature of 11.9°C. Native vegetation from c. 9 ka to 1 ka was a *Dacrydium cupressinum* (rimu)-dominant podocarp-hardwood forest, with Polynesian fires since c. 1 ka reducing the forest cover to fernland, grass and scrub by 400 years ago (McGlone 1983b). The modern soil is formed from multiple tephra layers including Rotomahana Mud, Kaharoa Tephra, Taupo Tephra, and Rotokawau Tephra overlying earlier eruptives (Fig. 5.6). It is mapped as the Rotoiti series (Rijske 1979), an ashy, mesic, Humic Udivitrand.

Stratigraphy and chronology

The section comprises 11 major tephra deposits aged from 1886 A.D. to c. 18 ka, most being derived from either the Haroharo or Tarawera complexes within the Okataina Volcanic Centre (Figs. 5.5, 5.6). The basal tephra exposed is the Okareka Tephra (aged c. 18 ka), which lies interbedded with tephric loess overlying lake sediments. All the tephras have been dated by the radiocarbon method except Okareka, the age of which is well constrained stratigraphically (Froggatt & Lowe 1990; Nairn 1992). The terrace on which the tephras lie relates to higher lake levels, with the highest stand (+ ≈10 m) in recent times occurring c. 7 ka following the Mamaku eruption. This would correspond today to a position at about the foot of the exposure. A brief description of the section is given in Table 5.4. Note that several of the paleosols at the Te Ngae section (e.g. Rotoma, Taupo) are not as well preserved as at other sites in the area.

Analyses of tephras and paleosols

The weathering of tephras and associated paleosols at this site, and several other sites in the Rotorua region, have been studied in detail by Green (1987). Part of the study examined the kinetics of glass weathering and implications for the formation of clay minerals, as described in Hodder et al. (1990). Similarly, an associated project for determining volcanic glass content in tephra-derived soils or paleosols using HF dissolution is reported by Lowe & Green (1992a).

The tephra sand and silt fractions are dominated by glass with plagioclase, quartz, and cristobalite making up the remainder of the felsic fractions (≥≈95% of the sand fraction), with ferromagnesian minerals (hypersthene, augite, biotite, calcic hornblende, cummingtonite, apatitie, and zircon) and Fe-Ti oxides (titanomagnetite) dominating the mafic fractions (≥≈5% of the sand fraction). The glass is highly siliceous (74-77% SiO_2 on a hydrous basis; Stokes et al. 1992).

The paleosols, notably the buried Bw horizons, were analysed using a variety of methods, and Green (1987) found that these tend to have lower bulk density, higher organic C%, and generally finer textures and higher clay contents than associated parent tephra materials. Although generally only weakly weathered, the degree of development of the paleosols, as indicated by wt% allophane on a whole sample basis and in the silt fraction, wt% clay, clay:sand ratio, and, to a lesser extent, by bulk density, is significantly correlated with effective time for weathering (i.e. time between successive eruptions). Fig. 5.7 demonstrates the relationship between time for weathering and clay content of buried Bw horizons on tephras in the Rotorua area. The time for weathering is greatest for the paleosol on Waiohau Tephra (c. 3320 years) and least for that on Kaharoa Tephra (c. 670 years) (Hodder et al. 1990). These correlations suggest that, in general, once a soil is capped by a succeeding tephra of sufficient thickness, soil forming processes effectively cease.

Table 5.4 Description of the Te Ngae section (after Green 1987)

A_p	0-18 cm	black(7.5YR 2/1)sandy clay, diffuse irregular boundary (Rotomahana Mud)
C	18-20	greyish yellow(2.5Y 6/2)sand, indistinct discontinuous boundary (Rotomahana Mud)
2uA	21-31	black(10YR 2/1)sandy loam, many pumice clasts, distinct irregular boundary (Kaharoa Ash)
2uBw	31-55	brownish black(7.5YR 3/2)loamy sand, abundant pumice, indistinct irregular boundary (Kaharoa Ash)
2uC	55-60	light grey(10YR 8/1)pumice lapilli, distinct discontinuous boundary (Kaharoa Ash)
3uBC	60-70	dark brown(7.5Y 3/4)sandy loam, soft vesicular pumice, diffuse discontinuous boundary (Taupo Pumice)
4uBw	70-80	brown(10YR 4/6)silt loam, few basalt fragments, indistinct irregular boundary (Rotokawau Ash)
4uC	80-100	grey(10YR 5/1)firm basalt, distinct irregular (Rotokawau basalt)
5uBw	100-110	brown(10YR 4/4)sandy loam, distinct irregular boundary (Whakatane Ash)
5uC	110-120	greyish yellow(2.5Y 7/2)coarse sand, indistinct wavy boundary (Whakatane Ash)
6uBw	120-135	yellowish brown(10YR 5/8)sandy loam, diffuse irregular boundary (Mamaku Ash)
6uBC	135-160	bright yellow brown(2.5Y 7/6)loamy sand, diffuse wavy boundary (Mamaku Ash)
6uC	160-183	light yellow(2.5Y 7/4)coarse sand, indistinct irregular boundary (Mamaku Ash)
6uC	183-194	dull yellowish brown(10YR 5/4)fine sand, discontinuous distinct boundary (Mamaku Ash)
6uC	194-220	light grey(2.5Y 7/1)coarse sand, distinct irregular boundary (Mamaku Ash)
6uC	220-230	light yellow(2.5Y 7/4)medium sand, distinct discontinuous boundary (Mamaku Ash)
6uC	230-234	dull yellowish orange(10YR 7/2)very fine sand, distinct discontinuous boundary (Mamaku Ash)
7uBw	234-275	dull yellow(2.5Y 6/4)loamy sand, distinct irregular boundary (Rotoma Ash)
7uBC	275-293	light yellow(2.5Y 7/3)fine loamy sand, distinct regular boundary (Rotoma Ash)
7uC	293-308	light brownish grey(7/2)medium sand, distinct irregular boundary (Rotoma Ash)
7uC	308-310	light yellow(2.5Y 7/3)fine sand, distinct irregular boundary (Rotoma Ash)
8uBw	310-330	dull yellow orange(10YR 6/4)sandy loam, diffuse wavy boundary (Waiohau Ash)
8uBC	330-346	dull yellow orange(10YR 7/3)loamy sand, diffuse wavy boundary (Waiohau Ash)
8uC	346-366	light yellow(2.5Y 7/3)coarse sand, indistinct irregular boundary (Waiohau Ash)
9uBw	366-384	dull yellow orange(10YR 6/3)sandy loam, indistinct wavy boundary (Rotorua Ash)
9uBC	384-395	dull yellow(2.5Y 6/3)fine sand, distinct wavy boundary (Rotorua Ash)
9uC	395-414	light yellow(2.5Y 7/3)showerbedded coarse sand, distinct smooth boundary (Rotorua Ash)
9uC	414-417	light yellow orange(10YR 8/4)fine sand, distinct wavy boundary (Rotorua Ash)
9uC	417-444	light yellow (2.5Y 7/4)showerbedded ash normally grading from fine sand to coarse lapilli, distinct smooth boundary (Rotorua Ash)
10uBw	444-458	dull yellow orange(10YR 6/4)sandy loam, distinct wavy boundary (Rerewhakaaitu Ash)
10uBC	458-468	greyish yellow(2.5Y 7/2)med sand, indistinct diffuse boundary (Rerewhakaaitu Ash)
10uCg	468-476	dull yellow orange(10YR 6/4)fine sand, regular distinct boundary (Rerewhakaaitu Ash)
11uC	476-512	dull yellow orange(10YR 6/3)silt loam, indistinct irregular boundary (tephric loess)
12uBC	512-524	dull yellow orange(10YR 6/4)loamy sand, diffuse wavy boundary (Okareka Ash)
13uC	524-563	dull yellow brown(10YR 5/4)silt loam, diffuse irregular boundary (tephric loess)
14uBw	563-570	dull yellowish brown(10YR 5/4)loamy sand (lake sediments)

Note: Horizon notation 'u' here indicates a buried horizon (cf. 'b' elsewhere)

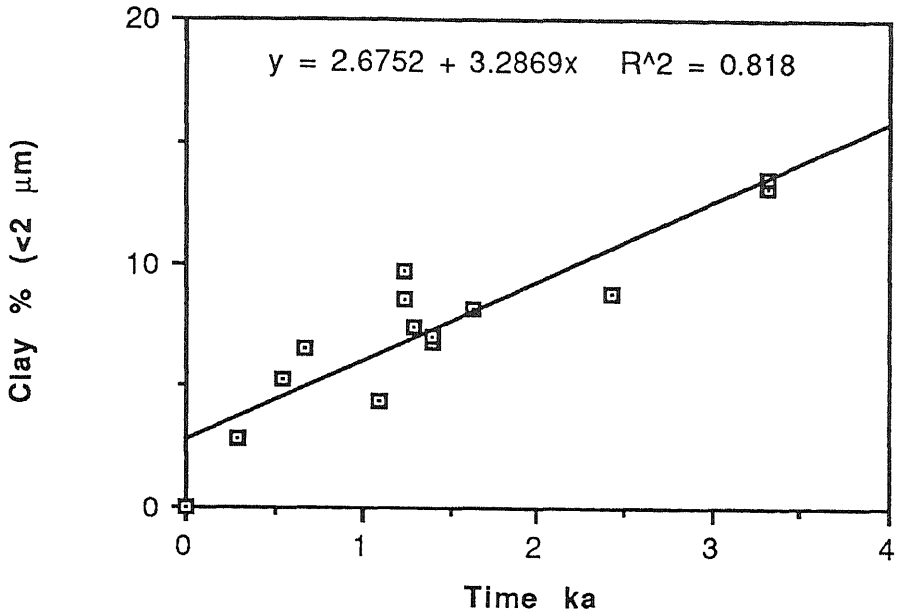

Fig. 5.7 Relationship between time for weathering of buried paleosols and clay content (based on data in Green 1987).

The secondary mineral assemblages and clay fractions were analysed using oxalate and pyrophosphate extraction techniques together with IR (Fig. 5.8), DTA (Fig. 5.9), and XRD analysis. The allophane and ferrihydrite contents on a whole soil basis are given in Table 5.5, allophane and ferrihydrite ranging up to 13.5% and 4.4%, respectively (in the basaltic Rotokawau Tephra paleosol). The whole sample analyses of allophane closely match the sum of analyses on separate fractions (Table 5.6). These latter results further emphasise the common occurrence of pedogenic aggregated clay in silt- and sand-sized fractions in tephra materials.

The clay fractions may contain a combination of Al-rich and Si-rich allophane, halloysite, volcanic glass, organic matter, oxides and hydroxides of Fe (including ferrihydrite), Al (gibbsite), and Si, and minor crystalline primary (residual) minerals; a summary is given in Table 5.7 (based mainly on IR data and including results of analyses from nearby Tikitere [U15/053436] and Democrat Road [V16/141150] sites).

Table 5.5 Clay content and allophane, ferrihydrite, and halloysite content of whole samples at Te Ngae (after Green 1987)

Tephra#	Hor.	Clay% (<2 μm)	Alloph.* wt%	Ferrih.* wt%	Halloy.† wt%
Tr	Ap	nd	2.0	1.3	
Ka	2A	6.1	2.7	1.3	
	2Bw	6.5	2.6	1.4	
	2Cu	0.9	0.8	neg	
Rw	4Bw	nd	13.5	4.4	
	4Cu	nd	8.9	3.7	
Wk	5Bw	7.1	6.4	1.8	
	5BC	3.8	4.5	1.1	
	5Cu	2.4	2.5	0.2	
Ma	6Bw	8.8	6.7	1.3	
	6BC	4.5	5.5	0.3	
	6Cu1	2.0	1.9	neg	
Rm	7Bw	3.7	3.3	0.2	
	7BC	4.2	5.5	0.2	
Wh	8Bw	13.6	9.2	1.0	4.7
	8BC	7.6	7.4	0.1	nd
	8Cu	3.5	5.3	neg	nd
Rr	9Bw	8.6	6.2	0.2	4.2
	9BC	5.3	5.5	0.1	nd
	9Cu1	2.1	3.7	neg	nd
Rk	10Bw	8.2	1.3	0.7	5.6
	10BC	6.1	1.6	0.5	nd
	10Cg	3.8	1.0	neg	nd
Ok	12BC	nd	1.4	0.1	nd

Abbreviations explained in Fig. 5.6
* Allophane and ferrihydrite estimated using acid oxalate and pyrophosphate extractions of Al, Si, Fe
† Halloysite estimated using DTA; neg = neglible; nd = not determined

Table 5.6 Comparison of allophane contents of buried Bw horizons determined by acid oxalate extraction on a whole soil basis (Table 5.5) and by separate determinations on sand, silt, and clay fractions (after Green 1987)

Paleosol	Wt% allophane in:				Wt% allophane
	Clay	Silt	Sand	Total	(bulk sample)
Ka	1.0	1.1	-	2.1	2.6
Wk	3.5	3.0	0.2	6.7	6.4
Ma	3.8	2.4	0.5	6.7	6.7
Wh	5.1	2.4	1.5	9.0	9.2
Rr	4.1	1.5	0.6	6.2	6.2
Rk	0.8	0.6	0.1	1.5	1.3

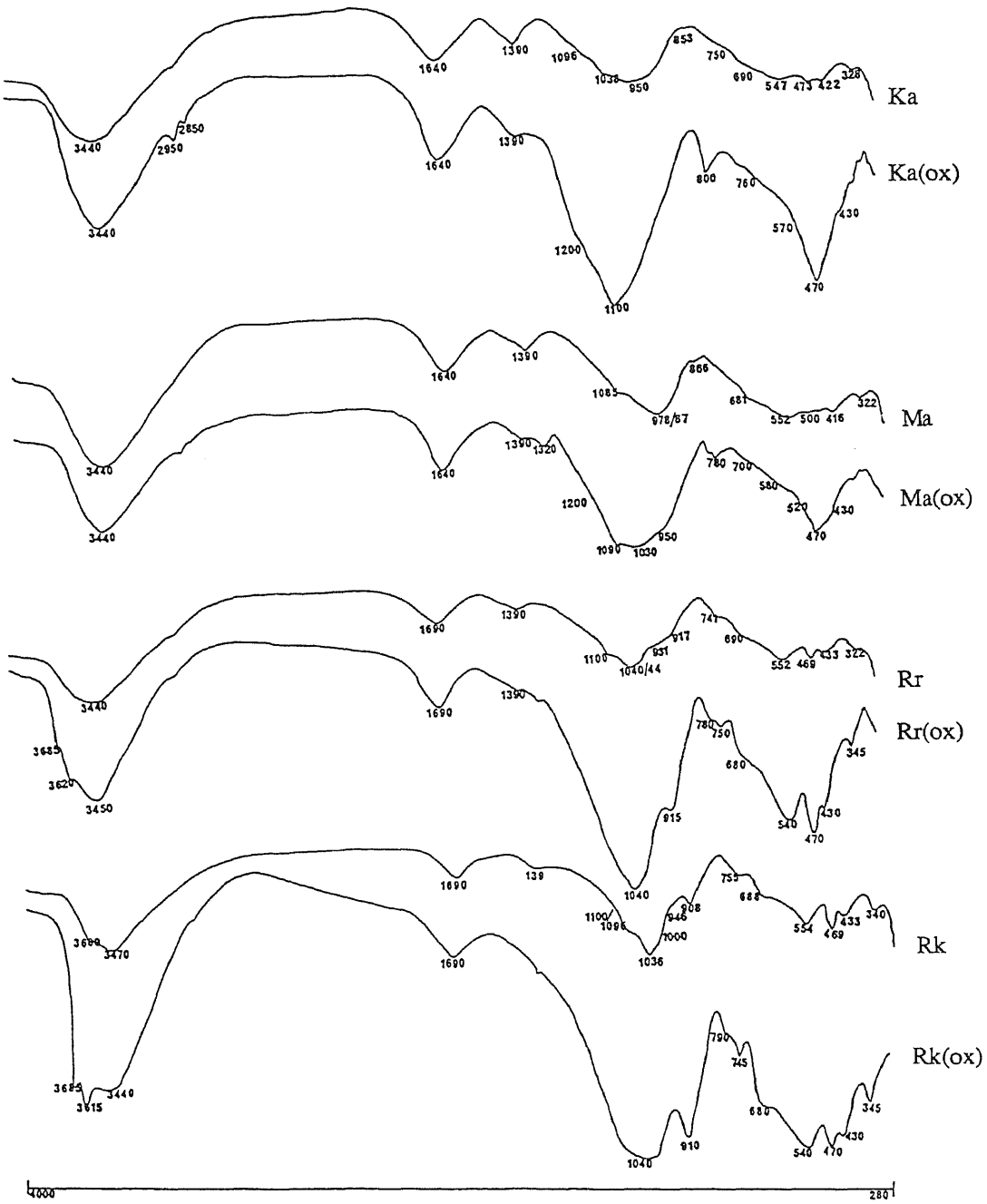

Fig. 5.8 Infrared spectra of clay fractions and ammonium oxalate residues (ox) of buried Bw horizons (paleosols) on four tephras at Te Ngae (abbreviations as in Fig. 5.6) (from Green 1987).

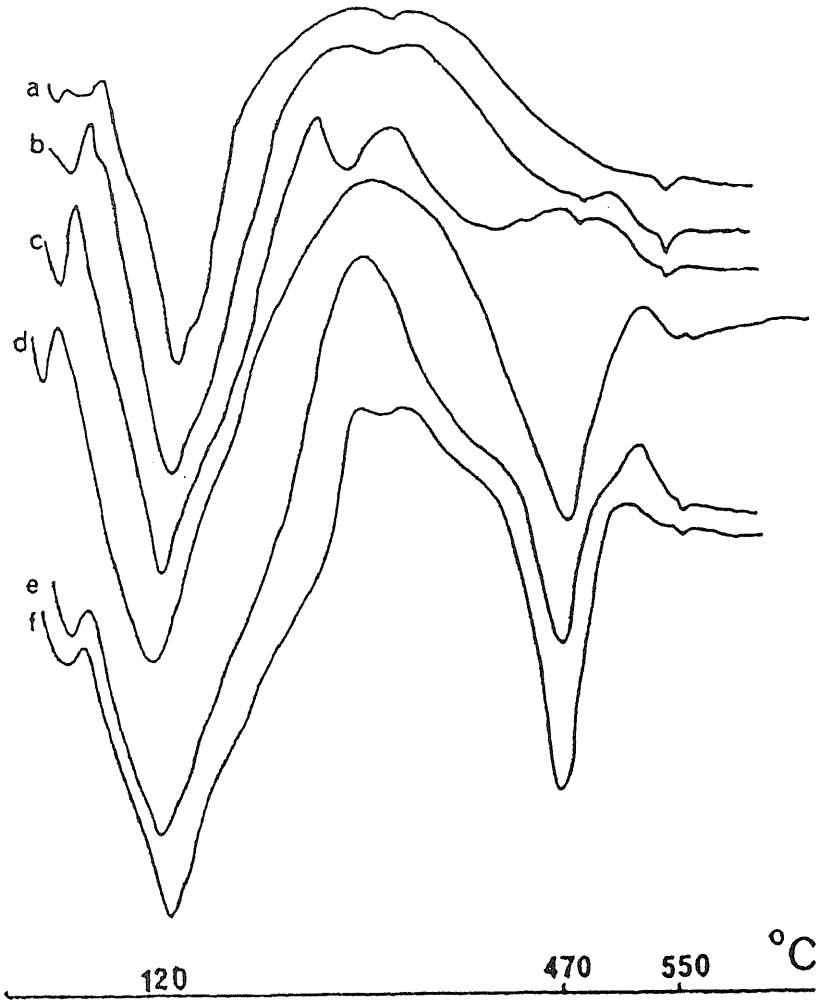

Fig. 5.9 DTA thermograms of clay fractions of buried Bw horizons (paleosols) on selected tephras at Te Ngae: a, Kaharoa; b, Whakatane; c, Mamaku; d, Waiohau; e, Rotorua; f, Rerewhakaaitu (from Green 1987).

Al-rich allophane predominates in the paleosols on the Te Ngae tephras deposited after Waiohau Tephra in the sequence (i.e. since c. 12 ka). At the same time, halloysite occurs in negligible quantities in these beds, instead occurring in appreciable quantities in paleosols with significant Si-rich allophane structures on the Waiohau, Rotorua, and Rerewhakaaitu tephras. The genesis of these clays essentially accords with the inferred paleoclimatic regime operative during the effective period of weathering at the land surface — climate was windier, drier and colder than present from c. 18 ka to about 12 ka, becoming moister and warmer from c. 12 ka to 8.5 ka or later, then becoming slightly drier and frostier with minor fluctuations in temperature to c. 1850 years ago, and finally attaining present day status (e.g. McGlone 1983b, 1988; Newnham et al. 1989). Thus conditions for the period from c. 18 ka to c. 12 ka were conducive to the formation of halloysite and Si-rich allophane (as in the Rerewhakaaitu paleosol) whereas after about 8.5 ka the conditions favoured stronger leaching and the formation of Al-rich allophane (as in the Rotoma, Mamaku, Whakatane, Taupo, and Kaharoa paleosols). However, variations in clay mineral assemblages between the Te Ngae and Democrat Rd sites (Table 5.7) for the Waiohau and Rotorua paleosols suggests that localised microenvironmental variations, such as perching due to textural changes, or some post-burial modification such as resilication through depth of burial, may have affected these (Green 1987).

Table 5.7 Clay mineral assemblages inferred from IR spectroscopy data for clay fractions in paleosols (Bw horizons) at Te Ngae, Democrat Rd, and Tikitere sections near Rotorua (after Green 1987)

Paleosol	Te Ngae	Democrat Rd Tikitere[T]
Ka	GL ≥Al- & Si-ALL >OM >>H, Q, +	
Tp		Al-ALL >GL > OM >>H, +
Wk	Al-ALL >Si-ALL ≥GL >OM > H, +	[T]Al-ALL >Si-ALL >GL >OM, H, Q, +
Ma	Al-ALL >Si-ALL >GL >OM, FE, H, +	
Rm		Al-ALL >GL > OM >Si-ALL >H, +
Wh	H ≥Si-ALL >GL >>OM, Al-ALL, +	Al-ALL >Si-ALL ≥GL >H >Q, +
Rr	Si-ALL >Al-ALL ≥GL ≥H >>OM, +	H >GL >Si-ALL > OM, +
Rk	H >GL >Si-ALL >OM, Al-ALL, +	

GL, glass; Al- and Si-ALL, Al-rich and Si-rich allophane; H, halloysite; OM, organic matter; FE, iron oxide mineral (e.g. ferrihydrite); Q, quartz; +, other Al and Si phase minerals (e.g. quartz, cristobalite, gibbsite).

Weathering kinetics

The kinetics of clay formation can be described in terms of a combination of parabolic and linear kinetics, reflecting the hydration of glass and the formation of clay minerals, respectively (Hodder et al. 1990). Such a two-stage model is consistent with the formation of clay minerals showing an Arrhenian temperature dependence and suggests, on the basis of calculated activation energies, that the process of formation of Al-rich allophane is diffusion controlled, whereas the rate of formation of Si-rich allophane is controlled by the chemical processes at the site of reaction (Hodder et al. 1990). This model is particularly appropriate for buried paleosols from tephra deposits such as those at Te Ngae where the time for weathering is comparatively short (a few hundred to few thousand years). The rate constant calculated for the weathering of rhyolitic tephras in the Rotorua area is 1.23 ka^{-1}, and the half-life of the glass is c. 18 ka (Green 1987).

STOP 4 — Whakarewarewa thermal area, Rotorua

Whakarewarewa is located just to the south of Rotorua City (Fig. 5.1) and is the last of New Zealand's five major geyserfields. More than 500 hot springs discharge from an area of <1 km^2. The geothermal systems in Rotorua, including Whakarewarewa, were closely monitored between 1982-1985 (Drew et al. 1985). Natural activity had dramatically decreased between 1967 and 1985, including a 30% drop in heat flow, and this has been clearly attributed to increased drawoff and inefficiencies by commercial and domestic users in the area. Legislation has since been passed limiting the number of wells and usage, and the geothermal systems have subsequently responded markedly.

The following notes are taken mainly from Simpson (1986).

Whakarewarewa thermal activity

Natural hydrothermal activity at Whakarewarewa has a variety of forms dependent on local vertical permeability and groundwater conditions. High vertical permeability allows upflow of alkaline chloride water which forms clear, near-boiling, sinter-depositing springs. Where vertical permeability is restricted, flashing of hydrothermal fluid produces a mixture of steam, CO_2 and H_2S which rises, heating and acidifying shallow groundwater and producing acid sulphate features. Alkaline chloride and acid sulphate activity are the endpoints between which all features fall depending on the degree to which deep and shallow waters interact. Any feature may change its character with time depending on variations in its supply conditions.

Springs that are predominantly alkaline chloride in character have relatively direct hydraulic connection to the underlying geothermal aquifer. Their activity is consequently directly influenced by changing pressures in this supply aquifer. In addition, they respond to rainfall, changes in groundwater storage, barometric pressure, and even wind speed and direction. The geometry of the conduits supplying alkaline chloride fluid may change over long periods due to mineral deposition or dissolution, while rather more abrupt changes may be induced by earth tremor. The variety of influences on alkaline chloride activity and the fact that each spring responds uniquely implies that modelling and prediction of spring activity is very complex and cannot be generalised. This is particularly true of geysers.

Acid sulphate features are very diverse in appearance and activity. In contrast to alkaline chloride features, they do not form massive sinter deposits, and they have a variable chemistry that may fluctuate rapidly in response to climatic conditions. The fairly typical opaque, milky colour of acid sulphate springs is due to temperature-dependent oxidation of sulphide ions to free colloidal sulphur. Theoretically, as aquifer pressures decline there should be increased steam production and a corresponding increase in acid sulphate activity.

Geysers are the principal focus of public attention at Whakarewarewa. By their nature they are highly variable. They are also difficult to monitor because their discharges are so widely dispersed. Geyser activity at Whakarewarewa is now restricted mainly to Geyser Flat where Waikorohihi, Pohutu, Prince of Wales' Feathers, and Te Horu (Fig. 5.10) are essentially multiple vents of a single system. Mahanga may be connected with these other vents but there is no evidence to suggest Kereru is also connected. Only four of these geysers now erupt frequently on a daily basis. (This situation may have improved in the past few years with the restrictions on well usage in Rotorua.)

Guided tour

During the tour, starting at the Maori Arts and Crafts Institute Building (Fig. 5.10), we will initially see the Rotowhio Model Pa, a replica of a 19th century fortified Maori village. This is followed by a typical mud pool, Ngamakaiakoko (Frog Pond), produced by perched, oxidised acidic water fed by steam and vapour escaping from chloride water at depth and by rainfall. The nature of the activity is directly related to viscosity of the mudpool and hence to rainfall.

We then move on to Geyser Flat and the geysers, which are aligned along the Te Puia Fault. The centre piece is the incomparable Pohutu Geyser. Typically, Pohutu erupts for 25-40% of each day, eruptions varying in number from 5 to 25 depending mainly on wind strength and direction. Over more than 100 years, estimates of the height of Pohutu's column have varied from 15 to 30 m. In August 1985 measurements of 5 separate eruption columns gave heights in the range 16.0-19.8 m. Prince of Wales' Feathers erupts in sympathy with the cycle of Pohutu, and on average is in eruption 90-95% of a day, mostly to only 1-2 m, but plays strongly to 6 m height immediately preceding and during eruptions of Pohutu.

We will finish by seeing a number of hydrothermal features including collapse pits and alkaline chloride springs, notably Parekohoru in the Whakarewarewa Village. This is a classic example of an alkaline chloride spring, and its deep vent (sounded to 19 m) is lined with silica deposited from the cooling geothermal fluid. The water is very clear and at a temperature of ≈90°C and with a pH >9. The chloride concentration is usually about 580 ppm. The spring was formerly known as Champagne Pool because of the fine stream of bubbles which rose constantly. Today the water temperature is somewhat lower and so the bubbling is no longer evident. Water levels in this and the nearby spring, Korotiotio, dropped in the early 1980s. Discharge from Parekohoru is now so low that it has to be channelled into the nearby (private) baths for use by local people.

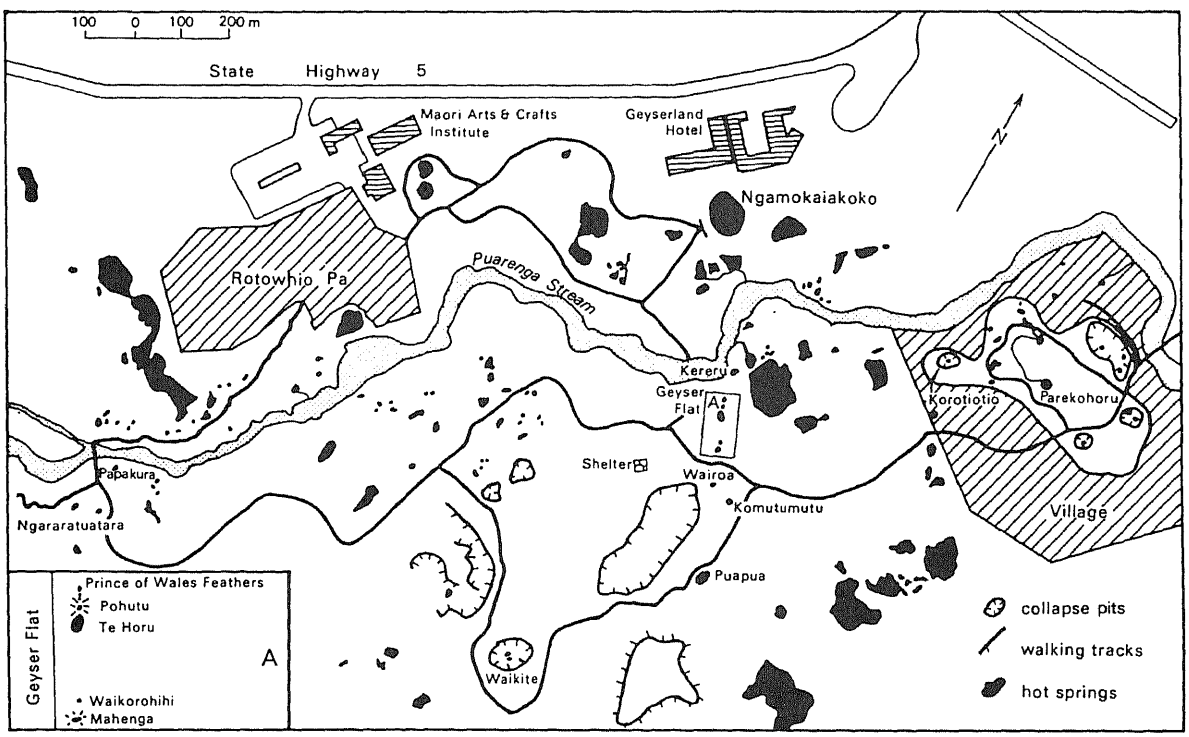

Fig. 5.10 Map of part of Whakarewarewa thermal area (from Houghton 1982).

6. DAY 3: ROTORUA—TAUPO—TOKAANU

Outline of Day 3 (Thursday 16 July)

8.00-8.30 am	Depart Lake Plaza Hotel, Rotorua, and travel to Waiotapu Thermal Park (31 km)
8.30-10.30 am	STOP 1 — Waiotapu Thermal Park, and morning tea
10.30-11.15 am	Travel to Wairakei (43 km)
11.15-12.00 noon	STOP 2 — Taupo soil on 1.85 ka Taupo Tephra, Wairakei
12.00-12.10 pm	Travel to Huka Falls (4 km)
12.10-12.30 pm	STOP 3 — View Huka Falls (Waikato River)
12.30-12.45 pm	Travel to Cherry Island, Taupo (8 km)
12.45-1.45 pm	STOP 4 — Lunch at Cherry Island, Taupo
1.45-2.00 pm	Travel to De Brett Hotel area (7 km)
2.00-2.45 pm	STOP 5 — 10 ka sequence of pumiceous tephra beds and paleosols, (De Brett section, Taupo)
2.45-3.00 pm	Travel into Taupo township (4 km)
3.00-3.30 pm	STOP 6 — Afternoon tea in Taupo
3.30-4.30 pm	STOP 7 — Free hour in Taupo
4.30-5.30 pm	Travel to Tokaanu Hotel, Tokaanu (60 km). Overnight stop.
	Dinner
	Evening: Hot pool at Tokaanu Hotel (or Tokaanu Thermal Baths)

Today we travel entirely within the Taupo Volcanic Zone, essentially following its eastern margin from Waiotapu southwards (Fig. 6.1). We begin by crossing the southern margins of the Rotorua Caldera (at Whakarewarewa) and then travel through a generally hilly landscape dominated by thick, eroded, pyroclastic deposits (both ignimbrite and fall units), rhyolite lava domes, and their reworked products in the form of fluvial and lacustrine sediments. The terrain is riddled with faults, mainly striking NE-SW (e.g. Fig. 5.5). Areas of hydrothermal activity, past and present, are also evident. Road cuttings show numerous tephra layers — mostly derived from the Okataina volcano — and weak paleosols. Soils are typically made up of layered or 'multisequal' rhyolitic parent tephras forming generally Udivitrands or Hapludands depending on the thickness of surficial, coarse pumiceous tephras (Kaharoa and Taupo). In the vicinity of Waimangu-Waiotapu, the Rotomahana Mud (from the 1886 A.D. Tarawera eruption; Nairn 1979) is sufficiently thick to form local Vitrandic or Typic Udorthents.

After Waiotapu, we climb on to vast, generally flat-lying welded ignimbrite sheets, erupted from centres in the TVZ, forming the so-called Kaingaroa Plateau. Airfall tephras and paleosols mantle this landscape (those visible in road cuts are mainly post 20 ka in age), with extensive Taupo Tephra deposits, erupted 1.85 ka, forming the parent materials for many soils (Udivitrands grading to Haplorthods) within a radius of ≈100 km or so of Lake Taupo. Taupo Tephra lacks cobalt and attempts at farming this area in the 1920s failed because of a Co deficiency-related stock disease, so called 'bush sickness' (selenium is also low). Apart from patches of pastoral farming, most of this central volcanic region is planted in exotic *Pinus radiata* (Monterey pine) forests (some *Eucalyptus* species, *P. ponderosa*, Douglas fir, etc., are also grown). Although exotic timber trees were first grown late last century, plantings by both state and private interests boomed in the 1926-1936 period, particularly with the availability of cheap land and labour during the financial depression. Radiata pine was found to be the most suitable timber species, growing almost all year round and exploiting nutrient and moisture reserves in buried paleosols, and maturing in only ≈30 years (pulping trees mature in 20-25 years).

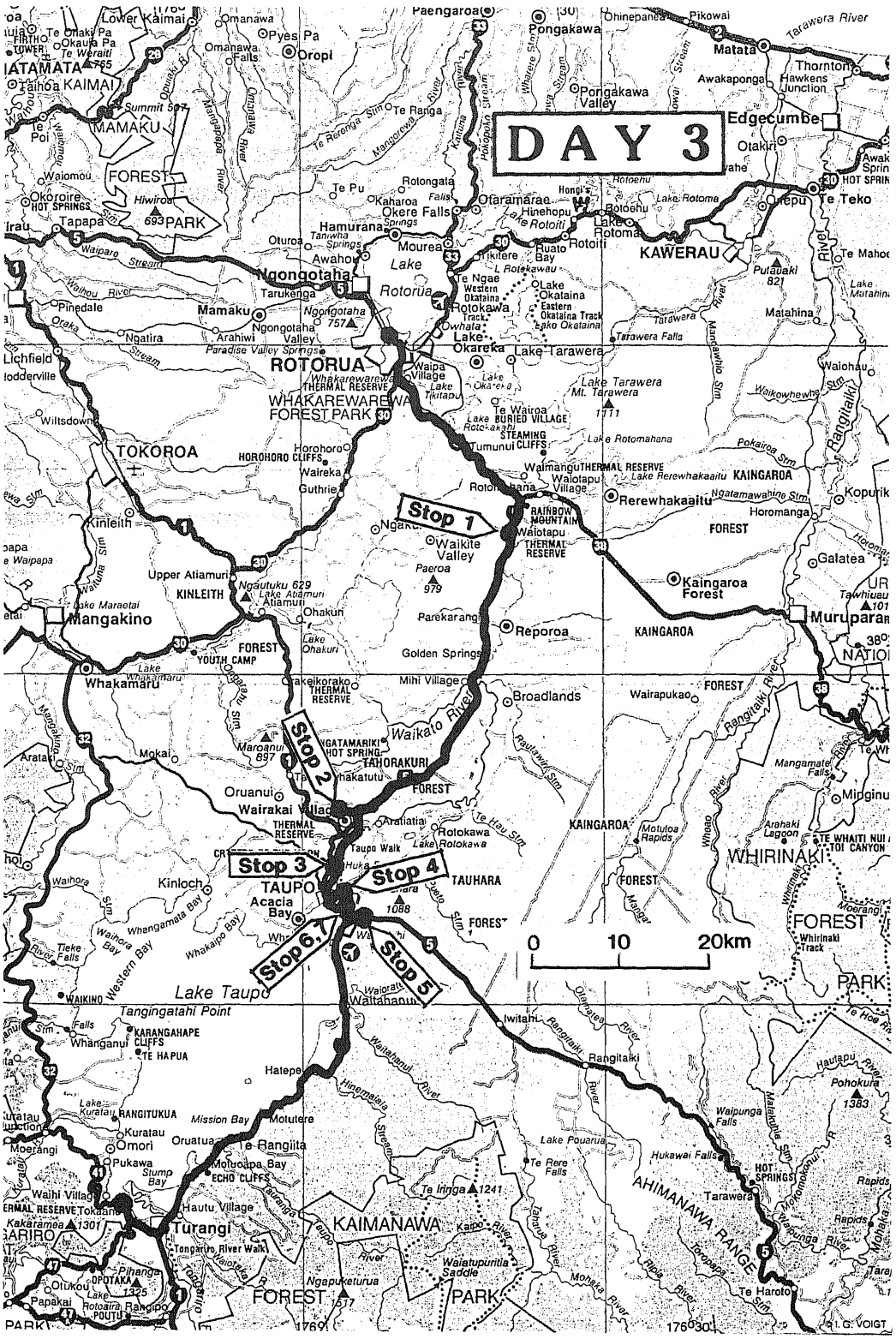

Fig. 6.1 Tour route and stops, Day 3 .

North of Taupo, we pass through the Wairakei geothermal field, New Zealand's first major geothermal power project (completed 1958), and cross the Waikato River outlet from Lake Taupo. If the weather is favourable, we might see the andesitic stratovolcanoes — Tongariro (1967 m), Ngauruhoe (2287 m), and Ruapehu (2797 m) — of Tongariro National Park to the south of the lake. These represent an extreme contrast in eruption styles and volumes to Taupo.

The final part of our journey today skirts the eastern, downward-sloping, 'flanks' of the Taupo volcano, in which Lake Taupo lies at 357 m altitude. This volcano is one of the world's two most productive rhyolite volcanoes, the other being Okataina (Wilson 1993). The northern part comprises a caldera complex created largely by the extreme Kawakawa (22.6 ka) eruption, modified by further collapse after the powerful Taupo (1.85 ka) eruption; the southern part is mainly a volcanotectonic collapse structure (Lowe & Green 1992; Wilson 1993). The lake had high stands at 495 m and 390 m after the Kawakawa and Taupo eruptions, respectively, with some transient lower lake levels in between (Wilson 1993). The outlet is cut into Kawakawa ignimbrite and graded to resistant silicified volcaniclastic sediment and ignimbrite at Huka Falls. Lake Taupo is New Zealand's largest (623 km^2) and 10th deepest (185 m) lake, and has a volume of ≈60 km^3.

Finally, we cross the Tongariro River at Turangi (set up to service the Tongariro power development scheme), past the Tokaanu Power Station and over the tailrace canal near the small rhyolite dome of Maunganamu, and arrive at Tokaanu Hotel, Tokaanu.

STOP 1 — Waiotapu Thermal Park, Waiotapu

Most of the following notes on the geology, mineralogy, and thermal features of Waiotapu are based on Simmons & Browne (1991) and Simmons et al. (1992). They have been supplied by Dr Stuart Simmons, Geothermal Institute, University of Auckland, who will lead us through the area. Broader review material is also contained in Browne & Lloyd (1986) and Hedenquist (1986). Soils of the area are described by Vucetich & Wells (1978).

The Waiotapu thermal area lies at 380 m altitude. Mean annual rainfall is 1320 mm and mean annual temperature is 10°C (Vucetich & Wells 1978).

Geology

Waiotapu geothermal field, located within a fault angle depression, lies south of Okataina and east of Kapenga volcanic centres (Fig. 6.2). Its relation to recent volcanism is uncertain but work in progress suggests that the field may relate to ignimbrite eruptions (?Kaingaroa) from a previously unrecognised rhyolitic centre along the eastern boundary of TVZ between the Okataina and Maroa centres. The field has the largest area of surface activity of any system in TVZ (18 km^2 and 540 MW_t). Seven holes penetrating to depths of 500 to 1100 m were drilled in near N-S alignment (Figs. 6.2, 6.3), but due to poor discharge the field was never developed for steam production. Early geological and geophysical studies are described in Healy et al. (1963). More recently, Waiotapu has been studied with respect to its geochemical evolution and as an analogue to an active ore-depositing system (Hedenquist 1983, 1991; Hedenquist & Henley 1985; Hedenquist & Browne 1989).

The stratigraphy of the area comprises near flat lying felsic ignimbrites, tuffs, and lacustrine sedimentary rocks (Table 6.1; Fig. 6.4). Basement greywacke was not encountered in any of the drill holes. The northern part of the field is bounded by two dacite domes (Maungakakaramea and Maungaongonga) that rise 400 m above their bases, and a rhyolite dome (Trig 8566) lies to the west of the field (Figs. 6.2, 6.3). The main structural feature is the Ngapouri Fault, a NE-SW trending splay off the Paeroa Fault which cuts between the two dacite domes.

Table 6.1 Summary of stratigraphy of Waiotapu (after Hedenquist 1986)*

Rock Unit	Lithology	Thickness (m)	Approx. Age
Ash (fh)	At least five rhyolitic ash beds and interbedded alluvium	<10	1.85 ka to 14.7 ka
Oruanui ignimbrite or Kawakawa Fm (fh)	Fine rhyolitic ash with abundant accretionary lapilli	<50	22.6 ka
Earthquake Flat Breccia (fh)	Unwelded rhyolite pumice breccia, biotite-rich		50 ka
Huka Group (fh)	Lacustrine silts and sands, stratigraphically extensive over Taupo volcanic zone	40-120	0.1 Ma to 0.4 Ma
Maungakakaramea Dacite (md)	Lava domes and flows of dacite	up to 1000(?)	0. 16 Ma
Kaingaroa Ignimbrite (kg)	Upper welded lenticulite and lower unwelded breccia		0.24 ± 0.05 Ma[1]
Matahina Ignimbrite (ma)	Poorly welded pumiceous tuff		0.28 ± 0.03 Ma[1]
Onuku Breccia Formation (ob)	Pumiceous pyroclastics, reworked to silts, sandstones correlative with Huka Formation	~50	
Rangitaiki	Moderately welded quartzose ignimbrite		0.36 ± 0.03 Ma[1]
Crystal-rich tuff (qb)	Moderately welded quartzose, biotite ignimbrite		
Waiora Formation (W2)	Pumiceous pyroclastics and lacustrine sediments of the lower Huka Group		
Haparangi Rhyolite (hal)	Lava domes and flows of rhyolite, with intrusive equivalents	up to 1100	
Waiotapu Ignimbrite (wi)	Moderately to highly welded quartz-poor lenticular ignimbrite; occurrence of spherulitic zones common with one 50 ± m zone of lithophysae about one-half of the way into the sheet	~250	0.59 ± 0.06 Ma[2]
Tuff	Crystal lithic tuff (breccia), reworked	20-90	
Ngakoro Andesite (nk)	Augite-hypersthene intrusive (?) sill; no surface equivalent	50	
Paeroa Ignimbrite (po-A, B, -C)	Three moderately welded ignimbrite sheets separated by tuff breccias	>100	0.332 ± 0.02 Ma[3] 0.390 ± 0.03 Ma[1]
Torlesse Supergroup	**Graywacke and argillite basement underlying the volcanics of the Taupo volcanic zone**		Mesozoic

* Ages and stratigraphic relationships of some units are currently being revised.
Sources: 1, Nairn (1989); 2, Grindley & Mumme (1991); 3, Pringle et al. (1992)

Minor NNE trending faults are inferred from the alignment of thermal features in the central part of the field; further south, the apparent intersection of E-W and NNE-SSW trending structures coincides with four hydrothermal explosion craters. More than 20 such hydrothermal explosion craters and associated breccia deposits occur at Waiotapu (Fig. 6.2). Several C-14 ages indicate that these eruptions took place around 900 years ago and were perhaps synchronous with (early) rhyolitic eruptions associated with the Kaharoa eruptive episode at Mt Tarawera, 15 km northeast of Waiotapu (Lloyd 1959; Cross 1963; Hedenquist & Henley 1985; Lowe & Hogg 1992). Explosion or eruption craters are sometimes confused with collapse features, which form through dissolution, but the two can usually be distinguished from their morphology and the presence or absence of a breccia apron.

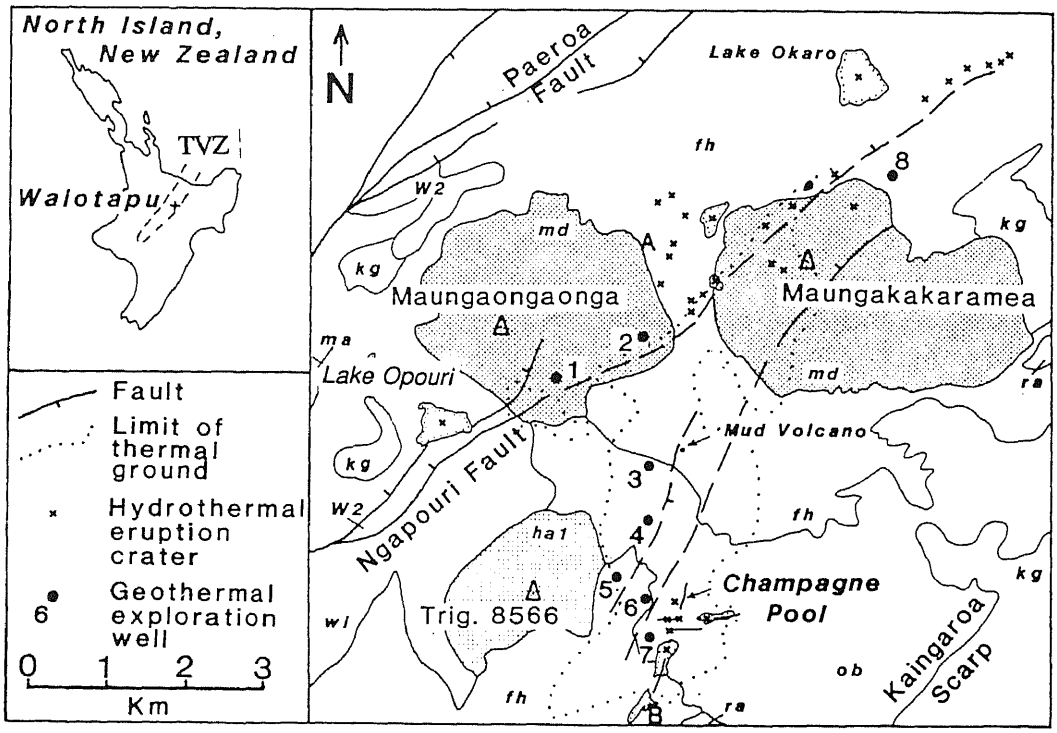

Fig. 6.2 Simplified geology of the Waiotapu area (unit abbreviations are in Table 6.1) and locations of hydrothermal eruption vents and drillholes (from Hedenquist & Henley 1985).

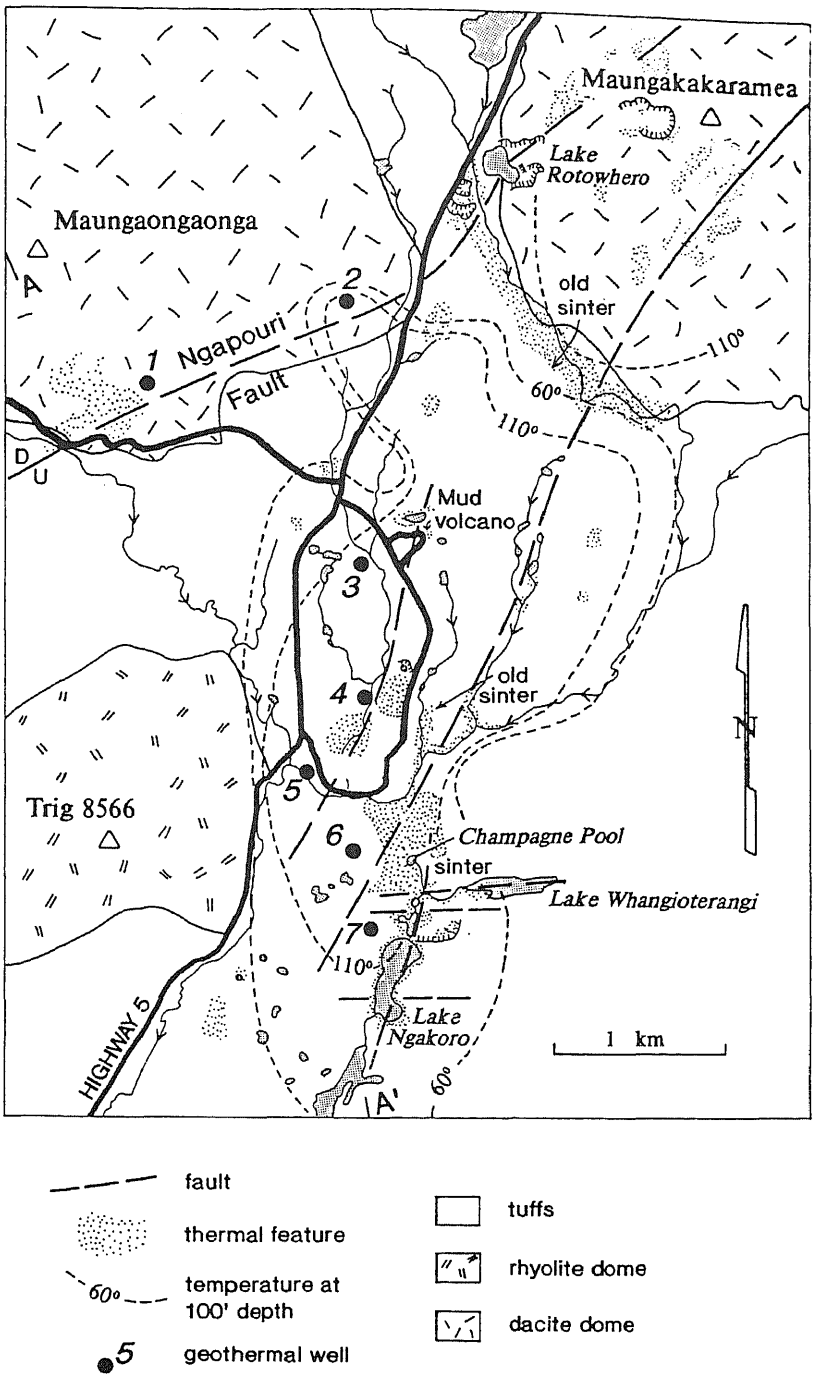

Fig. 6.3 Major thermal features at Waiotapu (after Lloyd 1959). Note: 100' is ≈30 m.

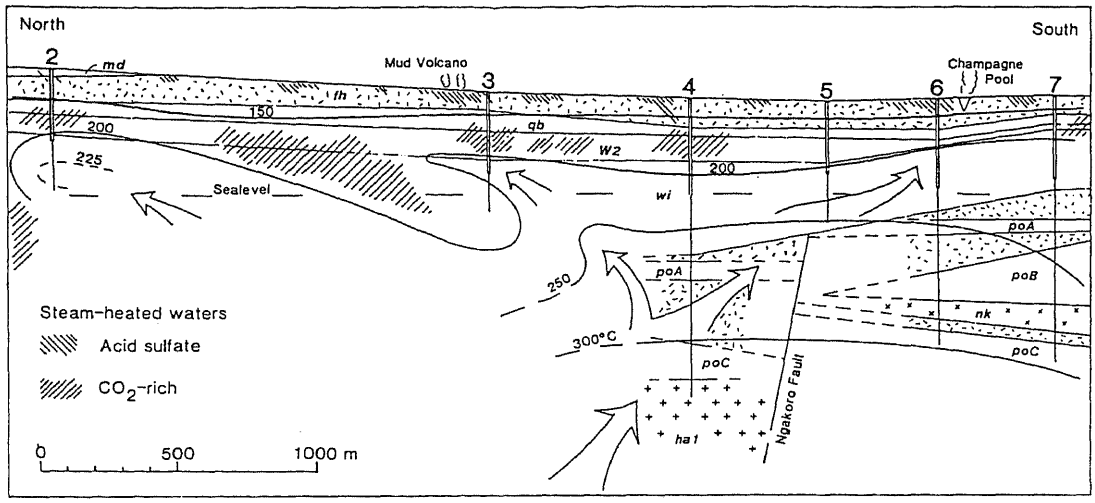

Fig. 6.4 N-S section through the Waiotapu system showing geology, distribution of steam-heated waters, isotherms, and flow paths of thermal fluids. Geological unit abbreviations are in Table 6.1. (From Hedenquist & Browne 1989.)

Soils

The main soils within and close to the Waiotapu thermal area have been mapped as Waikokomuka silty sands, formed mostly from hydrothermally altered Taupo Tephra deposits. They owe their chief properties to the accelerated weathering and leaching resulting from continuing hydrothermal activity. Pumice lapilli in the subsoils can be readily crushed by hand, in contrast to quite hard lapilli in cooler soils outside the thermal area. Vegetation cover is incomplete where soil temperatures are apparently too high for normal plant growth, and kanuka trees under these conditions are typically dwarfed and shallow rooted (Vucetich & Wells 1978). A series of pH measurements on soils sampled over the 0.8 km from Waiotapu Hotel to the thermal area (along Waiotapu Loop Rd) show a steady increase in acidity from 5.2 to 3.4. Insufficient data are available to classify the soils accurately but they may qualify as Udivitrands (if not sufficiently andic, then they might be Andic or Vitrandic Udorthents instead, because crystalline clays — alunite, illite, kaolinite, montmorillonite — tend to dominate over allophanic clays in these materials).

A profile description of a soil near a fumarole on Wiers Rd (after Vucetich & Wells 1978) is:

0-5 cm L	Dark brown loose kanuka leaves,
5-15 cm Ah	black sand; v. friable; loose; soft crumb structure; distinct boundary,
15-25 cm Bw	v. dark greyish brown silty sand; v. friable; weakly developed fine crumb and granular structure; numerous roots; distinct boundary,
25-35 cm BC	dark brown silty sand; weakly compact; structureless,
35 cm on	yellowish brown sand.

Towards the southern and northern margins of the thermal area, the altered Taupo materials are buried by ejecta from hydrothermal eruptions from which the Waiotapu and Ngahewa soils, respectively, are formed. A profile description of the Waiotapu stony silt loam on a 5° slope (after Vucetich & Wells 1978) is:

0-5 cm Ah	Dark brown silt loam with stones; v. friable; weakly developed v. soft crumb and granular structure; sharp boundary,
5-13 cm AC	dark brown stony silt loam; firm to friable; soft fine crumb structure,
13-23 cm C	pale brown stony silt loam; streaked brownish yellow; firm; structureless; merging boundary,
23 cm on 2C	pinkish white stony clay loam; massive.

These soils have pHs 3.8-4.5 and are likely to be Udorthents. Beyond the Waiotapu thermal area most soils are of the Taupo series (Vucetich & Wells 1978).

Thermal features and hydrology

Waiotapu (meaning 'sacred waters') is characterised by a large area of steaming ground and fumarolic activity associated with collapse craters, mud pools, and alteration due to acid-sulphate fluids, which form above the water table. Photographs, paintings, and eyewitness descriptions of the 19th century indicate former widespread steaming ground on the flanks and near the summit of Maungakakaramea (Rainbow Mountain). This thermal activity has declined in the last 60 years but nevertheless is responsible for the notable variegated colours of rocks exposed there. Springs discharging chloride waters lie at the water table and deposit siliceous sinter, but many are diluted by bicarbonate or sulphate waters (Fig. 6.5). Champagne Pool is situated in the south-central part of the field and is the only feature from which undiluted chloride waters discharge.

The subsurface hydrology was deduced from drill hole data and spring chemistry (Hedenquist & Browne 1989; Hedenquist 1991). Deep fluids ascend along temperature and pressure gradients that are close to boiling in the vicinity of Champagne Pool and near well 4. Temperature inversions at shallow levels (<300 m depth) encountered in wells 2 and 3, coupled with fluid chemistry (Figs. 6.4, 6.5), are interpreted to result from incursion of CO_2-rich steam heated waters (Hedenquist & Browne 1989). The southern part of the field is dominated by a southerly outflow towards the Waikato River (Fig. 6.6). Spring waters are dominated by chloride with variable amounts of bicarbonate and sulphate (Fig. 6.7).

Mineralogy

Despite the large areal extent of thermal activity, unaltered rocks dominate surface exposures. Surficial hydrothermal alteration is restricted to steaming ground, bubbling mudpots, and fumaroles, where alunite (natroalunite), kaolinite, amorphous silica, montmorillonite, cristobalite, and native sulphur occur. (Some properties of the platy kaolinite at Waiotapu are described in Wells et al. 1985.) Beneath the surface, acid-sulphate alteration is intense but is restricted to depths between 25 and 135 m (Figs. 6.8, 6.9). At greater depths, minor mordenite exists but is superseded by laumontite at about 170°C, and montmorillonite is rare. The deep alteration assemblage (>200°C) includes albite, adularia, K-mica, chlorite, epidote, and wairakite. Pyrite is ubiquitous and pyrrhotite occurs below 400 m depth. Calcite, quartz, and subordinate adularia fill fractures and veinlets. An example of a phase diagram relating the hydrothermal mineralogy and mineral chemistry to the fluid chemistry by means of component activities is given in Fig. 6.10 (Hedenquist 1986).

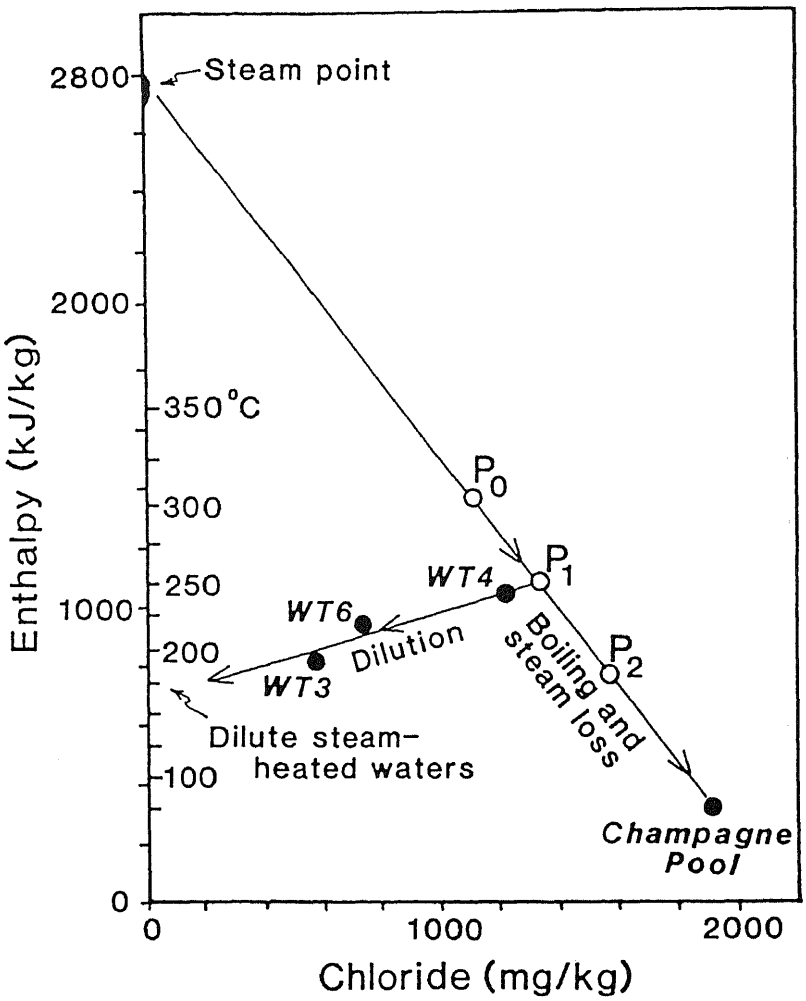

Fig. 6.5 Chloride-enthalpy plot of fluids discharged from Waiotapu wells and Champagne Pool. Undiluted fluid discharges from Champagne Pool and Wt-4 and originates from a parent fluid in the deep reservoir at ≈300°C. The other fluids are variably diluted by CO_2-rich steam-heated water (Hedenquist & Browne 1989).

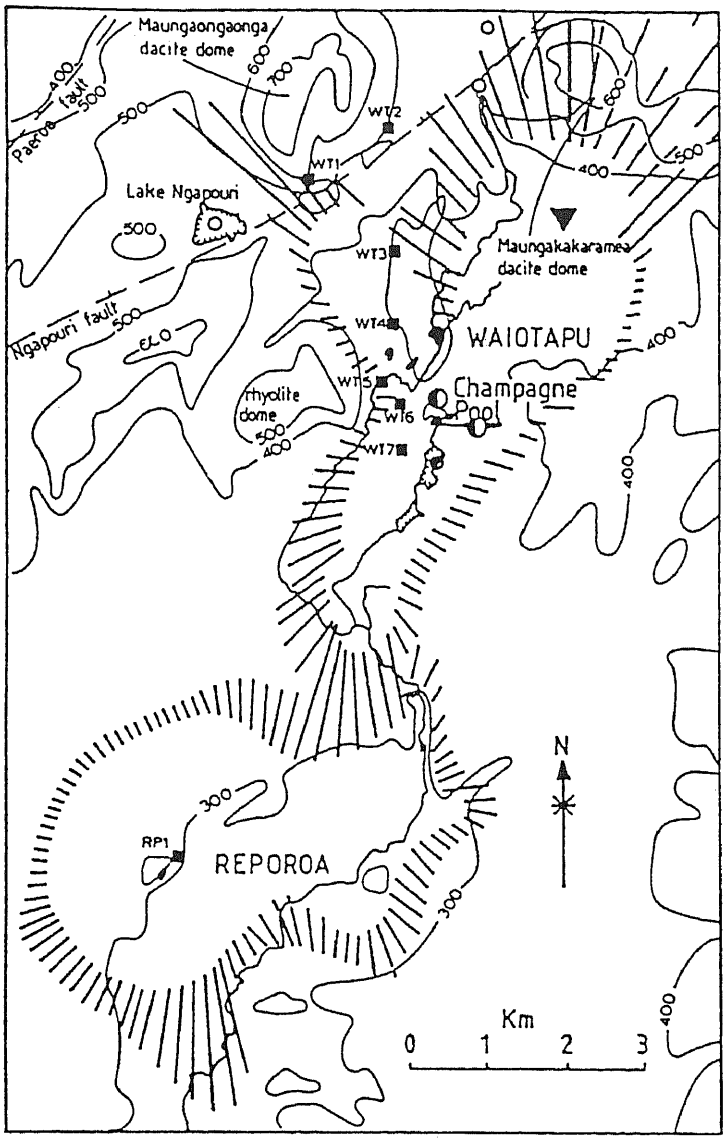

Fig. 6.6 The <10 Ωm resistivity anomaly for the Waiotapu and Reporoa geothermal areas, showing an outflow tongue of chloride water extending from Waiotapu to Reporoa (Healy & Hochstein 1973). (From Henley 1985.)

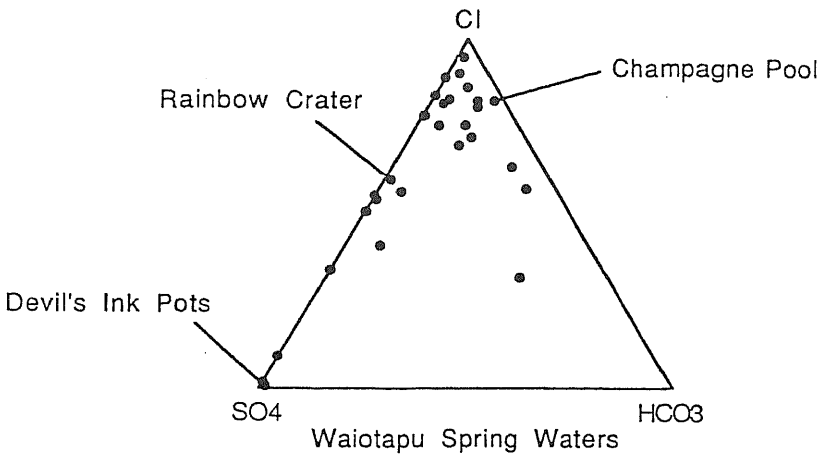

Fig. 6.7 Composition of spring waters at Waiotapu in terms of major anions (from Simmons et al. 1992; data from Hedenquist 1991).

Rare mineralisation in drill cores is characterised by disseminations of sphalerite, galena, and chalcopyrite, but none reaches 'ore' grade; gold and silver attain maximum concentrations of 0.2 ppm Au and 70 ppm Ag (Hedenquist & Henley 1985).

Spectacular mineralization is evident in Champagne Pool where orange precipitates, amorphous arsenic, and antimony sulphur compounds, containing up to 80 ppm Au and 175 ppm Ag, are accumulating at the margins of the pool. Thallium and mercury attain 320 and 170 ppm, respectively, in the precipitates (Weissberg 1969). These precipitates were not depositing in about 1930, so far as is known (e.g. Grange 1937), but in 1887 bright red precipitates were forming at Bridal Veil Falls, according to unpublished field notes of A.P.W. Thomas. Hedenquist & Henley (1985) suggested that the subsurface environment beneath Champagne Pool is a favourable site for precious metal deposition as here temperatures cool by boiling from 250 to 175°C. Champagne Pool itself represents a unique environment of mineralisation in that dissolved CO_2 maintains sufficiently low pH to stabilize precipitation of amorphous arsenic and antimony sulphur compounds which then adsorb Au and Ag from solution (Hedenquist & Henley 1985; Renders & Seward 1989; Webster 1990).

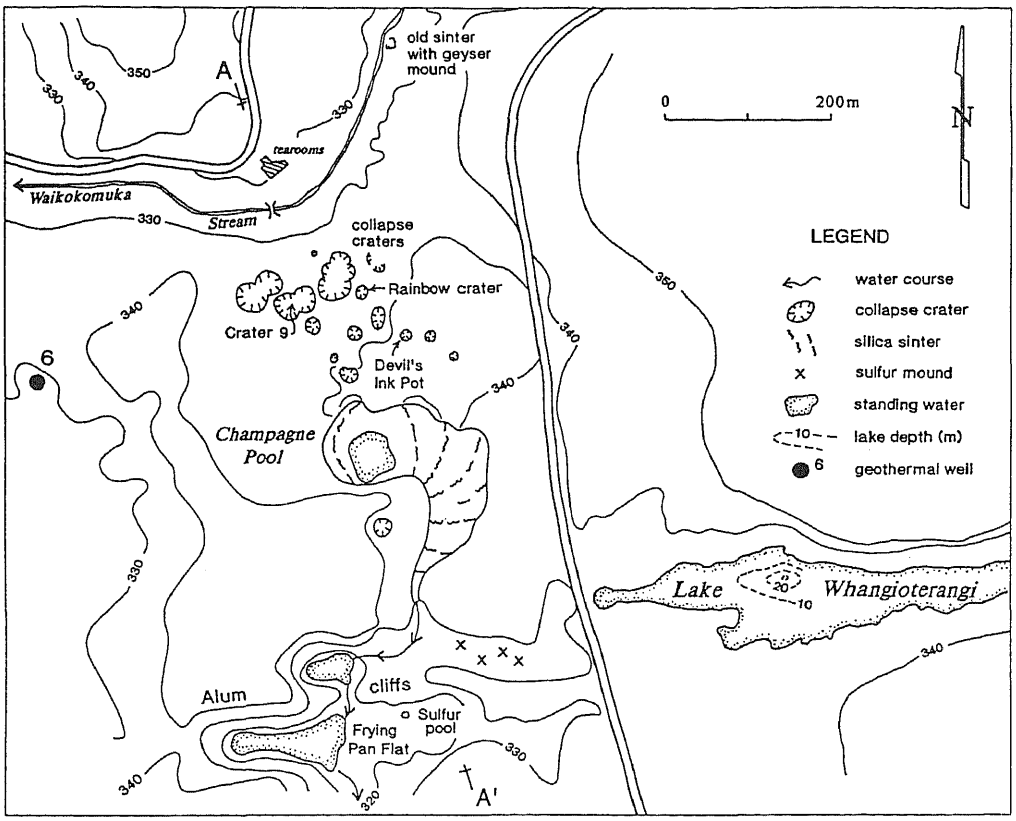

Fig. 6.8 Location of thermal features near Champagne Pool (from Simmons et al. 1992).

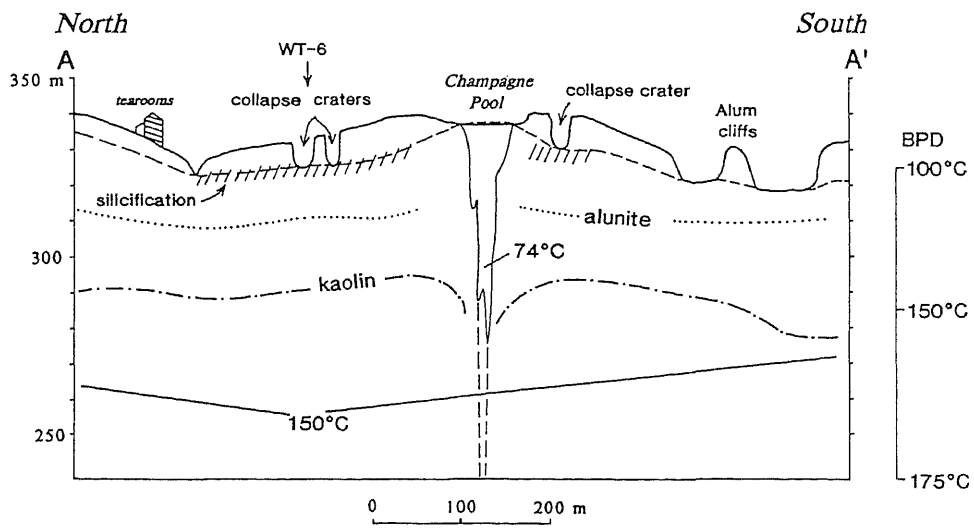

Fig. 6.9 N-S cross section through the collapse craters-Champagne Pool area, showing the water table and subsurface distribution of alunite and kaolinite. BDP is boiling temperature at depth indicated (from Simmons et al. 1992).

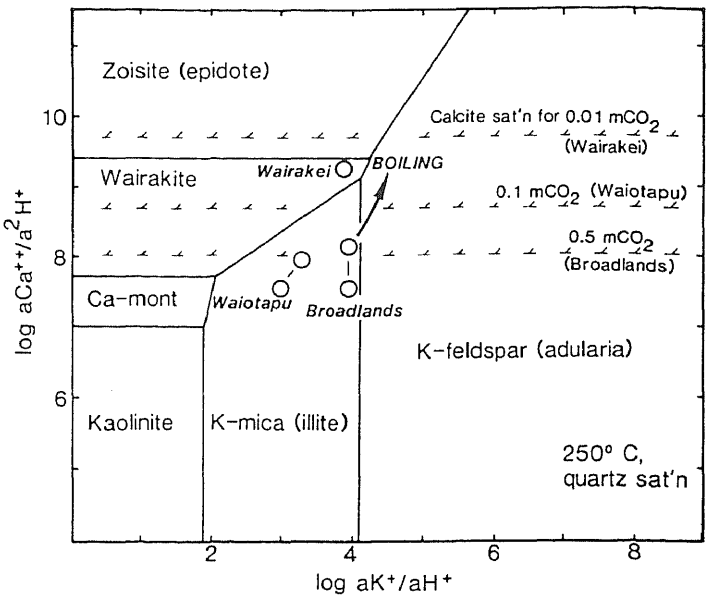

Fig. 6.10 Phase diagram relating hydrothermal mineralogy and mineral chemistry to fluid chemistry (from Hedenquist 1986).

Guided tour

Collapse pits

From the tea rooms we cross the Waikokomuka Stream (Fig. 6.8). Tuffs exposed on the south bank are coated with a mixture of amorphous silica and alunite which precipitated directly from mixed acid-sulphate-chloride waters draining into the stream. Underlying this veneer, the tuffs are silicified because of mixing between acid-sulphate and chloride waters at the water table. Unaltered Oruanui Ignimbrite crops out 2 m above stream level on the right side of the path, and contains numerous accretionary lapilli (chalazoidites or pisolites).

Twenty metres further along the path is an area of collapse pits ('craters'). Based on a conservative estimate, 70 million kg of rocks (density = 1.5 g cm^{-3}) were dissolved by acid-sulphate fluids to create unstable ground which then collapsed. Ground surrounding the collapse features contains cristobalite and sulphur, whereas alunite and kaolinite occur in mud pools on the pit floors. Notice how the ground resonates in places. Some of the deep pits (e.g. Rainbow Crater) contain a mixture of acid-sulphate and chloride waters, marking the location of the water table; other pit floors (e.g. Devil's Ink Pot) are perched above the water table and contain only acid-sulphate waters. In the vicinity of the Devil's Ink Pot, the surface is littered with fragmentary lithic material which is the explosion breccia erupted from the hydrothermal vent now occupied by Champagne Pool.

A feature of special interest is the presence of oil slicks and globules on the surface of some of the boiling pools. This occurs elsewhere in the Waiotapu area, notably at Kerosene Creek, near Rainbow Mountain. The petroleum is thought to be derived from carbonaceous material buried below the surface and undergoing distillation by thermal heat (Clark 1989).

Champagne Pool

This is a steep-sided, conical-shaped hydrothermal explosion crater 60 m deep. An inferred stockwork fracture pattern in rocks below the pool forms a vertical conduit which taps deep reservoir fluids at ≈230°C. Within the pool, the temperature is a constant 74°C from top to bottom because of rapid convection. Orange-coloured precipitates near the edge contain the amorphous arsenic and antimony sulphur compounds rich in gold and silver. The fluid effervesces CO_2 and bubbles nucleate at depths of only about 1 m below the surface. The high concentration of dissolved CO_2 results in a pH ≈5. Note that the water level in Champagne Pool is about 10 m higher here than in the surrounds.

In exposures south of Champagne Pool, hydrothermal explosion deposits overlie Taupo Tephra (1.85 ka). The breccia clasts are thought to derive from depths of <170 m; the large ballistic block is Oruanui Ignimbrite (Hedenquist & Henley 1985).

Lake Ngakoro Lookout

Alum Cliffs crater, directly below the lookout, is floored by pools discharging acid-sulphate-chloride waters, but also contains the dormant Waiotapu Geyser which discharged chloride water during the 1980s. To the south, Lake Ngakoro, and possibly Frying Pan Flat, are also hydrothermal explosion vents. To the east is Sulfur Mound Valley, which is a drained portion of Lake Whangioterangi, also visible from here.

We now walk around the base of Alum Cliffs and along the edge of Frying Pan Flat. Note evidence that there was indeed a geyser at the base of the cliffs.

Lake Whangioterangi

The interesting feature here is the zone of upwelling in the centre of the lake (25 m deep), which is the surface expression of a sublacustrine spring. Molten sulphur occurs on the lake bottom, as does a rather expensive sampler borrowed from the former DSIR!

Sulfur Mound Valley

This is a drained western portion of Lake Whangioterangi. The yellow mounds consist of vesicular suphur clasts and are interspersed among finely laminated beds of cristobalite; these are sublacustrine hydrothermal deposits. The vesicular sulphur clasts indicate that the sulphur was molten.

Mud Volcano

At the turn of the century, this mud volcano was over 2 m high and its base had a diameter twice this. The mud contains kaolinite, opal CT, quartz, and finely disseminated pyrite. The mud is 100°C in places and the fluid pH is 2.5

Lady Knox Geyser

This is artificial. It was constructed around 1906 by a Mr Scanlon (then chief warden of the Waiotapu prison farm) from a vigorously boiling spring. The orifice was restricted by an iron pipe surrounded by an artificial pumice cone and the geyser induced to erupt by soaping. Sinter deposits have since covered the structure, giving it a natural appearance (Lloyd 1959).

STOP 2 — Taupo sand on 1.85 ka Taupo Tephra, Wairakei

Taupo Tephra eruption 1850 years ago

The most recent eruption of the rhyolite Taupo volcano was the dramatic Taupo Tephra eruption about 1850 years ago, the most powerul and destructive eruptive episode since the Kawakawa eruption c. 22.6 ka. The Taupo eruption ejected at least 90 km^3 of pyroclastic material (Froggatt & Lowe 1990) and was centred on the Waitahanui Basin-Horomatangi Reefs area in the northeastern part of Lake Taupo (Lowe & Green 1992). It consisted of several closely-spaced phases (Fig. 6.11), climaxing in an exceptionally powerful and intense ultraplinian eruption that led to wholesale caldera collapse, over an area of ≈100 km^2, and generation of the Taupo ignimbrite (e.g. see Walker 1980; Wilson & Walker 1985; Wilson 1985, 1993; Houghton & Wilson 1986). Independent methods indicate that the height of the eruption column must have been 50-55 km, and that this ultraplinian phase lasted ≈6-17 h. The Taupo ignimbrite, with a volume (30 km^3) at least as great as that of all the earlier phases combined, is estimated to have been emplaced over about 400 s as a series of batches of material which coalesced to form a concentrated flow that travelled essentially radially outwards at speeds exceeding 200-300 m s^{-1} (Wilson 1985). The extreme violence of the flow caused it to be spread thinly over the landscape to generate an archetypal 'low-aspect ratio' ignimbrite with a range of facies and lateral variations (Walker & Wilson 1983)

Lake Taupo was esentially emptied during the eruption, generating what has been described as a 'volcanogene waterspout'. The fully water-charged column erupting from Taupo led to the Rotongaio ash member being deposited as wet mud into small gullies cut into the preceding Hatepe plinian deposits (Fig. 6.11). The lake probably took about 20-30 years to refill, reaching about 33 m above its present level to form several wave-cut benches (Lowe & Green 1992; Wilson 1993). It then fell to its modern level when the exit channel, the Waikato River, was re-established. Large blocks of pumiceous rhyolite (giant floated pumices) found in lake sediments overlying the Taupo Tephra deposits are inferred to be fragments that have spalled off a subaqueous dome (either Horomatangi Reefs or Waitahanui Bank), which was extruded perhaps 30 years after the Taupo eruption (Wilson 1993).

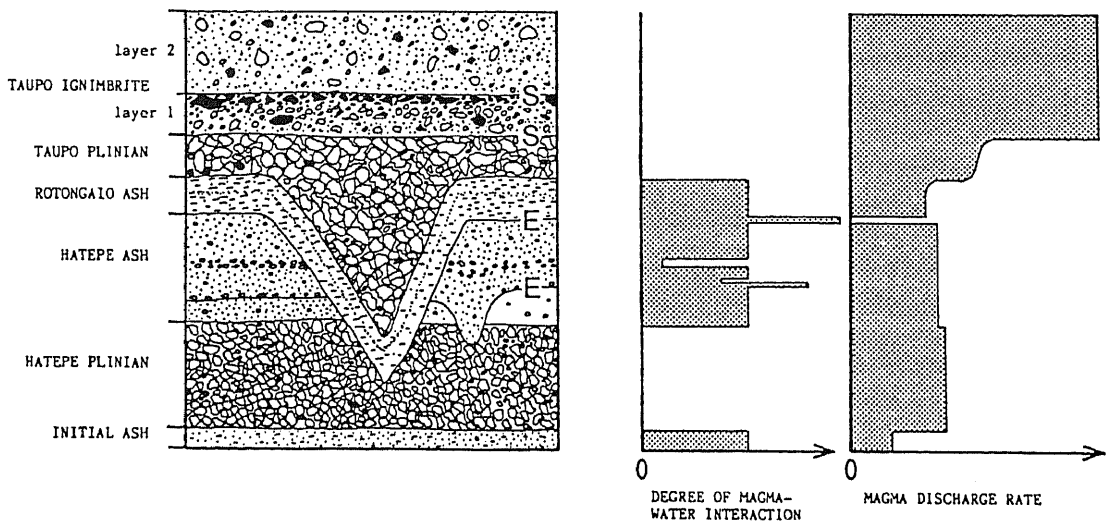

Fig. 6.11 Units making up the Taupo eruption sequence and associated magma-water interaction and magma discharge rate. E and S denote fluvial and pyroclastic-flow erosion surfaces, respectively. (From Houghton & Wilson 1986.)

The error-weighted mean of 41 radiocarbon ages on material associated with the eruption is 1850 ± 10 years BP, equivalent to a calendar date in the range 138—230 A.D. (mean c. 214 A.D.; Froggatt & Lowe 1990). A putative correlation between Roman and Chinese records of atmospheric phenomena was used by Wilson et al. (1980) to suggest a calendar date of c. 186 A.D. but the historical basis is disputed (Froggatt & Lowe 1990). However, this date does approximate (perhaps coincidentally) a date of 177 A.D. (1 s.d. range 166—195 A.D.) obtained by dendrochronology on trees buried by the ignimbrite. Fruit and seeds preserved in the buried forest, and the lack of an outer latewood ring, indicate that the eruption took place in late summer to early autumn (Froggatt & Lowe 1990; Clarkson et al. 1992).

Taupo sand profile developed on Taupo Tephra, Wairakei

The soil we will inspect is on privately owned land that was previously part of the Wairakei Research Station, DSIR. It was a reference soil for the 1981 'Soils with Variable Charge' North Island tour (Parfitt et al. 1981). The exposure is at U17/799834 at 450 m altitude near the crest of a hill about 500 m N of Wairakei village. Mean annual rainfall is 1280 mm. Native vegetation was probably a podocarp-dominated forest (Rijske & Vucetich 1980; Clarkson et al. 1992). Analyses of humus and phytoliths in the A horizon of Taupo soils show a higher degree of humification (type A humic acid) in the upper part than in the lower part, implying that the main source of phytolith changed from forest to grassland-type vegetation (Hosono et al. 1991). This change probably relates to the (partial) destruction of forests after ≈1000 years ago by Polynesians (e.g. McGlone 1983a; Newnham et al. 1989). The parent materials of the soil comprise pumiceous members of the Taupo Tephra Formation (erupted 1.85 ka), which overlie a weak paleosol on an earlier Taupo eruptive (Waimihia Tephra, 3.2 ka). The soil is friable to loose in the upper 1 m or so, and is somewhat excessively drained and droughty in summer. It is classed as an ashy/pumiceous, mesic, Typic Udivitrand.

Similar Taupo series soils occur on easy rolling and rolling terraces in the area, with deeper soils of the Oruanui series (Andic Haplorthods) at higher altitudes. In the valleys on flat to undulating terraces are shallow, compact Atiamuri series (probably Typic Udivitrands) formed from coarse, valley-ponded Taupo ignimbrite (visible from the hill top) (Rijske & Vucetich 1980). The Wairakei geothermal area to the south of S.H. 1 is also visible from the hill top.

The soil profile description is given in Table 6.2 with chemical, physical, and mineralogical data listed in Tables 6.3—6.4 (New Zealand Soil Bureau profile SB9577). Particle size grading curves are shown in Fig. 6.12. The clay fraction is dominated by allophane (Al/Si ≈2 to 2.5) and glass, with allophane making up ≈1-2% on a whole soil basis in the A and B horizons (Si_o x 7; Table 6.3). Ferrihydrite is ≈0.5% or less (Fe_o x 1.7; Table 6.3). Dry bulk densities in these soils generally range from ≈0.6 g cm^{-3} in topsoils to a maximum of ≈1.0 g cm^{-3} in subsoils (Read 1974).

Table 6.2 Profile description for Taupo sand, Wairakei (from Parfitt et al. 1981)

Profile	Depth (cm)	
Ap	0- 9	very dark brown (10YR 2/2) gritty sand; friable; weakly developed medium and fine nut structure breaking to crumb and granular structure; many fine lapilli (2-6 mm) of yellowish brown(10YR 5/6) colour; few fine black (10YR 2/1) pieces of charcoal; many fine roots; distinct smooth boundary,
Bw	9-24	yellowish brown (10YR 5/6) and olive yellow (2.5Y 6/6) gravelly sand; friable; weakly developed medium block structure breaking to crumb and single grain; many fine grey (10YR 5/1) rhyolite fragments; few medium (10 mm) yellowish brown (10YR 5/6) lapilli; many fine roots; few coarse roots; indistinct irregular boundary,
BC	24-34	pale brown (10YR 6/3) gritty sand; very friable; weakly developed crumb and granular structure; many fine grey (10YR 5/1) rhyolite fragments and few yellowish brown (10YR 5/6) lapilli; many fine roots; distinct irregular boundary,
C1	34-64	very dark grey (10YR 3/1) and very pale brown (10YR 7/4) fine gravel (2-5 mm); mainly rhyolite (max. size to 50 mm) loose; single grain; few black (10YR 2/1) carbonised branches (40-50 mm); abundant fine roots; distinct irregular boundary,
C2	64-95	yellow (10YR 7/6) pumice lapilli; loose; single grain; strong brown (7.5YR 4/6) and yellowish brown (10YR 5/8) iron staining on lapilli; lapilli vary from 5 to 100 mm; many medium grey (10YR 5/1) rhyolite fragments (4-8 mm) few reddish brown (5YR 4/4) rhyolite fragments; few fine roots; sharp smooth boundary,
C3	95-102	grey (10YR 5/1) loamy sand; friable; weakly developed medium block structure breaking to weakly developed fine blocky and crumb structure; many distinct dark yellowish brown (10YR 6/6) tubular staining; sharp smooth boundary, (Rotongaio Ash)
C4	102-103	very pale brown (10YR 7/4) pumice gravel (2-10 mm); loose; single grain; sharp smooth boundary,
C5	103-104	light grey (2.5Y 7/2) gritty loamy sand; firm; massive; sharp smooth boundary,
2Ah	104-108	dark brown (7.5YR 3/4) loamy sand; slightly greasy; soft; massive breaking to single grain; sharp smooth boundary,
2C	108-113	brown (10YR 5/3) and yellowish brown (10YR 5/6) gritty sand; loose; single grain; abundant fine lapilli (5-10 mm); distinct smooth boundary,
3Bw	*on*	yellowish brown (10YR 5/6) gritty loamy sand; slightly greasy; slightly firm; weakly developed medium blocky breaking to crumb and single grain; many fine (2-3 mm) lapilli.

Table 6.3 Chemical and mineralogical data, Taupo sand, Wairakei (from Parfitt et al. 1981)

Depth (cm)	Hor.	pH H_2O	pH KCl	pH ΔpH	pH NaF	Exchangeable cations (meq/100 g) Ca	Mg	K	Na	H (KCl)	Al (KCl)	Extr. Acidity (pH 8.2)	Acidity-Al (meq/100 g)	CEC (meq/100 g) ECEC	NH_4OAc (pH 7)	Σ Cations (pH 8.2)	Base saturation (%) Σ bases CEC NH_4OAc	Σ bases Σ Cations
0-9	Ap	5.0	4.2	-0.8	10.0	3.2	0.29	0.65	0.05		1.9	31.1	29.2	6.1	17.3	35.3	24	12
9-24	Bw	5.5	4.6	-0.9	10.7	1.1	0.03	0.57	0.06		0.60	14.5	13.9	2.4	6.3	16.3	29	11
24-34	BC	5.9	5.0	-0.9	10.3	0.7	0.03	0.90	0.07		0.08	6.3	6.2	1.8	3.5	8.0	49	21
34-64	C1	6.4	5.1	-1.3	8.1	2.3	0.21	0.97	0.63		0.00	3.0	3.0	4.1	4.6	7.1	89	58
64-95	C2	6.7	5.8	-0.9	9.3	1.0	0.06	1.18	0.24		0.03	1.6	1.6	2.5	2.9	4.1	86	61
95-102	C3	6.3	4.9	-1.4	9.4	0.9	0.07	1.58	0.50		0.03	1.5	1.5	3.1	3.7	4.6	84	67

Depth (cm)	Hor.	Total C (%)	Total N (%)	P (mg/100 g) H_2SO_4 (0.5 M)	P Inorg.	P Org.	P Retention (%)	Dithion. cit. (%) Fe	Dithion. cit. (%) Al	Tamm ox. (%) Fe	Tamm ox. (%) Al	Tamm ox. (%) Si	Pyrophos. (%) Fe	Pyrophos. (%) Al	Reserves (meq/100 g) K_c	Reserves (meq/100 g) Mg_r	Extractable S (ppm)
0-9	Ap	5.3	0.35	73	84	49	44	0.37	0.43	0.29	0.66	0.11	0.19	0.43	0.09	1.2	10
9-24	Bw	1.4	0.08	52	62	22	44	0.26	0.31	0.20	0.75	0.25	0.08	0.22	0.11	1.4	3
24-34	BC	0.4	0.03	24	32	11	29	0.20	0.14	0.13	0.42	0.15	0.03	0.10	0.13	1.7	3
34-64	C1	0.3	0.01	33	36	4	5	0.23	0.06	0.18	0.04	0.01	0.03	0.03	0.13	2.8	0
64-95	C2	0.2	0.01	24	32	3	11	0.22	0.11	0.14	0.13	0.07	0.03	0.04	0.16	2.2	4
95-102	C3	0.1	0.01	9	17	1	11	0.21	0.06	0.18	0.12	0.06	0.03	0.04	0.34	1.7	3

Depth (cm)	Hor.	Clay Fraction (%) Mica-Smectite	Mica-Vermiculite	Smectite	Vermiculite	Interlayered Hydrous Micas	Mica	Kaolinite	Halloysite	Gibbsite	Quartz	Cristobalite	Allophane	Feldspar	Glass	Hematite	Sand Fraction (%) Quartz	Feldspar (acid)	Andesine	Glass	Muscovite	Biotite	Hornblende	Augite	Hypersthene	Epidote	Quartz Ag	Apatite	Magnetite	Plant opal
0-9	Ap							23					2		75		S		c	A		tr	tr	tr	S			tr	R	
9-24	Bw							7					14		79				S	A					S				R	
24-34	BC							3					9		88				S	A				tr	S				R	
34-64	C1							3					5		92		S		C	A			R	tr	c		R		R	
64-95	C2												6		94		R		c	A				R	R				tr	
95-102	C3											5	3	5	87				S	A					S				S	

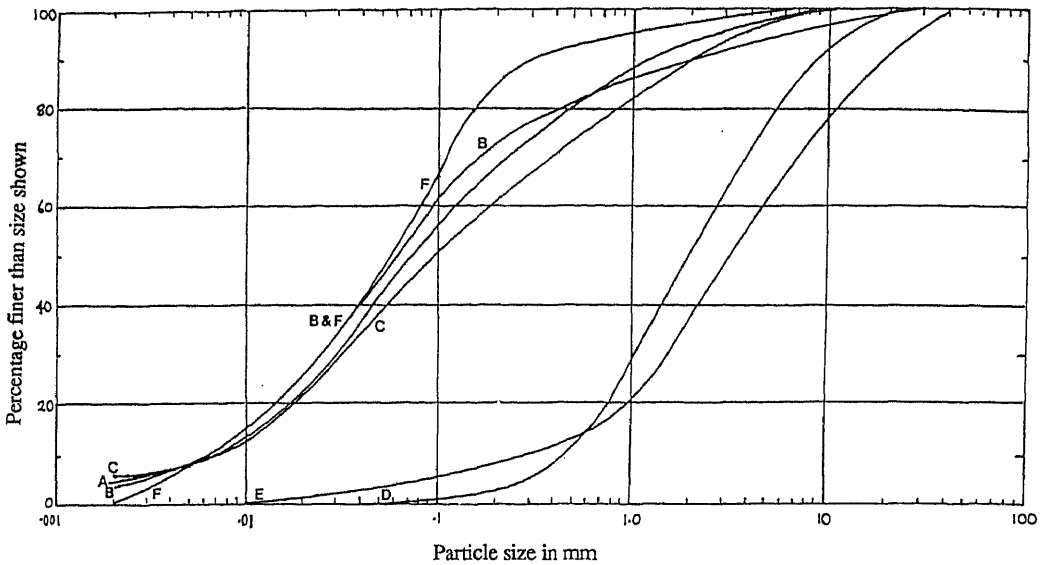

Fig. 6.12 Size grading curves for Taupo sand, Wairakei. A, 0-9 cm; B, 9-24 cm; C, 24-34 cm; D, 34-64 cm; E, 64-95 cm; F, 95-102 cm (from Parfitt et al. 1981).

Table 6.4 Particle size data and 1500 kPa water retention, Taupo sand, Wairakei (from Parfitt et al. 1981)

Depth (cm)	Hor.	Sand		Silt	Clay	Stones (%)	15 bar water	
		2-0.1 mm (%)	0.1-0.05 mm (%)	0.05-0.002 mm (%)	<0.002 mm (%)		Field moist (%)	Air Dry (%)
0-9	Ap	40	18	38	4	(7)	12.9	10.3
9-24	Bw	30	19	48	3	(10)	7.8	4.6
24-34	BC	41	14	41	4	(12)	4.6	2.5
34-64	C1	98	2	0	0	(52)	2.6	2.0
64-95	C2	82	3	15	0	(66)	6.0	1.6
95-102	C3	35	21	43	1	(4)	4.6	2.4

STOP 5 — 10 ka sequence of pumiceous tephra beds and paleosols, De Brett section (Taupo)

Late Quaternary tephras from Taupo volcano

The De Brett section on the Napier-Taupo road is the type section for a number of Taupo eruptives of Holocene age (Vucetich & Pullar 1973; Froggatt & Lowe 1990). The first radiocarbon date published in New Zealand (NZ1, 1820 ± 150 yr BP; on Hatepe Lapilli) was obtained near here (Baumgart 1954), and the section is now a registered 'geological monument'. The deposits are highly siliceous with pumiceous glass (SiO_2 75-76%, hydrous basis), plagioclase feldspar, quartz, and minor hypersthene, augite, and Fe-Ti oxides, being the dominant minerals (Froggatt & Lowe 1990; Stokes et al. 1992). Some units also contain rock fragments and obsidian clasts.

The general stratigraphy and chronology is summarised in Fig. 6.13 but very recent work by Wilson (1993) has shown that this is an oversimplified interpretation. He has now identified a total of 28 eruptions post-dating the 22.6 ka Kawakawa eruption, the first at c. 17.2 ka and the latest at c. 1.82 ka. The deposits of seven eruptions largely correspond to previously defined tephra formations (Karapiti, Poronui, Opepe, Waimihia, Whakaipo, Mapara, and Taupo), but the Motutere and Hinemaiaia are reinterpreted to represent the products of 12 eruptions, while the remaining nine eruptions are newly recognised. All of the eruptions have originated from within Lake Taupo, the vent positions being noticeably concentrated along a 55 km-long NE-SW lineament along the eastern side of the lake (Wilson 1993). The eruption deposits reflect great variations in parameters such as dispersal characteristics of the fall deposits, the formation of pyroclastic flows, the degree of magma-water interaction, vesicularity, and so on. Eruption volumes vary by more than three orders of magnitude between 0.01 and >44 km^3, and repose periods by more than two orders of magnitude from ≈20 to 6000 years. Wilson (1983) has shown that the repose periods in the sequence are not randomly distributed but show 'self-similar properties'. The repose period before or after any eruption is unrelated to the erupted volume so that prediction of the time and size of the (inevitable) next eruption is impossible. It appears that in terms of time and erupted volume, the post-Kawakawa record at Taupo is best considered as eruptive 'noise' superimposed on the more uniform, longer term activity in the central TVZ, where very large eruptions (> 100 km^3), such as Kawakawa, occur at more evenly spaced intervals of one per 40 000 to 60 000 years (Wilson 1993).

Clay mineralogy of paleosols on Whakaipo and Mapara tephras

Green (1987) analysed the weak paleosols formed on Whakaipo (2.7 ka) and Mapara (2.1 ka) tephra deposits here as part of a wider study on the weathering of buried paleosols (e.g. Stop 3, Day 2; Hodder et al. 1990). The site is at U18/799731 and 376 m altitude with a mean annual rainfall of 1011 mm and a mean annual temperature of 11.6°C. Native vegetation was probably podocarp-dominated forest. The time for weathering of the Whakaipo Tephra paleosol is ≈550 ± 50 years; that for the Mapara Tephra is ≈290 ± 50 years.

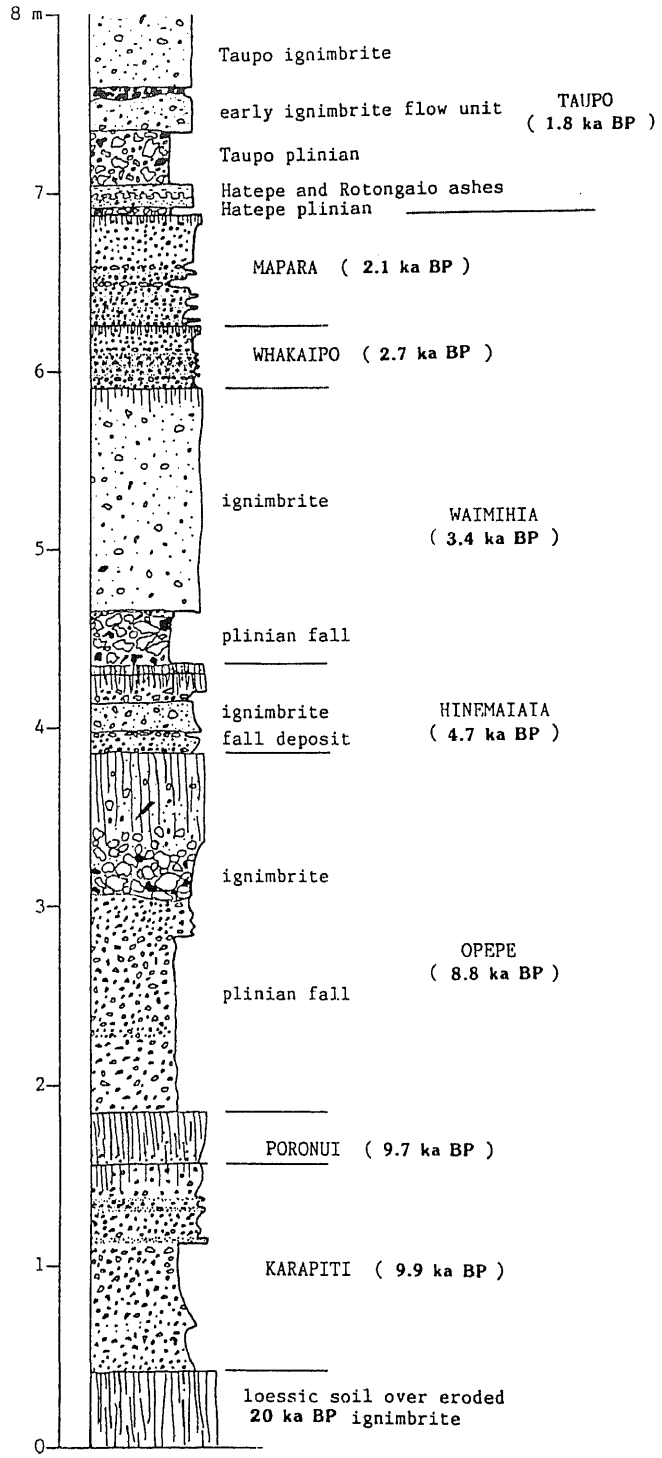

Fig. 6.13 Composite stratigraphic section through the post-10 ka pyroclastic deposits and paleosols, De Brett section (from Houghton & Wilson 1986).

An abbreviated profile description of these beds is (from Green 1987):

0-100 cm	Taupo Ignimbrite
100-130 cm	Taupo Lapilli
130-140 cm	Hatepe & Rotongaio ashes
140-145 cm	Hatepe Ash
145-155 cm 5Bwb	Reddish grey (2.5YR 4/1) gritty loamy sand; many dark lithic fragments; distinct wavy boundary (Mapara Tephra),
155-165 cm 5BCb	brownish grey (7.5YR 5/1) fine to coarse sand; distinct bounday (Mapara Tephra),
165-205 cm 5Cb	dull yellow orange (10YR 7/3) fine sand to coarse lapilli, distinct wavy bounday (Mapara Tephra),
205-213 cm 6Bwb	greyish brown (7.5YR 4/2) gritty loamy sand; distinct wavy bounday (Whakaipo Tephra),
213-219 cm 6BCb	dull yellow orange (10YR 7/3) medium sand; many lithic and pumice lapilli; distinct wavy bounday (Whakaipo Tephra),
219-240 cm 6Cb	pale yellow (2.5Y 7/3) shower-bedded coarse sand to coarse lapilli, distinct wavy bounday (Whakaipo Tephra),
on	paleosol on Waimihia Tephra.

The paleosols (buried Bw horizons) were analysed using acid oxalate and pyrophosphate dissolution techniques (Table 6.5), together with IR spectroscopy and DTA (Figs. 6.14, 6.15). The oxalate analyses on whole samples indicate that allophane (Al/Si is ≈2.0) predominates. However, Green (1987) interpreted from all the analyses that the clay fractions in both paleosols are dominated by glass followed by Si-rich allophane, followed in turn by organic matter, Al-rich allophane, ferrihydrite, and traces of halloysite and quartz. The apparent co-existence of both Si-rich and Al-rich allophane, and traces of halloysite, suggests that Si in soil solution may be near 10 g/m^3 and perhaps fluctuates with seasons or vegetational effects, or varies between weathering microsites.

Table 6.5 Selected analyses of paleosols on Whakaipo and Mapara tephras, De Brett section (after Green 1987)

	Sand %	Silt %	Clay† %	Org. C %	Al*o* %	Al*p* %	Al/Si ratio	Si*o* %	Fe*o* %	Fe*p* %	Alloph. %	Ferrihyd. %
Mp	65	32	3	0.1	0.06	neg	2.0	0.03	0.04	neg	0.2*	0.1
Wo	66	29	5	0.6	0.27	neg	2.1	0.13	0.21	neg	1.0*	0.4

neg = negligible † clay <2 μm, silt 2-63 μm, sand >63 μm

* Allophane wt% in the clay, silt, and sand fractions in Mp are 0.15, 0.06, 0.00, respectively (total 0.2); in Wo, they are 0.97, 0.63, 0.00, respectively (total 1.6).

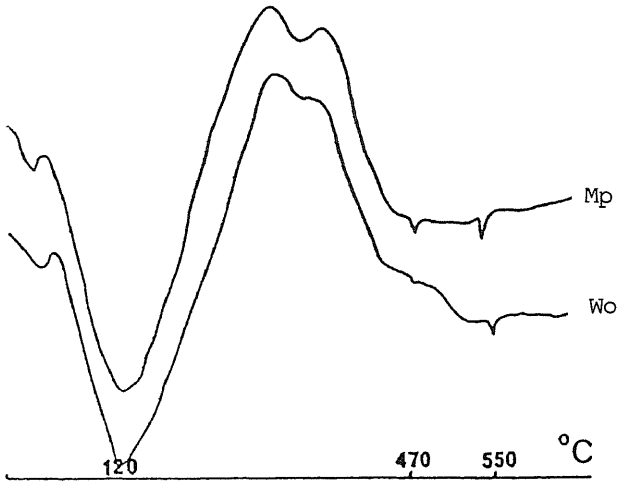

Fig. 6.14 DTA thermograms of the clay fraction of paleosols on Mapara (Mp) and Whakaipo (Wo) tephras at the De Brett section. The 460°C endotherm, halloysite; 550°C endotherm, silica phase change, probably quartz (from Green 1987).

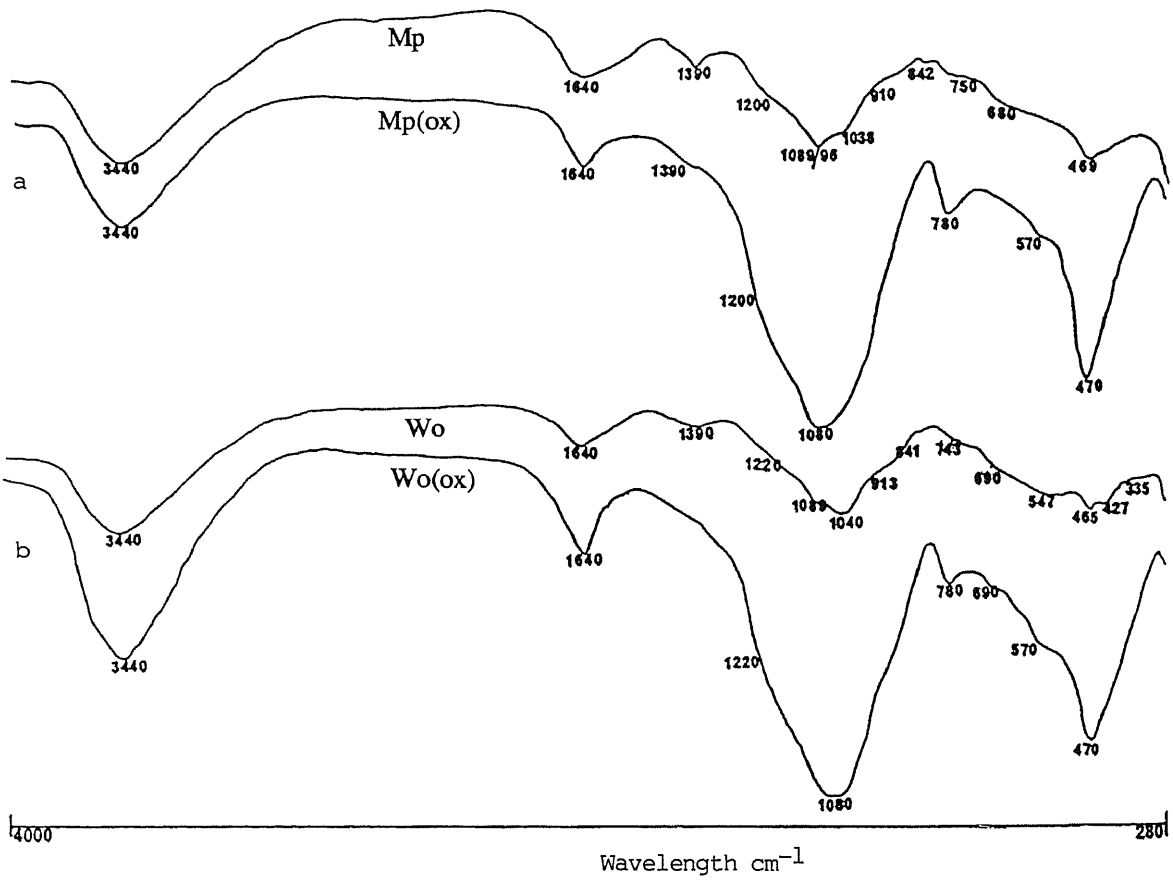

Fig. 6.15 Infrared spectra of (a) Mapara paleosol, Mp, and oxalate residue, Mp(ox), and (b) Whakaipo paleosol, Wo, and oxalate residue, Wo(ox), at the De Brett section (from Green 1987).

7. DAY 4: TOKAANU—WAITOMO—HAMILTON—AUCKLAND

Outline of Day 4 (Friday 16 July)

8.00-9.30 am	Depart Tokaanu Hotel and travel to Taumaranui via Waituhi Saddle (70 km)
9.30-10.00 am	STOP 1 — Morning tea at Taumaranui
10.00-11.30 am	Travel to Waitomo Hotel, Waitomo (107 km)
11.30-12.45 pm	STOP 2 — Lunch at Waitomo Hotel
12.45-1.00 pm	Travel to Waitomo Cave (1 km)
1.00-2.00 pm	STOP 3 Waitomo Cave tour
2.00-3.15 pm	Travel to Hamilton (79 km)
3.15-4.00 pm	STOP 4 — Ferrihydrite deposits, Waikato River area, Hamilton
4.00-5.00 pm	STOP 5 — Afternoon tea at Waikato Museum, and museum viewing, Hamilton
5.00-7.00 pm	Travel to Travellers' International Hotel, Auckland (126 km). Overnight stop. Evening: Farewell Dinner Party (8.00 pm) Next morning (Sat 17 July): Breakfast; Flights to Australia

The route today covers nearly 400 km (Fig. 7.1) and so we have time for only one scientific stop. However, there are many other features of interest to see on the journey. We initially skirt around the southern margins of Lake Taupo, passing the fumaroles of the Waihi Steaming Cliffs, and then climb over andesite lavas and around rhyolite domes draped with both andesitic and rhyolitic tephras. We also pass through occasional outcrops of pinkish Whakamaru Ignimbrite (0.35 Ma). If weather conditions are appropriate, we may pause briefly at Waituhi Saddle (869 m) for a view of the stratovolcanoes of Tongariro National Park. The terrain is then dominated by uplifted sedimentary rocks, mainly Miocene mudstones and flysch (alternating sandstone-mudstone) deposits, and Mesozoic greywacke. Smectite and illite are the dominant clay minerals in the Miocene sediments with smaller amounts of chlorite, kaolinite, and interstratified minerals (chlorite-smectite, chlorite-vermiculite, illite-smectite, and illite-chlorite-smectite) (Hume & Nelson 1982). Landscape features roughly parallel major N-S and NE-SW trending fault structures.

Around Te Kuiti (home of the current Prime Minister), Oligocene calcareous sandstones, siltstones, and especially limestones appear, often forming distinctive bluffs, isolated crags, and sinkholes (tomos). Drainage is mainly underground and numerous caves, including Waitomo (meaning 'water cavern'), occur in the region. As one might expect by now, much of the area is mantled by tephra deposits of varying thickness and composition, with Andisols common except on steep and eroded slopes where, typically, Inceptisols may form. Sheep and some beef farming are the main land uses in the region.

North of Otorohanga we see the low-angle, basaltic composite cones of the Alexandra Volcanics (aged between 2.74 and 1.60 Ma) that lie on a remarkably straight NW-orientated (300°) line. The steepish terrain then gives way to the rolling, tephra-draped lowlands and pastures of the Hamilton Basin. After Hamilton, we follow the Waikato River through Huntly, centre of a coal mining region (local coal measures are Eocene in age), and eventually return to Auckland and the tour conclusion.

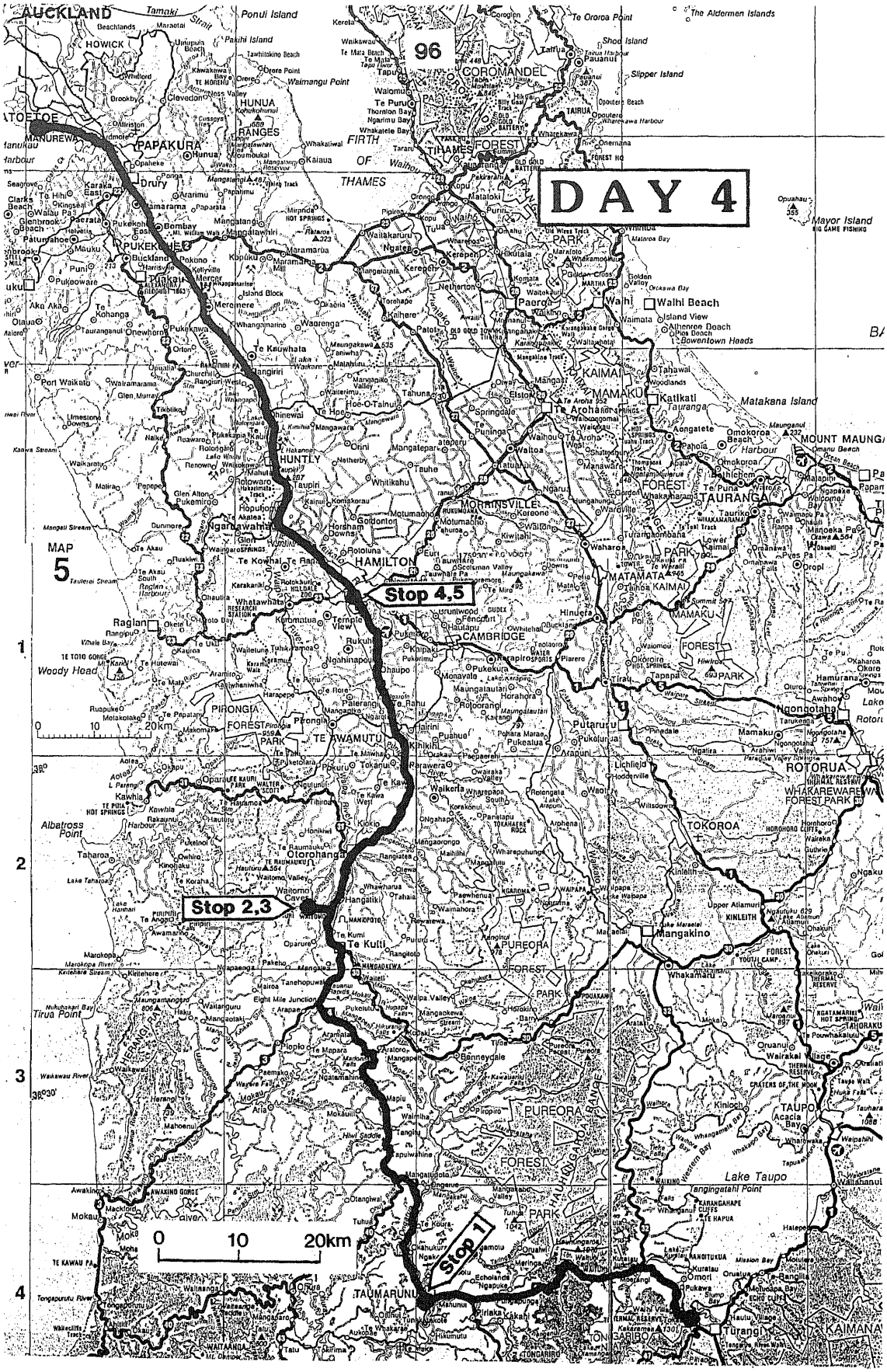

Fig. 7.1 Tour route and stops, Day 4.

STOP 4 - Ferrihydrite deposits near the Waikato River, Hamilton

Ferry Bank

The main site, known as the 'Ferry Bank ferrihydrite', is in the heart of Hamilton City (population ≈100 000) on the left bank of the Waikato River near the Waikato Museum of Art and History (Fig. 7.2). (Prior to the first bridge construction in 1879, this area marked the ferry bank landing for transport across the river.) The naturally-occurring ferrihydrite is found in several drains and gutter seepages alongside walking tracks by the river. The water in the drains has passed through the c. 19-15 ka volcanogenic sediments making up the Hinuera Formation, which are in places capped with thin tephra deposits (see Stop 5, Day 1). Ferrihydrite is a poorly crystalline iron oxide mineral with high specific surface area (typically 200-500 $m^2 g^{-1}$) that is a widespread minor constituent in New Zealand soils — minor in the sense of mass% concentration (usually <5%) but highly significant in terms of the area of reactive surfaces in the soils (Childs 1987a, 1992a; see also Section 3 above).

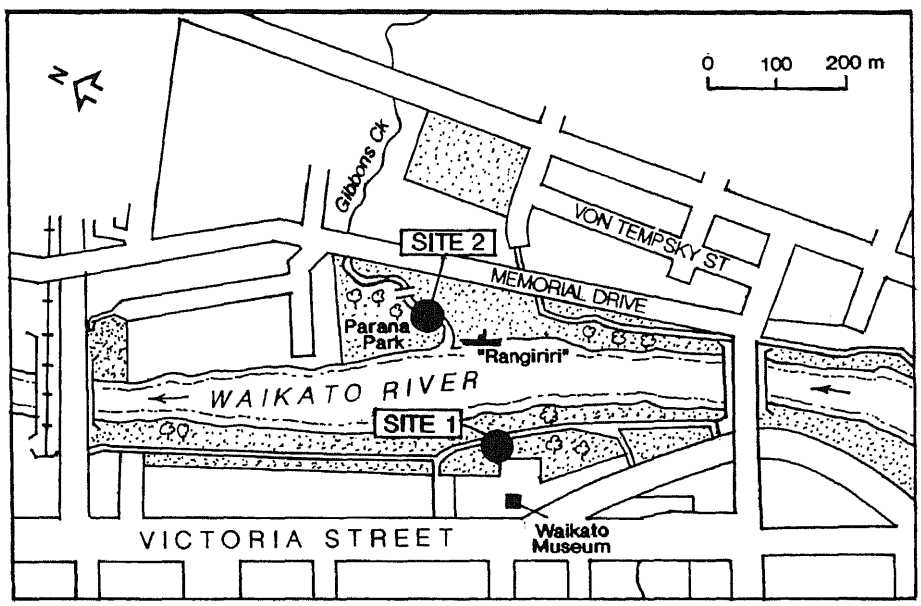

Fig. 7.2 Location of ferrihydrite sites near Waikato River, Hamilton. Site 1, Ferry Bank seepage/drains; Site 2, Gibbons Creek.

The Ferry Bank ferrihydrite is not a major one but it illustrates the rapid oxidation of groundwaters containing the products of volcanogenic or tephra weathering that often give rise to the formation of ferrihydrite in New Zealand. Natural ferrihydrites commonly contain up to ≈9% Si, which is thought to inhibit the growth of arrays of atoms sufficiently to prevent the formation of more crystalline iron such as goethite and hematite. The best deposits of natural ferrihydrite in New Zealand occur half way up the slopes of Mts Ruapehu and Taranaki (Childs et al. 1982, 1986) — not suitable places to visit on a field trip in July!

The XRD pattern of the ferrihydrite at this site consists of two very broad bands (centred about 0.26 nm and 0.15 nm) with a very small third band (about 0.22 nm) (Fig. 7.3). Material such as this is often referred to as 'two-' or 'three-line' ferrihydrite (Childs 1992a). Analysis by XRF of a Ferry Bank sample is given in Table 7.1, which also includes analyses of two samples from Mt Taranaki for comparison.

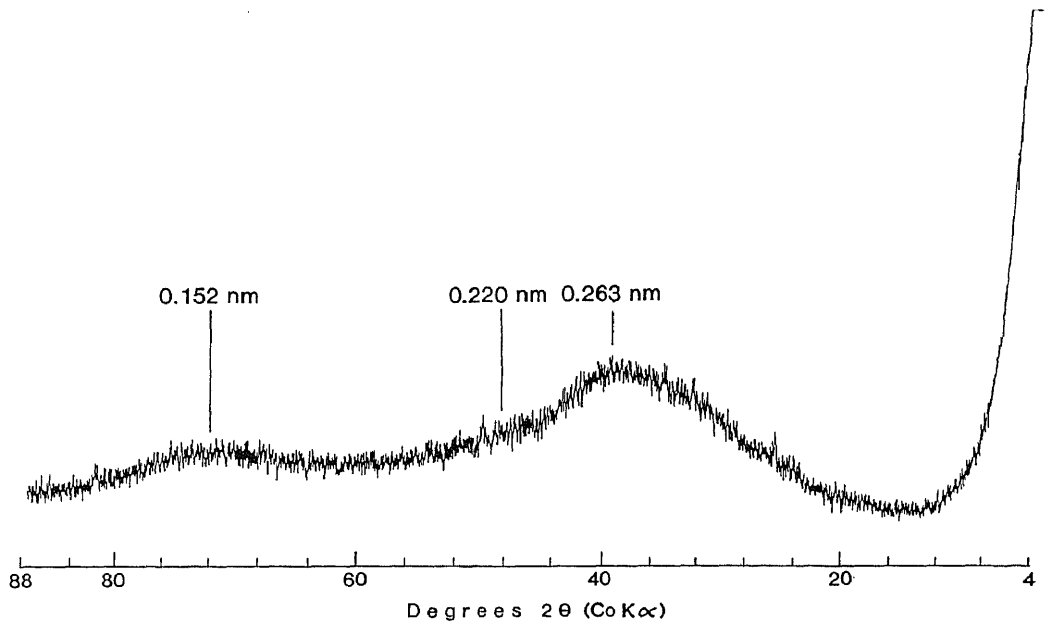

Fig. 7.3 XRD pattern of Ferry Bank ferrihydrite, Hamilton (C.W. Childs pers. comm. 1993).

Gibbons Creek

If time permits, we may visit a nearby second site, Gibbons Creek, draining into the right bank of the Waikato River in Parana-Memorial Park near the old paddle steamer *P.S. Rangiriri* (Fig. 7.2). This stream was artificially regraded by the Hamilton City Council in 1983-84 and the thin reddish yellow deposits — probably ferrihydrite — on each of the water falls have appeared since that time. The stream drains a gully cut into the Hinuera Formation. The lowest reaches cut through Taupo Pumice Alluvium, which was deposited as an aggradational terrace soon after the Taupo Tephra eruption c. 1.85 ka.

Table 7.1 XRF analysis* of the Ferry Bank ferrihydrite near Waikato Museum, Hamilton (from C.W. Childs pers. comm. 1993), and of Kokowai Springs ferrihydrite, Taranaki (from Childs et al. 1986)

	Ferrybank			*Kokowai Springs*		
				PC1020[a]	PC1022[b]
Fe	41.59	Fe_2O_3	59.47	Fe 53.9	44.7
Mn	0.05	MnO	0.06	Mn 0.03	0.55
Ti	0.04	TiO	0.07	Ti 0.02	0.04
Ca	0.36	CaO	0.50	Ca 0.21	0.67
K	0.26	K_2O	0.31	K <0.01	0.06
S	<0.01	SO_3	nd	S nd	nd
P	0.32	P_2O_5	0.73	P 0.37	0.09
Si	8.99	SiO_2	19.25	Si 4.69	8.16
Al	0.81	Al_2O_3	1.54	Al 0.44	0.65
Mg	0.08	MgO	0.14	Mg 0.09	0.12
Na	<0.07	Na_2O	<0.09	Na 0.24	<0.20
H2O[+]†	17.75	H2O[+]	17.75	H2O[+] 10.1	14.0
		Total	99.81		

* Wt% on oven-dry basis † H2O[+] = weight loss on ignition at 1000°C for 1 h
a Sample A: thick, extensive deposits at main spring vent
b Sample B: thin deposit (0.01 mm) on boulders downstream from vent

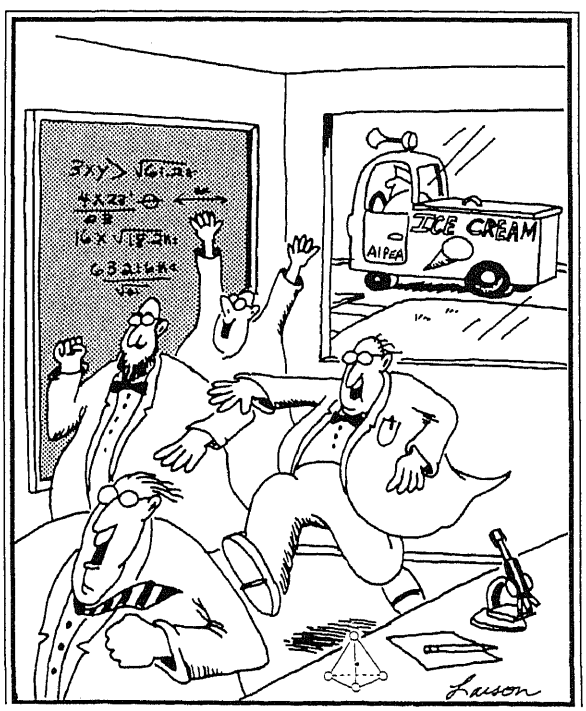

(From Larson, G. 1989. *The Far Side Gallery 2*. Futura Publications, London.)

8. REFERENCES

Ahn, J.H.; Peacor, D.R. 1987. Kaolinization of biotite: TEM data and implications for an alteration mechanism. *American Mineralogist* 72: 353-356.

Allbrook, R.F. 1983. Some physical properties of allophane soils from the North Island, New Zealand. *New Zealand Journal of Science* 26: 481-492.

Alloway, B.V.; McGlone, M.S.; Neall, V.E.; Vucetich, C.G. 1992a. The role of Egmont-sourced tephra in evaluating the paleoclimatic correspondence between the bio- and soil-stratigraphic records of central Taranaki, New Zealand. *Quaternary International* 13/14: 187-194.

Alloway, B.V.; Stewart, R.B.; Neall, V.E.; Vucetich, C.G. 1992b. Climate of the last glaciation in New Zealand, based on aerosolic quartz influx in an andesitic terrain. *Quaternary Research* 38: 170-179.

Alloway, B.V.; Pillans, B.J.; Sandhu, A.S.; Westgate, J.A. 1993. Revision of the marine chronology in the Wanganui Basin, New Zealand, based on the isothermal plateau fission-track dating of tephra horizons. *Sedimentary Geology* 82: 299-310.

Barratt, B.C. 1988. Micromorphology and pedogenesis in a Late Pleistocene succession of tephric loesses and paleosols near Tapapa, Mamaku Plateau, North Island, New Zealand (Abstract). In Eden, D.N.; Furkert, R.J. (eds) *Loess: Its Distribution, Geology and Soils* A.A. Balkema, Rotterdam: 7-8.

Baumgart, I.L. 1954. Some ash showers of the central North Island. *New Zealand Journal of Science and Technology* B35: 456-467.

Berryman, K. 1992. A stratigraphic age of Rotoehu Ash and late Pleistocene climate interpretation based on marine terrace chronology, Mahia Peninsula, North Island, New Zealand. *New Zealand Journal of Geology and Geophysics* 35: 1-7.

Birrell, K.S.; Pullar, W.A. 1973. Weathering of paleosols in Holocene and late Pleistocene tephras in central North Island, New Zealand. *New Zealand Journal of Geology and Geophysics* 35: 1-7.

Birrell, K.S.; Pullar, W.A.; Heine, J.C. 1971. Pedological, chemical, and physical properties of organic horizons of paleosols underlying the Tarawera Formation. *New Zealand Journal of Science* 14: 187-218.

Birrell, K.S.; Pullar, W.A.; Searle, P.L.1977. Weathering of Rotoehu Ash in the Bay of Plenty district. *New Zealand Journal of Science* 20: 303-310.

Bishop, N. 1992. *Natural History of New Zealand.* Hodder & Stoughton, Auckland. 199 p.

Briggs, R.M.; McDonough, W.F. 1990. Contemporaneous convergent margin and intraplate magmatism, North Island, New Zealand. *Journal of Petrology* 31: 813-851.

Briggs, R.M.; Itaya, T.; Lowe, D.J.; Keane, A.J. 1989. Ages of Pliocene-Pleistocene Alexandra and Ngatutura Volcanics, western North Island, New Zealand, and some geological implications. *New Zealand Journal of Geology and Geophysics* 32: 417-427.

Briggs, R.M.; Gifford, M.G.; Moyle, A.R.; Taylor, S.R.; Norman, M.D.; Houghton, B.F.; Wilson, C.J.N. in press. Geochemical zoning and eruptive mixing in ignimbrites from Mangakino volcano, Taupo Volcanic Zone, New Zealand. *Journal of Volcanology and Geothermal Research*

Browne, P.R.L.; Lloyd, E.F. 1986. Water dominated geothermal systems and associated mineralisation. *New Zealand geological Survey Record* 11: 145-212.

Browne, P.R.L.; Graham, I.J.; Parker, R.J.; Wood, C.P. 1992. Subsurface andesite lavas and plutonic rocks in the Rotokawa and Ngatamariki geothermal systems, Taupo Volcanic Zone, New Zealand. *Journal of Volcanology and Geothermal Research* 51: 199-215.

Buhay, W.M.; Clifford, P.M.; Schwarcz, H.P. 1992. ESR dating of the Rotoiti Breccia in the Taupo Volcanic Zone, New Zealand. *Quaternary Science Reviews* 11: 267-271.

Childs, C.W. 1985. Towards understanding soil mineralogy II. Notes on ferrihydrite. *New Zealand Soil Bureau Laboratory Report* CM7. 16p.

Childs, C.W. 1987a. Weighted mean concentrations of minerals in New Zealand soils. 1. Ferrihydrite. *New Zealand Soil Bureau Scientific Report* 81. 28p.

Childs, C.W. 1987b. Weighted mean concentrations of minerals in New Zealand soils. 3. Crystalline iron oxides. *New Zealand Soil Bureau Scientific Report* 83. 18p.

Childs, C.W. 1992a. Ferrihydrite: A review of structure, properties and occurrence in relation to soils. *Zeitschrift fuer Pflanzenernaehrung und Bodenkunde* 154: 441-448.
Childs, C.W. 1992b. Soil- and geo-chemistry: rattling nodules to heat engines. *New Zealand Soil News* 40: 5-16.
Childs, C.W.; Parfitt, R.L. 1987. Weighted mean concentrations of minerals in New Zealand soils. 2. Allophane/imogolite. *New Zealand Soil Bureau Scientific Report* 82. 20 p.
Childs, C.W.; Downes, C.J.; Wells, N. 1982. Hydrous iron oxide minerals with short range order deposited in a spring/stream system, Tongariro National Park, New Zealand. *Australian Journal of Soil Research* 20: 119-129.
Childs, C.W.; Wells, N.; Downes, C.J. 1986. Kokowai Springs, Mount Egmont, New Zealand: chemistry and mineralogy of the ochre (ferrihydrite) deposit and analysis of the waters. *Journal of the Royal Society of New Zealand* 16: 85-99.
Childs, C.W.; Palmer, R.W.P.; Ross, C.W. 1990. Thick iron oxide pans in soils of Taranaki, New Zealand. *Australian Journal of Soil Research* 28: 245-257.
Childs, C.W.; Parfitt, R.L.; Lee, R. 1983. Movement of aluminium as an inorganic complex in some podzolised soils, New Zealand. *Geoderma* 29: 139-155.
Childs, C.W.; Parfitt, R.L.; Newman, R.H. 1990. Structural studies of Silica Springs allophane. *Clay Minerals* 25: 329-341.
Churchman, G.J. 1986. Towards understanding soil mineralogy I. An introduction to clay minerals in soils. *New Zealand Soil Bureau Laboratory Report* CM6. 28p.
Churchman, G.J. 1990. Relevance of different intercalation tests for distinguishing halloysite from kaolinite in soils. *Clays and Clay Minerals* 38: 591-599.
Churchman, G.J.; Carr, R.M. 1975. The definition and nomenclature of halloysites. *Clays and Clay Minerals* 23: 382-388.
Churchman, G.J.; Gilkes, R.J. 1989. Recognition of intermediates in the possible transformation of halloysite to kaolinite in weathering profiles. *Clay Minerals* 24: 579-590.
Churchman, G.J.; Tate, K.R. 1987. Stability of aggregates of different size grades in allophanic soils from volcanic ash in New Zealand. *Journal of Soil Science* 38: 19-27.
Churchman, G.J.; Theng, B.K.G. 1984. Interactions of halloysites with amides: mineralogical factors affecting complex formation. *Clay Minerals* 19: 161-175.
Churchman, G.J.; Aldridge, L.P.; Carr, R.M. 1972: The relationship between the hydrated and dehydrated states of an halloysite. *Clays and Clay Minerals* 20: 241-246.
Churchman, G.J.; Whitton, J.S.; Claridge, G.G.C.; Theng, B.K.G. 1984. Intercalation method using formamide for differentiating halloysite from kaolinite. *Clays and Clay Minerals* 32: 241-248.
Clark, R.H. 1989. *New Zealand From the Road.* Heinemann Reed, Auckland. 177p.
Clarkson, B.R.; Clarkson, B.D.; Patel, R.N. 1992. The pre-Taupo eruption (*c.* AD 130) forest of the Bennydale-Pureora district, central North Island, New Zealand. *Journal of the Royal Society of New Zealand* 22: 61-76.
Cole, J.W. 1990. Structural control and origin of volcanism in the Taupo volcanic zone, New Zealand. *Bulletin of Volcanology* 52: 445-492.
Cole, J.W.; Graham, I.J.; Hackett, W.R.; Houghton, B.F. 1986. Volcanology and petrology of the Quaternary composite volcanoes of Tongariro Volcanic Centre, Taupo Volcanic Zone. *Royal Society of New Zealand Bulletin* 23: 7-20.
Cox, J.E. 1973. Guidebook for Excursion 4 Northland. *IX INQUA Congress,* Christchurch: 85-138.
Cradwick, P.D.G.; Farmer, V.C.; Russell, J.D.; Masson, C.R.; Wada, K.; Yoshinaga, N. 1972. Imogolite, a hydrated alumium silicate of tubular structure. *Nature* 240: 187-189.
Cross, D. 1963. Soils and geology of some hydrothermal eruptions in the Waiotapu district. *New Zealand Journal of Geology and Geophysics* 6: 70-87..
Crozier, M.J.; Gage, M.; Pettinga, J.R.; Selby, M.J.; Wasson, R.J. 1992. The stability of hillslopes. In: Soons, J.M.; Selby, M.J. (eds) *Landforms of New Zealand Second Edition.* Longman Paul, Auckland: 63-90.
Darby, D.J.; Williams, R.O. 1991. A new deodetic estimate of deformation in the Central Volcanic Region of the North Island, New Zealand. *New Zealand Journal of Geology and Geophysics* 34: 127-136.

Davoren, A. 1976. A pedological study of the Kauroa Ash Formation at the University of Waikato. Unpublished M.Sc. thesis, University of Waikato, Hamilton.

Dixon, J.B. 1989. Kaolin and serpentine group minerals. In Dixon, J.B.; Weed, S.B. (eds) 1989. *Minerals in Soil Environments (Second Edition)*. Soil Science Society of America Book Series 1: 467-525.

Dixon, J.B.; McKee, T.R. 1974. Internal and external morphology of tubular and spheroidal halloysite particles. *Clays and Clay Minerals* 22: 127-137.

Dixon, J.B.; Weed, S.B. (eds) 1989. *Minerals in Soil Environments (Second Edition)*. Soil Science Society of America Book Series 1. 1244p.

Donoghue, S.L.; Stewart, R.B.; Palmer, A.S. 1991. Morphology and chemistry of olivine phenocrysts of Mangamate Tephra, Tongariro Volcanic Centre, New Zealand. *Journal of the Royal Society of New Zealand* 21: 225-236.

Drees, L.R.; Wilding, L.P.; Smeck, N.E.; Senkayi, A.L. 1989. Silica in soils: quartz and disordered silica polymorphs. In Dixon, J.B.; Weed, S.B. (eds) 1989. *Minerals in Soil Environments (Second Edition)*. Soil Science Society of America Book Series 1: 913-974.

Drew, S.; Simpson, B.M.; Robinson, R.; Paul, D. 1985. The Rotorua Geothermal Field. A report of the Rotorua Geothermal Monitoring Programme and Task Force 1982-1985. DSIR, Ministry of Works, and Ministry of Energy. 48p.

Eden, D.N.; Hunt, J.L.; Whitton, J.S.; Kennedy, N.M.; Lowe, D.J. in prep. Element chemistry, mineralogy, and other properties of a 140 000 year old tephra, loess, and paleosol sequence from Mamaku Plateau, central North Island, New Zealand. Unpublished manuscript.

Eggleton, R.A.; Fitzpatrick, R.W.1988. New data and a revised structural model for ferrihydrite. *Clays and Clay Minerals* 36: 111-124.

Ewart, A. 1966. Review of mineralogy and chemistry of the acidic volcanic rocks of Taupo Volcanic Zone, New Zealand. *Bulletin Volcanologique* 29: 147-172.

Fanning, D.S.; Keramidas, V.Z.; El-Desoky, M.A. 1989. Micas. In Dixon, J.B.; Weed, S.B. (eds) 1989. *Minerals in Soil Environments (Second Edition)*. Soil Science Society of America Book Series 1: 551-634.

Farmer, V.C. 1982. Significance of the presence of allophane and imogolite in podzol Bs horizons for podzolization mechanisms: a review. *Soil Science and Plant Nutrition* 28: 571-578.

Farmer, V.C.; Fraser, A.R.; Tait, J.M. 1979. Characterization of the chemical structures of natural and synthetic aluminosilicate gels and sols by infrared spectroscopy. *Geochimica et Cosmochimica Acta* 43: 1417-1420.

Farmer, V.C.; McHardy, W.J.; Palmieri, F.; Violante, A.; Violante, P. 1991. Synthetic allophanes formed in calcareous environments: nature, conditions of formation, and transformations. *Soil Science Society of America Journal* 55: 1162-1166.

Farmer, V.C.; Palmieri, F.; Violante, A.; Violante, P. 1991a. Amorphous hydroxyaluminium silicates formed under physiological saline conditions, and in $CaCO_3$-buffered solutions. Stability and significance for Alzheimer plaque precipitates. *Clay Minerals* 26: 281-287.

Fieldes, M.; Perrott, K. W. 1966. The nature of allophane in soils. Part 3. Rapid field and laboratory test for allophane. *New Zealand Journal of Science* 9: 623-629.

Froggatt, P.C. 1988. Paleomagnetism of Last Glacial loess from two sections in New Zealand. In Eden, D.N.; Furkert, R.J. (eds) *Loess: Its Distribution, Geology and Soils* A.A. Balkema, Rotterdam: 59-68.

Froggatt, P.C.; Lowe, D.J. 1990. A review of late Quaternary silicic amd some other tephra formations from New Zealand: their stratigraphy, nomenclature, distribution, volume, and age. *New Zealand Journal of Geology and Geophysics* 33: 89-109.

Froggatt, P.C.; Nelson, C.S.; Carter, L.; Griggs, G.; Black, K.P. 1986. An exceptionally large late Quaternary eruption from New Zealand. *Nature* 319: 578-582.

Gamble, J.A.; Smith, I.E.M.; Graham, I.J.; Kokelaar, B.P.; Cole, J.W.; Houghton, B.F.; Wilson, C.J.N. 1990. The petrology, phase relations and tectonic setting of basalts from the Taupo Volcanic Zone, New Zealand and the Kermadec Island Arc — Havre Trough, SW Pacific. *Journal of Volcanollogy and Geothermal Research* 43: 235-270.

Goh, K.M. 1972. Amino acid levels as indicators of paleosols in New Zealand soil profiles. *Geoderma* 7: 33-47.

Grange, L.I. 1937. The geology of the Rotorua-Taupo Subdivision, Rotorua and Kaimanawa Divisions. *New Zealand Geological Survey Bulletin* 37. 138p.

Green, B.E. 1987.Weathering of buried paleosols on late Quaternary rhyolitic tephras, Rotorua region, New Zealand. Unpublished M.Sc thesis, University of Waikato, Hamilton.

Green, J.D.; Lowe, D.J. 1985. Stratigraphy and development of c. 17 000 year old Lake Maratoto, North Island, New Zealand, with some inferences about postglacial climatic change. *New Zealand Journal of Geology and Geophysics* 28: 675-699.

Grindley, G.W.; Mumme, T.C. 1991. Magnetic stratigraphy and correlation of ignimbrite eruptions of the Mangakino Basin and Tokoroa Plateau. *New Zealand Geological Survey Record* 43: 25-36.

Hackwell, K. 1983. The international significance of New Zealand's indigenous forests. *Nature Conservation Council Information Leaflet* 19. 17p.

Healy, J. 1992. Central volcanic region. In Soons, J.M.; Selby, M.J. (eds) *Landforms of New Zealand Second Edition.* Longman Paul, Auckland: 256-286.

Healy, J.; Hochstein, M.P. 1973. Horizontal flow in hydrothermal systems. *New Zealand Journal of Hydrology* 12: 71-82.

Healy, J.; Grindley, G.W. et al. 1963. Waiotapu geothemal field. *DSIR Bulletin* 155.

Hedenquist, J.W. 1983. Waiotapu, New Zealand: the geochemical evolution and mineralization of an active hydrothermal system. Unpublished PhD thesis, University of Auckland, Auckland.

Hedenquist, J.W. 1986. Geothermal systems in the Taupo Volcanic Zone: their characteristics and relation to,volcanism and mineralisation. *Royal Society of New Zealand Bulletin* 23: 134-168.

Hedenquist, J.W. 1991. Boiling and dilution in the shallow portion of the Waiotapu geothermal system. *Geochemica et Cosmochimica Acta* 55: 2753-2765.

Hedenquist, J.W.; Henley, R.W. 1985. Hydrothermal eruption in the Waiotapu geothermal system, New Zealand: their origin, associated breccias and relation to precious metal deposition. *Economic Geology* 80: 1640-1668.

Hedenquist, J.W.; Browne, P.R.L. 1989. The evolution of the Waiotapu geothermal system, New Zealand, based on the chemical and isotopic comparison of its fluids, minerals and rocks. *Geochemica et Cosmochimica Acta* 53: 2235-2257.

Heming, R.F.; Barnet, P.R. 1986. The petrology and petrochemistry of the Auckland Volcanic Field. *The Royal Society of New Zealand Bulletin* 23: 64-75.

Henley, R.W. 1985. The geothermal framework for epithermal deposits: Geology and Geochemistry of Epithermal Systems (B.R. Gerger & P.M. Bethke eds). *Reviews in Economic Geology* 2: 1-24.

Henmi, T.; Parfitt, R.L. 1980. Laminar opaline silica from some volcanic ash soils in New Zealand. *Clays and Clay Minerals* 28: 57-60.

Hewitt, A.E. 1992. New Zealand Soil Classification. *DSIR Land Resources Scientific Report* 19. 133p.

Hodder, A.P.W.; Green, B.E.; Lowe, D.J. 1990. A two-stage model for the formation of clay minerals from tephra-derived volcanic glass. *Clay Minerals* 25: 313-327.

Hogg, A.G. 1974. A pedological study of the Hamilton Ash Formation at Te Uku. Unpublished M.Sc. thesis, University of Waikato, Hamilton.

Hosono, M.; Oba, Y.; Sase, T.; Utsugawa, T.; Aoki, K. 1991. Holocene volcanic ash soils at Waimangu Road tephra section, North Island, New Zealand: soil formation-vegetation relationship. *Quaternary Research (Tokyo)* 30: 91-101 (in Japanese).

Houghton, B.F. 1982. Geyserland: a guide to the volcanoes and geothermal areas of Rotorua. *Geological Society of New Zealand Guidebook* 4. 48p.

Houghton, B.F.; Wilson, C.J.N. 1986. Explosive rhyolitic volcanism: the case studies of Mayor Island and Taupo volcanoes. *New Zealand Geological Survey Record* 12: 33-100.

Houghton, B.F.; Weaver, S.D.; Wilson, C.J.N.; Lanphere, M.A. 1992. Evolution of a Quaternary peralkaline volcano: Mayor Island, New Zealand. *Journal of Volcanology and Geothermal Research* 51: 217-236.

Huang, P.M. 1991. Ionic factors affecting the formation of short-range ordered aluminosilicates. *Soil Science Society of America Journal* 55: 1172-1180.

Hume, T.M.; Nelson, C.S. 1982. X-ray diffraction analytical procedures and some mineralogical characteristics for South Auckland region sediments and sedimentary rocks, with special reference to their clay fraction. *University of Waikato, Department of Earth Sciences Occasional Report* 10. 33p.

Hume, T.M.; Sherwood, A.M.; Nelson, C.S. 1975. Alluvial sedimentology of the Upper Pleistocene Hinuera Formation, Hamilton basin, New Zealand. *Journal of the Royal Society of New Zealand* 5: 421-462.

Jamieson, A. 1992. Volcanic Auckland. *New Zealand Geographic* 16: 90-113.

Kamp, P.J.J. 1984. Neogene and Quaternary extent and geometry of the subducted Pacific Plate beneath North Island, New Zealand: implications for Kaikoura tectonics. *Tectonophysics* 108: 241-266.

Kamp, P.J.J. 1986. Late Cretaceous-Cenozoic tectonic development of the southwest Pacific region. *Tectonophysics* 121: 225-251.

Kamp, P.J.J. 1992. Tectonic architecture of New Zealand. In Soons, J.M.; Selby, M.J. (eds) *Landforms of New Zealand Second Edition.* Longman Paul, Auckland: 1-30.

Kamp, P.J.J.; Green, P.F.; White, S.H. 1989. Fission track analysis reveals character of collisional tectonics in New Zealand. *Tectonics* 8: 169-195.

Kear, D.S.; Schofield, J.C. 1978. Geology of the Ngaruawahia Subdivision. *New Zealand Geological Survey Bulletin* 88. 168p.

Kennedy, N.M. 1982. Tephric loess in Rotorua-Bay of Plenty region, North Island, New Zealand. In Wasson, R.J. (ed) *Quaternary Dust Mantles of Australia, New Zealand and China* Australian National University, Canberra: 119-122.

Kennedy, N.M. 1988. Late Quaternary loess associated with the Mamaku Plateau, North Island, New Zealand. In Eden, D.N.; Furkert, R.J. (eds) *Loess: Its Distribution, Geology and Soils* A.A. Balkema, Rotterdam: 71-80.

Kennedy, N.M.; Pullar, W.A.; Pain, C.F. 1978. Late Quaternary land surfaces and geomorphic changes in the Rotorua Basin, North Island, New Zealand. *New Zealand Journal of Science* 21: 249-264.

Kermode, L.O. 1983. Tour 8 — Auckland volcanoes. *Geological Society of New Zealand Annual Conference,* Auckland. 32p.

Kermode, L.O. 1992. Geology of the Auckland urban area. Scale 1: 50 000. "Institute of Geological and Nuclear Sciences Geological Map 2". 1 sheet and notes (63 p.). Institute of Geological and Nuclear Sciences Ltd, Lower Hutt.

Kimber, R.W.L.; Kennedy, N.M.; Milnes, A.R. in press. Amino acid racemization dating of a 140,000 year-old tephra-loess-palaeosol sequence on the Mamaku Plateau near Rotorua, New Zealand. *Australian Journal of Earth Sciences*

Kirkman, J.H. 1975. Clay mineralogy of some tephra beds of Rotorua area, North Island, New Zealand. *Clay Minerals* 10: 437-449.

Kirkman, J.H. 1976a. Clay mineralogy of thirteen paleosols developed in Holocene and late Pleistocene tephras of central North Island, New Zealand. *New Zealand Journal of Geology and Geophysics* 19: 179-187.

Kirkman, J.H. 1976b. Clay mineralogy of Rotomahana sandy loam soil, North Island, New Zealand. *New Zealand Journal of Geology and Geophysics* 19: 35-41.

Kirkman, J.H. 1977. Possible structure of halloysite disks and cylinders observed in some New Zealand rhyolitic tephras. *Clay Minerals* 12: 199-216.

Kirkman, J.H. 1980a. Mineralogy of the Kauroa Ash Formation of south-west and west Waikato, North Island, New Zealand. *New Zealand Journal of Geology and Geophysics* 23: 113-120.

Kirkman, J.H. 1980b. Clay mineralogy of a sequence of andesitic tephra beds of western Taranaki, New Zealand. *Clay Minerals* 15: 157-163.

Kirkman, J.K. 1981a. Morphology and structure of halloysite in New Zealand tephras. *Clays and Clay Minerals* 29: 1-9.

Kirkman, J.H. 1981b. Some primary mineral to clay mineral transformations in New Zealand tephras and tephra-derived soils. Programme and abstracts, Soils with Variable Charge Conference, Palmerston North, New Zealand: 169-170.

Kirkman, J.H.; McHardy, W.J. 1980. A comparative study of the morphology, chemical composition and weathering of rhyolitic and andesitic glass. *Clay Minerals* 15: 165-173.

Kirkman, J.H.; Pullar, W.A. 1978. Halloysite in late Pleistocene rhyolitic tephra beds near Opotiki, coastal Bay of Plenty, North Island, New Zealand. *Australian Journal of Soil Research* 16: 1-8.

Kodama, H.; Ross, G.J. 1991. Tiron dissolution method used to remove and characterize inorganic components in soils. *Soil Science Society of America Journal* 55: 1180-1187.

Kohn, B.P.; Pillans, B.J.; McGlone, M.S. 1992. Zircon fission track age for middle Pleistocene Rangitawa Tephra, New Zealand: stratigraphic and paleoclimatic significance. *Palaeogeography, Palaeoclimatology, Palaeoecology* 95: 73-94.

Limmer, A.W.; Wilson, A.T. 1980. Amino acids in buried paleosols. *Journal of Soil Science* 31: 147-153.

Lloyd, E.F. 1959. The hot springs and hydrothermal eruptions of Waiotapu. *New Zealand Journal of Geology and Geophysics* 2: 141-176.

Lowe, D.J. 1986. Controls on the rates of weathering and clay mineral genesis in airfall tephras: a review and New Zealand case study. In Colman, S.M.; Dethier, D.P. (eds) *Rates of Chemical Weathering of Rocks and Minerals*. Academic Press, Orlando: 265-330.

Lowe, D.J. 1988. Stratigraphy, age, composition, and correlation of late Quaternary tephras interbedded with organic sediments in Waikato lakes, North Island, New Zealand. *New Zealand Journal of Geology and Geophysics* 31: 125-165.

Lowe, D.J. 1990. Tephra studies in New Zealand: an historical review. *Journal of the Royal Society of New Zealand* 20: 119-150.

Lowe, D.J.; Green, J.D. 1992. Lakes. In Soons, J.M.; Selby, M.J. (eds) *Landforms of New Zealand Second Edition*. Longman Paul, Auckland: 107-143.

Lowe, D.J.; Green, B.E. 1992a. A hydrofluoric acid dissolution method for determining volcanic glass content of tephra-derived soils (Andisols). *Australian Journal of Soil Research* 30: 573-581.

Lowe, D.J.; Hogg, A.G. 1992. Application of new technology liquid scintillation spectrometry to radiocarbon dating of tephra deposits, New Zealand. *Quaternary International* 13/14: 135-142.

Lowe, D.J.; Nelson, C.S. 1983. Guide to the nature and methods of analysis of the clay fraction of tephras from the South Auckland region, New Zealand. *University of Waikato, Department of Earth Sciences Occasional Report* 11. 69p.

McCraw, J.D. 1967. The surface features and soil pattern of the Hamilton Basin. *Earth Science Journal* 1: 59-74.

McGlone, M.S. 1983a. Polynesian deforestation of New Zealand: a preliminary synthesis. *Archaeology in Oceania* 18: 11-25.

McGlone, M.S. 1983b. Holocene pollen diagrams, Lake Rotorua, North Island, New Zealand. *Journal of the Royal Society of New Zealand* 13: 53-65.

McGlone, M.S. 1985. Plant biogeography and the late Cenozoic history of New Zealand. *New Zealand Journal of Botany* 23: 723-749.

McGlone, M.S. 1988. New Zealand. In Huntley, B.; Webb, T.III (eds) *Vegetational History*. Kluwer Academic Publishers: 557-599.

McIntosh, P.D. 1979. Halloysite in a New Zealand tephra and paleosol less than 2500 years old. *New Zealand Jounal of Science* 22: 49-54.

McIntosh, P.D. 1980. Weathering products in Vitrandept profiles under pine and manuka, New Zealand. *Geoderma* 24: 225-239.

McLeod, M. 1992. Soils of part northern Matamata County, North Island, New Zealand. *DSIR Land Resources Scientific Report* 18. 96p.

McQueen, D.J. 1975. A study of the Horotiu-Te Kowhai soil complex. Unpublished M.Sc. thesis, University of Waikato, Hamilton.

Mizota, C. 1982. Clay mineralogy of a Dystrandept and an Haplaquod from Northland, New Zealand. *Soil Science and Plant Nutrition* 28: 293-301.

Mizota, C.; van Reeuwijk, L.P. 1989. Clay mineralogy and chemistry of soils formed in volcanic material in diverse climatic regions. *ISRIC, Wageningen, Soil Monograph* 2. 185p.

Mizota, C.; Toh, N.; Matsuhisa, Y. 1987. Origin of cristobalite in soils derived from volcanic ash in temperate and tropical regions. *Geoderma* 39: 323-330.

Molloy, L. 1988. *Soils in the New Zealand Landscape*. New Zealand Society of Soil Science and Mallinson Rendel, Wellington. 239 p.

Murphy, R.P.; Seward, D. 1981. Stratigraphy, lithology, paleomagnetism, and fission track ages of some ignimbrite formations in the Matahana Basin, New Zealand. *New Zealand Journal of Geology and Geophysics* 24: 325-331.

Nagasawa, K.; Noro, H. 1987. Mineralogical properties of halloysites of weathering origin. *Chemical Geology* 60: 145-149.

Nairn, I.A. 1979. Rotomahana-Waimangu eruption, 1886: base surge and basalt magma. *New Zealand Journal of Geology and Geophysics* 22: 363-378.

Nairn, I.A. 1989. Geological Map of New Zealand 1:50 000. Sheet V16C Mount Tarawera. New Zealand Geological Survey DSIR, Wellington.

Nairn, I.A. 1992. The Te Rere and Okareka eruptive episodes — Okataina Volcanic Centre, Taupo Volcanic Zone, New Zealand. *New Zealand Journal of Geology and Geophysics* 35: 93-108.

Neall, V.E. 1979. Sheets P19, P20, & P21 *New Plymouth, Egmont, and Manaia* (1st ed) "Geological Map of New Zealand 1: 50 000". Three maps and notes (36 p.). New Zealand Department of Scientific and Industrial Research, Wellington.

Neall, V.E. 1984. Properties of Andisols important to pasture and horticulture. *Proceedings Sixth International Soil Classification Workshop, Chile & Ecuador*. Part 1: 109-120.

Neall, V.E.; Stewart, R.B.; Smith, I.E.M. 1986. History and petrology of the Taranaki volcanoes. *The Royal Society of New Zealand Bulletin* 23: 251-263.

Nelson, C.S. 1988. Revised age of a late Quaternary tephra at DSDP Site 594 off eastern South Island and some implications for correlation. *Geological Society of New Zealand Newsletter* 82: 35-40.

Nelson, C.S.; Hendy, C.H.; Jarrett, G.R.; Cuthbertson, A.M. 1985a. Near synchroneity of New Zealand alpine glaciations and Northern Hemisphere continental glaciations during the past 750 ka. *Nature* 318: 361-363.

Nelson, C.S.; Froggatt, P.C.; Gosson, G.J. 1985b. Nature, chemistry, and origin of late Cenozoic megascopic tephras in Leg 90 cores from the southwest Pacific. In: Kennett, J.P.; von der Borch, C.C. et al. (eds) *Initial Reports of the Deep Sea Drilling Project* 90, Washington: 1161-1173.

Newnham, R.M.; Lowe, D.J. 1991. Holocene vegetation and volcanic activity, Auckland Isthmus, New Zealand. *Journal of Quaternary Science* 6: 177-193.

Newnham, R.M.; Lowe, D.J.; Green, J.D. 1989. Palynology, vegetation and climate of the Waikato lowlands, North Island, New Zealand, since c. 18,000 years ago. *Journal of the Royal Society of New Zealand* 19: 127-150.

Nichol, R. 1992. The eruption history of Rangitoto: reappraisal of a small New Zealand myth. *Journal of the Royal Society of New Zealand* 22: 159-180.

Nicholson, C.M. 1986. A geomechanical investigation of the Hamilton Ash Formation using the Iowa Borehole Shear Device and selected laboratory tests. Unpublished M.Sc. thesis, University of Waikato, Hamilton.

Orbell, G.E.; Parfitt, R.L.; Furkert, R.J. (compilers) 1981. Guide book for Tour 6 Specialist North Auckland, New Zealand. *Soils With Variable Charge Conference*, Palmerston North, New Zealand. 105p.

Otowa, M. 1986. Morphology and classification. In Wada, K. (ed) *Ando Soils of Japan*. Kyushu University Press: 3-20.

Pain, C.F. 1975. Some tephra deposits in the south-west Waikato area, North Island, New Zealand. *New Zealand Journal of Geology and Geophysics* 18: 541-550.

Parfitt, R.L. 1980. Chemical properties of variable charge soils. In Theng, B.K.G. (ed) *Soils With Variable Charge*. New Zealand Society of Soil Science, Lower Hutt: 167-194.

Parfitt, R.L. 1986. Towards understanding soil mineralogy III. Notes on allophane. *New Zealand Soil Bureau Laboratory Report* CM10. 19p.

Parfitt, R.L. 1990a. Allophane in New Zealand — a review. *Australian Journal of Soil Research* 28: 343-360.

Parfitt, R.L. 1990b. Soils formed in tephra in different climatic regions. *Transactions XIV Congress of the International Society of Soil Science, Kyoto,* VII: 134-139.

Parfitt, R.L.; Childs, C.W. 1983. Comment on clay mineralogy of two Northland soils New Zealand. *Soil Science and Plant Nutrition* 29: 555-559.

Parfitt, R.L.; Childs, C.W. 1988. Estimation of forms of Fe and Al: a review, and analysis of contrasting soils by dissolution and Moessbauer methods. *Australian Journal of Soil Research* 26: 289-296.

Parfitt, R.L.; Churchman, G.J. 1988. Clay minerals and humus complexes in five Kenyan soils derived from volcanic ash — a discussion. *Geoderma* 42: 365-367.

Parfitt, R.L.; Clayden, B. 1991. Andisols — the development of a new order in Soil Taxonomy. *Geoderma* 49: 181-198.

Parfitt, R.L.; Kimble, J.M. 1989. Conditions for formation of allophane in soils. *Soil Science Society of America Journal* 53: 971-977.

Parfitt, R.L.; Saigusa, M. 1985. Allophane and humus-aluminium in Spodosols and Andepts formed from the same volcanic ash beds in New Zealand. *Soil Science* 139: 149-155.

Parfitt, R.L.; Webb, T.H. 1984. Allophane in some South Island yellow-brown shallow and stony soils and high country and upland yellow-brown earths. *New Zealand Journal of Science* 27: 37-40.

Parfitt, R.L.; Wilson, A.D. 1985. Estimation of allophane and halloysite in three sequences of volcanic soils, New Zealand. *Catena Supplement* 7: 1-8.

Parfitt, R.L.; Furkert, R.J.; Henmi, T. 1980. Identification and structure of two types of allophane from volcanic ash soils and tephra. *Clays and Clay Minerals* 28: 328-334.

Parfitt, R.L.; Pollock, J.A.; Furkert, R.J. (compilers) 1981. Guide book for Tour 1 Pre-conference North Island, New Zealand. *Soils With Variable Charge Conference,* Palmerston North, New Zealand. 153p.

Parfitt, R.L.; Russell, M.; Kirkman, J.H. 1982. The clay mineralogy of yellow-brown loam soils. In Neall, V.E. (ed) *Soil Groups of New Zealand, Part 6.* New Zealand Society of Soil Science, Lower Hutt: 48-53.

Parfitt, R.L.; Russell, M.; Orbell, G.E.1983. Weathering sequence of soils from volcanic ash involving allophane and halloysite, New Zealand. *Geoderma* 29: 41-57.

Parfitt, R.L.; Saigusa, M.; Cowie, J.D. 1984. Allophane and halloysite formation in a volcanic ash bed under different moisture conditions. *Soil Science* 138: 360-364.

Parfitt, R.L.; Van der Gaast, S.J.; Childs, C.W. in press. A structural model for natural siliceous ferrihydrite. *Clays and Clay Minerals*

Percival, H.J. 1985. Soil solutions, minerals, and equilibria. *New Zealand Soil Bureau Scientific Report* 69. 21p.

Pillans, B.J. 1992. New Zealand Quaternary stratigraphy: an overview. *Quaternary Science Reviews* 10: 405-418.

Pillans, B.J.; Pullar, W.A.; Selby, M.J.; Soons, J.M. 1992. The age and development of the New Zealand landscape. In: Soons, J.M.; Selby, M.J. (eds) *Landforms of New Zealand Second Edition.* Longman Paul, Auckland: 31-62.

Porter, S.C. 1975. Equilibrium line of late Quaternary glaciers in the Southern Alps, New Zealand. *Quaternary Research* 5: 27-48.

Pringle, M.S.; McWilliams, M.; Houghton, B.F.; Lanphere, M.A.; Wilson, C.J.N. 1992. $^{40}Ar/^{39}Ar$ dating of Quaternary feldspar: Examples from the Taupo Volcanic Zone, New Zealand. *Geology* 20: 531-534.

Read, N.E. (ed) 1974. Soil groups of New Zealand. Part 1. Yellow-brown pumice soils. New Zealand Society of Soil Science, Lower Hutt. 251p.

Renders, P.J.; Seward, T.M. 1989. The adsorption of thio gold (I) complexes by amorphous As_2S_3 and Sb_2S_3 at 25 and 90°C. *Geochemica et Cosmochimica Acta* 40: 379-399.

Rijkse, W.C. 1979. Soils of Rotorua Lakes district, North Island, New Zealand. *New Zealand Soil Survey Report* 43. 124p.

Rijkse, W.C.; Vucetich, C.G. 1980. Soils of Wairakei research Station, North Island, New Zealand. *New Zealand Soil Survey Report* 57. 26p.

Russell, M.; Parfitt, R.L.; Claridge, G.G.C. 1981. Estimation of the amounts of allophane and other materials in the clay fraction of an Egmont loam profile and other volcanic ash soils, New Zealand. *Australian Journal of Soil Research* 19: 185-195.

Salter, R.T. 1979. A pedological study of the Kauroa Ash Formation at Woodstock. Unpublished M.Sc. thesis, University of Waikato, Hamilton.

Schulze, D.G. 1989. An introduction to soil mineralogy. In Dixon, J.B.; Weed, S.B. (eds) *Minerals in Soil Environments (Second Edition).* Soil Science Society of America Book Series 1: 1-34.

Schwertmann, U.; Taylor, R.M. 1989. Iron oxides. In Dixon, J.B.; Weed, S.B. (eds) *Minerals in Soil Environments (Second Edition).* Soil Science Society of America Book Series 1: 379-438.

Searle, E.J. 1981. *City of Volcanoes: a Geology of Auckland.* Second edition (edited by R.D. Mayhill). Longman Paul, Auckland. 195p.

Selby, M.J.; Lowe, D.J. 1992. The middle Waikato Basin and hills. In Soons, J.M.; Selby, M.J. (eds) *Landforms of New Zealand Second Edition.* Longman Paul, Auckland: 233-255.

Shepherd, T.G. 1984. A pedological study of the Hamilton Ash Group at Welches Road, Mangawara, North Waikato. Unpublished M.Sc. thesis, University of Waikato, Hamilton.

Shoji, S.; Fujiwara, Y. 1984. Active Al and Fe in the humus horizons of Andosols from northeastern Japan: Their forms, properties and significance in clay weathering. *Soil Science* 137: 216-226.

Simmons, S.F.; Browne, P.R.L. 1991. Active geothermal systems of the North Island, New Zealand. *Geological Society of New Zealand Miscellaneous Publication* 57. 70p.

Simmons, S.F.; Browne, P.R.L.; Brathwaite, R.L. 1992. Active and extinct hydrothermal systems of the North Island, New Zealand. *Society of Economic Geologists Guide Book Series* 15. 121p.

Simpson, B.M. 1986. Rotorua Geothermal Field. Handbook, International Volcanological Congress, New Zealand: 91-95.

Singleton, P.L. 1991. Soils of Ruakura — a window on the Waikato. *DSIR Land Resources Scientific Report* 5. 127p.

Singleton, P.L. 1992. Soil map unit descriptions for Ruakura Agricultural Centre, Hamilton. *DSIR Land Resources Technical Record* 88.

Singleton, P.L.; McLeod, M.; Percival, H.J. 1989. Allophane and halloysite content and soil solution silicon in soils from rhyolitic volcanic material, New Zealand. *Australian Journal of Soil Research* 27: 67-77.

Skinner, D.N.B. 1986. Neogene volcanism of the Hauraki Volcanic Region. *Royal Society of New Zealand Bulletin* 23: 21-47.

Soengkono, S.; Hochstein, M.P.; Smith, I.E.M.; Itaya, T. 1992. Geophysical evidence for widespread reversely magnetised pyroclastics in the western Taupo Volcanic Zone (New Zealand). *New Zealand Journal of Geology and Geophysics* 35: 47-55.

Soil Bureau Staff 1968. Soils of New Zealand Part 1. *New Zealand Soil Bureau Bulletin* 26 (1). 142 p.

Soil Survey Staff 1992. Keys to Soil Taxonomy (5th edition). *SMSS Technical Monograph* 19. Pocahontas Press, Blacksburg, Virginia. 566 p.

Soma, M.; Churchman, G.J.; Theng, B.K.G. 1992. X-ray photoelectron spectroscopic analysis of halloysites with different composition and particle morphology. *Clay Minerals* 27: 413-421.

Stern, T. A. 1987. Asymmetric back-arc spreading, heat flux and structure associated with the Central Volcanic region of New Zealand. *Earth and Planetary Science Letters* 85: 265-276.

Stevens, K.F.; Vucetich, C.G. 1985. Weathering of Upper Quaternary tephras in New Zealand, 2. Clay minerals and their climatic interpretation. *Chemical Geology* 53: 237-247.

Stewart, R.B.; Neall, V.E.; Syers, J.K. 1984. Accumulation of aerosolic quartz in an Andept chronosequence, North Island, New Zealand. *Geoderma* 37: 331-340.

Stewart, R.B.; Neall, V.E.; Syers, J.K. 1986. Origin of quartz in selected soils and sediments, North Island, New Zealand. *New Zealand Journal of Geology and Geophysics* 29: 147-152.

Stokes, S.; Lowe, D.J.; Froggatt, P.C. 1992. Discriminant function analysis and correlation of late Quaternary rhyolitic tephra deposits from Taupo and Okataina volcanoes, New Zealand, using glass shard major element composition. *Quaternary International* 13/14: 103-117.

Tatsumi, Y.; Tsunakawa, H. 1992. Cenozoic volcanism, stress gradient and back-arc opening in the North Island, New Zealand: Origin of Taupo-Rotorua Depression. *The Island Arc* 1: 40-50.

Theng, B.K.G. (ed) 1980. *Soils With Variable Charge*. New Zealand Society of Soil Science, Lower Hutt. 448 p.

Theng, B.K.G.; Russell, M.; Churchman, G.J.; Parfitt, R.L. 1982. Surface properties of allophane, halloysite and imogolite. *Clays and Clay Minerals* 30: 143-149.

Theng, B.K.G.; Churchman, G.J.; Whitton, J.S.; Claridge, G.G.C. 1984. Comparison of intercalation methods for differentiating halloysite from kaolinite. *Clays and Clay Minerals* 32: 249-258.

Tippett, J.M.; Kamp, P.J.J. in press. Fission track analysis of the Late Cenozoic vertical kinematics of continental Pacific crust, South Island, New Zealand. *Journal of Geophysical Research* (B series)

Tomlinson, A.I. 1975. Climate. In Wards, I. (ed) *New Zealand Atlas*. Government Printer, Wellington: 82-89.

Topping, W.W. 1973. Tephrostratigraphy and chronology of late Quaternary eruptives from the Tongariro Volcanic Centre, New Zealand. *New Zealand Journal of Geology and Geophysics* 16: 397-423.

Towns, D.R.; Atkinson, I.A.E. 1991. New Zealand's restoration ecology. *New Scientist* 1765: 30-33.

Tsutsuki, K.; Kuwatsuka, S. 1989. Degradation and stabilization of humus in buried volcanic ash soils. I. Humus composition, molecular size distribution of humic acids, and sugar composition of soils. *Soil Science and Plant Nutrition* 35: 207-216.

Vucetich, C.G.; Pullar, W.A. 1969. Stratigraphy and chronology of late Pleistocene volcanic ash beds in central North Island, New Zealand. *New Zealand Journal of Geology and Geophysics* 12: 784-837.

Vucetich, C.G.; Pullar, W.A. 1973. Holocene tephra formations erupted in the Taupo area, and interbedded tephras from other sources. *New Zealand Journal of Geology and Geophysics* 16: 745-780.

Vucetich, C.G.; Wells, N. 1978. Soils, agriculture, and forestry of Waiotapu region, central North Island, New Zealand. *New Zealand Soil Bureau Bulletin* 31. 100p.

Wada, K. 1980. Mineralogical characteristics of Andosols. In Theng, B.K.G. (ed) *Soils With Variable Charge*. New Zealand Society of Soil Science, Lower Hutt: 87-107.

Wada, K. 1985. The distinctive properties of Andosols. *Advances in Soil Science* Vol. 2. Springer-Verlag, New York: 173-229.

Wada, K. 1987. Minerals formed and mineral formation from volcanic ash by weathering. *Chemical Geology* 60: 17-28.

Wada, K. 1989. Allophane and imogolite. In Dixon, J.B.; Weed, S.B. (eds) *Minerals in Soil Environments (Second Edition)*. Soil Science Society of America Book Series 1: 1051-1087.

Wada, K.; Kakuto, Y. 1985. A spot test with toluidine blue for allophane and imogolite. *Soil Science Society of America Journal* 49: 276-278.

Wada, K.; Kakuto, Y.; Muchena, F.N. 1987. Clay minerals and humus complexes in five Kenyan soils derived from volcanic ash. *Geoderma* 39: 307-321.

Walker, G.P.L. 1980. The Taupo Pumice: product of the most powerful known (ultraplinian) eruption? *Journal of Volcanology and Geothermal Research* 8: 69-94.

Walker, G.P.L. 1984. Downsag calderas, ring faults, caldera sizes, and incremental caldera growth. *Journal of Geophysical Research* 89(B10): 8407-8416.

Walker, G.P.L.; Wilson, C.J.N. 1983. Lateral variations in the Taupo ignimbrite. *Journal of Volcanology and Geothermal Research* 18: 117-133.

Walker, G.P.L.; Self, S.; Wilson, L. 1984. Tarawera 1886, New Zealand — a basaltic plinian fissure eruption. *Journal of Volcanology and Geothermal Research* 21: 61-78.

Ward, W.T. 1967. Volcanic ash beds of the lower Waikato Basin, North Island, New Zealand. *New Zealand Journal of Geology and Geophysics* 10: 1109-1135.

Weatherhead, A.V. 1988. The occurrence of plant opal in New Zealand soils. *New Zealand Soil Bureau Record* 108. 53p.

Webster, J.G. 1990. The solubility of As_2S_3 and speciation of As in dilute and sulphide-bearing fluids at 25 and 90°C. *Geochemica et Cosmochimica Acta* 54: 1009-1017.

Weissberg, B.G. 1969. Gold-silver ore-grade precipitates from New Zealand thermal waters. *Economic Geology* 64: 95-108.

Wells, N.; Percival, H.J.; Churchman, G.J. 1985. Potential of five New Zealand clays for coating paper. *New Zealand Journal of Technology* 1: 109-114.

Whitton, J.S.; Churchman, G.J. 1987. Standard methods for mineral analysis of soil survey samples for characterisation and classification in New Zealand Soil Bureau. *New Zealand Soil Bureau Scientific Report* 79.

Wilson, C.J.N. 1985. The Taupo eruption, New Zealand. II. The Taupo ignimbrite. *Philosophical Transactions of the Royal Society, London* A314: 229-310.

Wilson, C.J.N. 1986. Reconnaissance stratigraphy and volcanology of ignimbrites from Mangakino Volcano. *Royal Society of New Zealand Bulletin* 23: 179-193.

Wilson, C.J.N. 1993. Stratigraphy, chronology, styles and dynamics of late Quaternary erptions from Taupo volcano, New Zealand. *Philosophical Transactions of the Royal Society, London* A343: 205-306.

Wilson, C.J.N.; Walker, G.P.L. 1985. The Taupo eruption, New Zealand. I. General aspects. *Philosophical Transactions of the Royal Society, London* A314: 199-228.

Wilson, C.J.N.; Ambraseys, N.N.; Bradley, J.; Walker, G.P.L. 1980. A new date for the Taupo eruption, New Zealand. *Nature* 288: 252-253.

Wilson, C.J.N.; Rogan, A.M.; Smith, I.E.M.; Northey, D.J.; Nairn, I.A.; Houghton, B.F. 1984. Caldera volcanoes of the Taupo Volcanic Zone, New Zealand. *Journal of Geophysical Research* 89(B10): 8463-8484.

Wilson, C.J.N.; Houghton, B.F.; Lloyd, E.F. 1986. Volcanic history and evolution of the Maroa-Taupo area, central North Island. *Royal Society of New Zealand Bulletin* 23: 194-223.

Wilson, C.J.N.; Houghton, B.F.; Lanphere, M.A.; Weaver, S.D. 1992. A new radiometric age estimate for the Rotoehu Ash from Mayor Island volcano, New Zealand. *New Zealand Journal of Geology and Geophysics* 35: 371-374.

Wood, I.A. 1991. Thermoluminescence dating gives new ages for some Auckland basalts. *Geological Society of New Zealand Miscellaneous Publication* 59A: 147.

Wright, I.; Carter, L.; Lewis, K. 1990. GLORIA survey of the oceanic-continental transition of the Havre-Taupo back-arc basin. *Geo-Marine Letters* 10: 59-67.

Yamamoto, K.; Tate, K.R.; Churchman, G.J. 1989. A comparison of the humic substances from some volcanic ash soils in New Zealand and Japan. *Soil Science and Plant Nutrition* 35: 257-270.

Yoshinaga, N. 1986. Mineralogical characterisitcs. II. Clay minerals. In Wada, K. (ed) *Ando Soils of Japan.* Kyushu University Press: 41-56.

Yoshinaga, N.; Tait, J.M.; Soong, R. 1973. Occurrence of imogolite in some volcanic ash soils of New Zealand. *Clay Minerals* 10: 127-130.

Young, A.W.; Campbell, A.S.; Walker, T.W. 1980. Allophane isolated from a podzol developed on a non-vitric parent material. *Nature* 284: 46-48.